creative commons
COMMONS DEED

저작자표시-비영리-변경금지 2.0 대한민국

이용자는 아래의 조건을 따르는 경우에 한하여 자유롭게

- 이 저작물을 복제, 배포, 전송, 전시, 공연 및 방송할 수 있습니다.

다음과 같은 조건을 따라야 합니다:

저작자표시. 귀하는 원저작자를 표시하여야 합니다.

비영리. 귀하는 이 저작물을 영리 목적으로 이용할 수 없습니다.

변경금지. 귀하는 이 저작물을 개작, 변형 또는 가공할 수 없습니다.

- 귀하는, 이 저작물의 재이용이나 배포의 경우, 이 저작물에 적용된 이용허락조건을 명확하게 나타내어야 합니다.
- 저작권자로부터 별도의 허가를 받으면 이러한 조건들은 적용되지 않습니다.

저작권법에 따른 이용자의 권리는 위의 내용에 의하여 영향을 받지 않습니다.

이것은 이용허락규약(Legal Code)을 이해하기 쉽게 요약한 것입니다.

Disclaimer

dCollection

ULSAN NATIONAL INSTITUTE OF
SCIENCE AND TECHNOLOGY

Mitochondria targeting peptides for highly efficient cancer therapy

Jae-Hyeong Park

Department of Chemistry

Graduate School of UNIST

ULSAN NATIONAL INSTITUTE OF
SCIENCE AND TECHNOLOGY

Mitochondria targeting peptides for highly efficient cancer therapy

A thesis
submitted to the Graduate School of UNIST
in partial fulfillment of the
requirements for the degree of
Master of Science

JaeHyeong Park

01. 13. 2017
Approved by

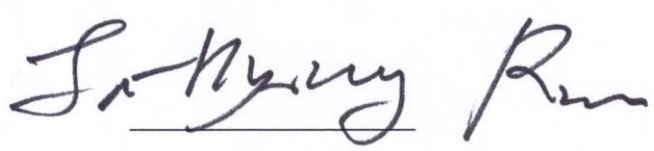

Advisor

Ja-Hyoung Ryu

ULSAN NATIONAL INSTITUTE OF
SCIENCE AND TECHNOLOGY

Mitochondria targeting peptides for highly efficient cancer therapy

Jae-Hyeong Park

This certifies that the thesis of JaeHyeong Park is approved.

01. 13. 2017

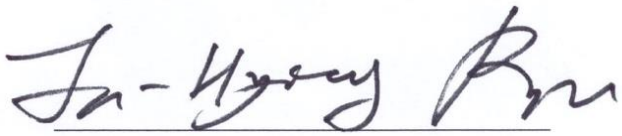

Advisor: Ja-Hyoung Ryu

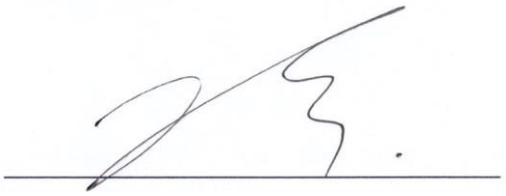

Tae Hyuk Kwon

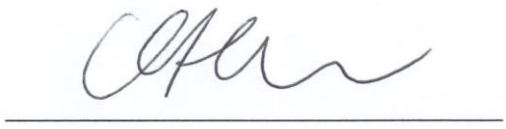

Hyun Woo Rhee

ULSAN NATIONAL INSTITUTE OF SCIENCE AND TECHNOLOGY

Abstract

Synthesis of *Cyclic mitochondria penetrating peptides (MPPs) coordinated with Ir(III) complex* and *pH-responsive charge conversion MPPs* , 2016, Jae-Hyeong Park, Graduate Program of Chemistry, Ulsan National Institute of Science and Technology(UNIST).

Selectively targeting and accumulating the photosensitizers (PS) inside the cancer cells have considerable interest. Herein, we report simple, biocompatible and robust technique for the conjugation of iridium to the MPPs complexes to target the mitochondria of cancer cells. While considering the organelle specific targeting, the mitochondria have received vital merits, upon their ability to induce apoptosis and they become an ideal target for several PDT agents. Cyclic $[HK(F_xr)_nH]$ and corresponding linear peptide $[K(F_xr)_nHH]$ were conjugated with Ir(III) complexes[Red and Green]. Ir(III) complexes and histidine (His) which has positively charged amino acid can easily bind through coordination between imidazole side chain of histidine (His) and metal which is highly efficient and easily synthesized through cyclization procedure. As a result, this effectively develop designed strategy for PDT agent based on Ir(III) complexes, which specifically targeted the mitochondria. Moreover, this cyclic modified complexes showed an improved PDT effect compared to linear one, meaning of a potent mitochondria-targeted PDT agents in antitumor therapy. Although both forms possess abundant charge, cyclic structure with rigidity is ability to result in an ideal interface for interaction with membrane constituent more than flexible structure.

Stimuli responsive degradation of chemical bonds are useful tools for the development of ‘smart materials’ which have remarkable applications in stimuli responsive drug delivery system. The pH is commonly applied to the cancer specific drug delivery system, because the pH near the tumor or in the tumor extracellular environment significantly acidic as pH 6-6.5 while the normal physiological pH is around 7.4**.** In this study, we designed and developed mitochondria targeting short peptide with charge conversion depending on pH values. The peptide sequences consists of F_xrF_xKK, possess positive charge and lipophilic character for targeting mitochondria. We conjugated drug (PU-10-COOH) as an inhibitor of HSP90 and maleic derivatives which are play a role of hydrolyzed in MPPs. Once maleic conjugated MPP extravagates into cell membrane through highly permeability, amide bonds within conjugate occur hydrolysis, reproducing intrinsic properties of MPP in the acidic tumor extracellular fluids (pH < 7) for cellular uptake and mitochondria targeting. Moreover, this platforms shows anticancer effect at 20 μM concentration. Therefore, we hope that this model conjugated peptides have a potent of cancer therapy agent

ULSAN NATIONAL INSTITUTE OF
SCIENCE AND TECHNOLOGY

ULSAN NATIONAL INSTITUTE OF SCIENCE AND TECHNOLOGY

Contents

Chapter 1. Introduction ----------1
1.1 Mitochondria penetrating peptides (MPPs) ---------- 1
1.2 Histidine-Ir(III) complex coordination method ---------- 2
1.3 Cyclic form Versus Linear peptide for cellular uptake ---------- 4
1.4 Cyclometalated Ir(III) complexes ---------- 5
1.5 Charge conversion delivery---------- 6
1.6 Thesis summary ---------- 7
1.7 References ---------- 8

Chapter 2. Cyclic Mitochondria-penetrating peptides (MPPs) with Ir(III) complex for mitochondria-targeted anticancer theranostics and photodynamic therapy ----- 11
2.1 Abstract ---------- 11
2.2 Introduction ---------- 11
2.3 Experimental ---------- 14
2.4 Results and Discussion ---------- 29
2.5 Conclusion ---------- 38
2.6 References ---------- 39

Chapter 3. pH-resoponsive Mitochondria Penetrating Peptide with PU-H71 derivatives for efficient anticancer therapy ---------- 41
3.1 Abstract ---------- 41
3.2 Introduction ---------- 41
3.3 Experimental ---------- 44
3.4 Results and Discussion ---------- 50
3.5 Conclusion ---------- 63
3.6 References ---------- 64

ULSAN NATIONAL INSTITUTE OF SCIENCE AND TECHNOLOGY

List of Schemes

Scheme 2. 1 Schematic representation of overall process for PDT by using Ir(III) complex modifications with MPPs. ---------- 13

Scheme 2. 2 Molecular structures of newly synthesized mitochondria targeting peptides. ---------- 15

Scheme 2. 3 Synthetic scheme of H_2O coordinated Ir(III) complexes (GREEN and RED). ---------- 19

Scheme 2. 4 Breakage of conjugation backbone of ABDA through $^1O_2$ oxidation. ---------- 26

Scheme 2. 5 Formation of new conjugation of DHR 123 through oxidation by $O2^{\bullet-}$---------- 26

Scheme 3. 1 Schematic representation of charge conversion MPP ---------- 43

Scheme 3. 2 synthesis of Pyrene- F_xrF_xKK ---------- 45

Scheme 3. 3 Overall schematic illustration of PU-10-COOH linker ---------- 46

ULSAN NATIONAL INSTITUTE OF SCIENCE AND TECHNOLOGY

List of Figures

Figure 1. 1 Kinetics of the luminogenic reaction with Ir(III) complex and peptides. ---------- 2

Figure 1. 2 Enhanced and selective cytotoxicity of Ir−HRGDH−KLA. ---------- 3

Figure 1. 3 FACS analysis of cellular uptake assays of cyclic peptide in SK-OV-3 cells ---------- 4

Figure 1. 4 Proposed mechanism for the photophysical processes of Irbtp–RhB. ---------- 5

Figure 1. 5 Schematic representation showing the preparation of the charge-conversional PIC micelle---------- 6

Figure 2. 1 MALDI-MS analysis of HKF_xr2H peptide. (M.W: 1,038 g/mol) ---------- 16

Figure 2. 2 MALDI-MS analysis of HKF_xr3H peptide. (M.W: 1,347 g/mol) ---------- 16

Figure 2. 3 MALDI-MS analysis of HKF_xr4H peptide. (M.W: 1,657 g/mol) ---------- 17

Figure 2. 4 MALDI-MS analysis of KF_xr2HH peptide. (M.W: 1,038 g/mol) ---------- 17

Figure 2. 5 MALDI-MS analysis of KF_xr3HH peptide. (M.W: 1,347 g/mol) ---------- 18

Figure 2. 6 MALDI-MS analysis of KF_xr4HH peptide. (M.W: 1,657 g/mol) ---------- 18

Figure 2. 7 MALDI-MS analysis of HKF_xr2H-Ir(Green). (M.W: 1,538 g/mol) ---------- 20

Figure 2. 8 MALDI-MS analysis of HKF_xr3H-Ir(Green). (M.W: 1,848 g/mol) ---------- 21

Figure 2. 9 MALDI-MS analysis of HKF_xr4H-Ir(Green). (M.W: 2,157 g/mol) ---------- 21

Figure 2. 10 MALDI-MS analysis of KF_xr2HH-Ir(Green). (M.W: 1,538 g/mol) ---------- 22

Figure 2. 11 MALDI-MS analysis of KF_xr3HH-Ir(Green). (M.W: 1,848 g/mol) ---------- 22

ULSAN NATIONAL INSTITUTE OF SCIENCE AND TECHNOLOGY

Figure 2. 12 MALDI-MS analysis of KF_xr4HH-Ir(Green). (M.W: 2,157 g/mol) ---------- 23

Figure 2. 13 Optical properties of peptide biding Ir(III) complex(Red). ---------- 24

Figure 2. 14 Each lifetime for peptide binding Ir(III) complexes by recording with time-correlated single photon counting (TCSPC). ---------- 25

Figure 2. 15 Absorbance change of ABDA for GREEN + peptide complexes. ---------- 27

Figure 2. 16 Absorbance change of ABDA for RED + peptide complexes. ---------- 27

Figure 2. 17 Analyses for peptide binding with Ir(III) aquo complexes. ----------29

Figure 2. 18 Live-cell confocal microscope images of HeLA cells after incubation with Red-Ir complex (Em: 583 nm) conjugated peptides (linear & cyclic) for 1h. ---------- 31

Figure 2. 19 Live-cell confocal microscopy images of HeLa cells after treatment for 1h, cyclic peptide-Ir(Green) and linear peptide-Ir(Green) treated with the mito tracker deep red FM.---------- 32

Figure 2. 20 FACS analysis to check the cellular uptake of Green Ir and Red Ir complex conjugated peptides in HeLA cells after 1h incubation. ---------- 33

Figure 2. 21 Flow cytometry analysis to measure the energy independent uptake mechanism in HeLA for cyclic and linear Red Ir peptides after 1h incubation at 37 ℃ and 4 ℃. ---------- 34

Figure 2. 22 Photodynamic therapy experiment for red iridium complex conjugated peptide. ------- 35

Figure 2. 23 Photodynamic therapy experiment for Green iridium complex. ---------- 36

Figure 2. 24 Flow-cytometry analysis to measure the extend of apoptosis mediated cell death in linear & cyclic Red Ir complex conjugated peptides in HeLA cells after 8h incubation and irradiation with light (300s), analyzed by annexin-V-FITC (FL1-H) and propidium iodide (FL3-H) staining assay. - 37

Figure 3. 1 MALDI-MS analysis of Pyrene-F_xrF_xKK.(M.W: 1,006 g/mol) ---------- 52

Figure 3. 2 Pyrene with MPP peptide after 1h incubation in HeLA cells. ---------- 53

ULSAN NATIONAL INSTITUTE OF SCIENCE AND TECHNOLOGY

Figure 3. 3 Cell viability analysis for Pyrene-MPP peptides. ---------- 53

Figure 3. 4 ^{1}H-NMR spectra of PUH71-COOH linker. ---------- 54

Figure 3. 5 MALDI-MS analysis of PUH71-F_xrF_xKK. ---------- 55

Figure 3. 6 Cell viability analysis for PuH71-MPP peptide and PuH71 drug in HeLA cells after 48h incubation using the Alamar blue dye assay. ---------- 55

Figure 3. 7 ^{1}H-NMR spectra of 8-mercaptoadenine. ---------- 56

Figure 3. 8 ^{1}H-NMR spectra of 1-iodo-3,4-methylenedioxybenzene. ---------- 57

Figure 3. 9 ^{1}H-NMR spectra of PU. ---------- 58

Figure 3. 10 ^{1}H-NMR spectra of PU-I. ---------- 59

Figure 3. 11 ^{1}H-NMR spectra of PU-10-$COOCH_3$ ---------- 60

Figure 3. 12 ^{1}H-NMR spectra of PU-10-COOH ---------- 61

Figure 3. 13 MALDI-MS analysis of PU-10-F_xrF_xKK. ---------- 62

Figure 3. 14 Cell viability analysis for Pu-10-MPP peptide (a) in HeLa cells after 24h incubation. (b) Compared cell viability of PU-H71, PU-H71-MPP and PU-10-MPP at concentration 2, 20 μM. ---------- 62

Figure 3. 15 MALDI-MS analysis of Pyrene-F_xrF_xKK-succinic anhydride. ---------- 63

Figure 3. 16 MALDI-MS analysis of Pyrene-F_xrF_xKK-citraconic anhydride. ---------- 64

Figure 3. 17 HPLC analysis of MPP-citraconic conjugate depending on reaction time at acidic pH 5.5. ---------- 64

ULSAN NATIONAL INSTITUTE OF
SCIENCE AND TECHNOLOGY

List of Tables

Table 1. 1 Evaluation of Mitochondrial Localization for Synthetic Peptide Conjugates ---------- 1

Table 2. 1 Quantification data of Each lifetime for peptide binding Ir(III) complexes by recording with time-correlated single photon counting (TCSPC). ---------- 25

ULSAN NATIONAL INSTITUTE OF SCIENCE AND TECHNOLOGY

List of Abbreviation

MPP	Mitochondria penetrating peptide
CPP	Cell penetrating peptide
Ir(III) or Ir	Iridium(III) complex
PDT	Photodynamic therapy
PS	Photosensitizers
K	Lysine
H	Histidine
R	Arginine
r	D- Arginine
F	Phenyl alanine
F_x	Cyclohexyl alanine
Tat	Transactivator of transcription peptide
ROS	Reactive oxygen species
$^1O_2$	Singlet oxygen
$O_2^{\bullet-}$	Superoxide radical
PEG	Polyethylene glycol
RES	Reticuloendothelial systems
HBTU	O-benzotriazole-N,N,N’,N’-tetramethyluronium hexafluorophosphate
DIPEA	N,N-diisopropylethylamine
TFA	Trifluoroacetic acid
ACN	Acetonitrile
DMF	Dimethylformamide
DCM	Dichloromethane
HPLC	High-performance liquid chromatography

ULSAN NATIONAL INSTITUTE OF SCIENCE AND TECHNOLOGY

ABDA	9,10-anthracenediyl-bis(methylene)dimalonic acid
DHR123	Dihydrorhodamine 123
TCSPC	Time-correlated single photon counting
SPPS	Solid phase peptide synthesis
IRF	Instrument response function
HeK293T	Noncancerous fibroblast cell
HeLa	Human cancer cells originating from cervix
PBS	Phosphate-buffered saline
FACS	Analyze the stained cells by flow cytometry
EC_{50}	Half maximal effective concentration
K_d	Dissociation constant
DMAP	4-Dimethylaminopyridine
DMSO	Dimethyl sulfoxide

ULSAN NATIONAL INSTITUTE OF SCIENCE AND TECHNOLOGY

Chapter 1. Introduction

1.1 Mitochondria penetrating peptides (MPPs)

Mitochondria is a candidate of interesting targets for organelle-specific cancer chemotherapy, since mitochondria have merits of important role, which possess not only energy production but programmed cell death [1,2]. However, a significant challenge to access of mitochondrial transporters within this organelle can be difficult, because the inner membrane have the impervious structure of the hydrophobic properties [3]. To solve this issue, mitochondria penetrating peptides (MPPs) have been develop. This MPPs are some kinds of cell-permeable peptides that are able to enter mitochondria membrane [4]. The sequences of the MPPs exhibits positive charge and lipophilic character for translocation both the plasma membrane and mitochondrial membranes. Among the amino acids, lysine (K) and arginine (R) provide positive charge, and phenylalanine (F) and cyclohexylalanine (F_X) residues have a lipophilicity. Delocalized lipophilic cationic units are known to predominantly accumulate in mitochondria in response to negatively charged intra-trans membrane potentials [4]. Moreover, arginine-based peptides such as Tat, which known as CPPs, have high levels of cellular uptake [5]. By altering aromatic (lipophilicity) and cationic residues, MPPs shows successful delivery for mitochondrial location. The sequence of MPPs are presented in Table 1.1.

Table 1. 1 Evaluation of Mitochondrial Localization for Synthetic Peptide Conjugates [27]. (*Reprinted with permission**)**

Compound	Charge	Log P[a]	Rr[b]
to-F_X-r-F_X-K-F_X-r-F_X-K (**1a**)[c]	+5	−2.2	+0.5
to-F-r-F-K-F-r-F-K (**1b**)	+5	−2.5	+0.1
to-F-r-F_X-K-F-r-F_X-K (**1c**)	+5	−2.3	+0.4
to-F-r-Y-K-F-r-Y-K (**1d**)	+5	−2.7	−0.4
to-F_X-r-F_X-K (**2a**)	+3	−1.1	+0.6
to-F-r-F-K (**2b**)	+3	−1.9	+0.2
to-F-r-F_X-K (**2c**)	+3	−1.4	+0.4
to-F-r-F_2-K (**2d**)	+3	−1.6	+0.6
to-F-r-Nap-K (**2e**)	+3	−1.6	+0.5
to-F-r-Hex-K (**2f**)	+3	−1.7	+0.5
to-F-r-Y_{Me}-K (**2g**)	+3	−2.0	+0.1
to-F-r-F_F-K (**2h**)	+3	−2.0	−0.1
to-F-r-Y-K (**2i**)	+3	−2.1	−0.2
to-Y-r-Y-K (**2j**)	+3	−2.4	−0.4

ULSAN NATIONAL INSTITUTE OF
SCIENCE AND TECHNOLOGY

1.2 Histidine-Ir(III) complex coordination method

Wang et al reported that through the combined coordination of Ir(III) complex, peptide luminogenic cyclization method developed an easy-to-use and versatile method [6]. Some cyclometalated Iridium(III) solvent complex can be ability to use a selective luminogenic probe [7]. Moreover, the imidazole unit of histidine side chains contained the pair of free electrons can be able to attach to metal ions. When in a peptide bond, an $–NH_2$ group in adjacent neighborhood of a histidine residue show negiligible influence on coordination of histidine residues with Ir(III) complex (Figure 1.1.a,b). But, N-terminally placed histidine can bind to Ir(III) complex.

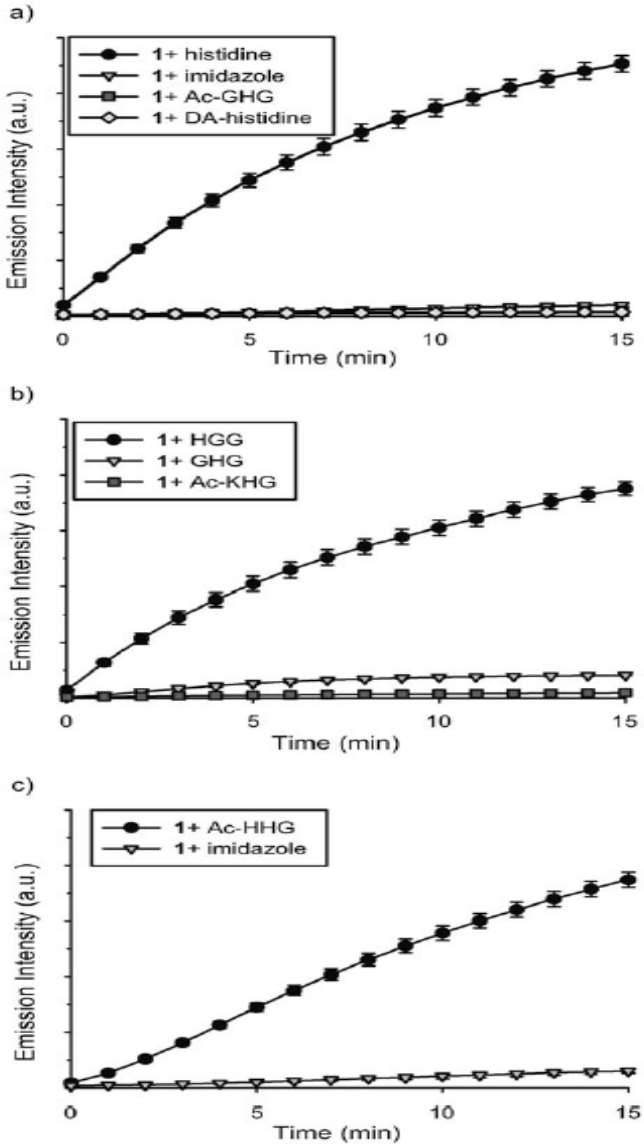

Figure 1. 1 Kinetics of the luminogenic reaction with Ir(III) complex and peptides [6]. (*Reprinted with permission)

ULSAN NATIONAL INSTITUTE OF SCIENCE AND TECHNOLOGY

Also, peptide with two histidine placed each terminus can be used to coordination with Ir(III) complex [8]. This peptide can make cyclic formation with the different ring sizes by placing other sequences of amino acid between two histidine. By utilizing these located sequences of amino acid, cyclic peptide with Ir(III) complex have ability to accumulate organelle with targeting peptide. Because peptide can be tethered to anticancer drug, these cyclic peptides are more beneficial in cancer. So, the combination of structural modification and phosphorescent labeling properties may provide multifunctional effect for biomedicine applications.

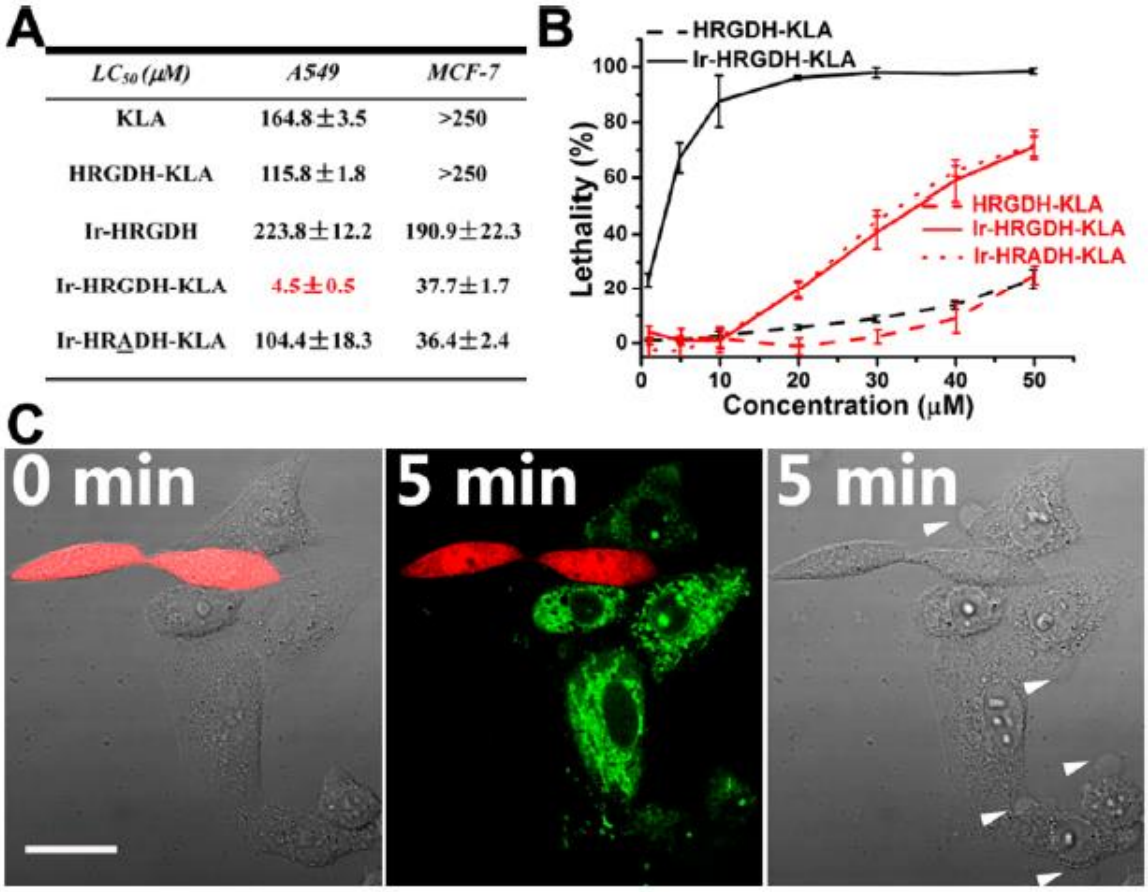

LC_{50} (μM)	A549	MCF-7
KLA	164.8±3.5	>250
HRGDH-KLA	115.8±1.8	>250
Ir-HRGDH	223.8±12.2	190.9±22.3
Ir-HRGDH-KLA	4.5±0.5	37.7±1.7
Ir-HRADH-KLA	104.4±18.3	36.4±2.4

Figure 1. 2 Enhanced and selective cytotoxicity of Ir−HRGDH−KLA [8]. (*Reprinted with permission).

ULSAN NATIONAL INSTITUTE OF SCIENCE AND TECHNOLOGY

1.3 Cyclic form Verses Linear peptide for cellular uptake

Cyclic peptides generally impermeable to the cell membrane. However, the combination of cell-penetrating peptide can be lead to overcome their applications against intracellular targets with resulted in cell-permeable [9]. Moreover, cyclic peptides exhibit a great potential as therapeutic agents, because the ability of a general intracellular delivery are more effective than linear form peptides [10]. As shown Figure 1.3.a, cyclic peptide (DOX-[W(RW)4]) shows more higher cellular uptake than linear peptide(DOX-[RW]5) [26]. Moreover, cyclic Tat entered living cells more effectively than linear Tat [11]. Although both forms possess abundant charge, cyclic structure with rigidity is ability to result in an ideal interface for interaction with membrane constituent more than flexible structure [11]. So, the cyclic form can be not only able to translocate into living cells compared to linear form but enhanced significantly transduction kinetics.

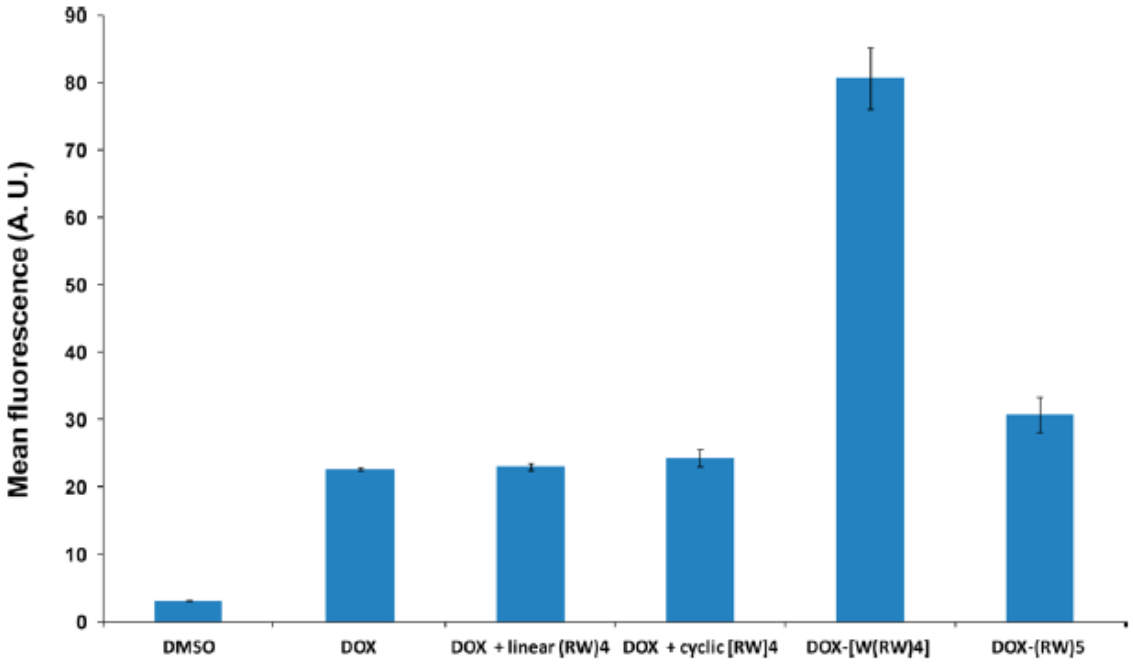

Figure 1. 3 FACS analysis of cellular uptake assays of cyclic peptide in SK-OV-3 cells [26]. (*Reprinted with permission)

ULSAN NATIONAL INSTITUTE OF SCIENCE AND TECHNOLOGY

1.4 Cyclometalated Ir(III) complexes

Recently, cyclometalated iridium(III) complexes are widely developed as biosensing agents, which exhibit superior photophysical properties, e.g, high quantum yield, large stokes shifts, long lived phosphorescence, good phtostability, cell permeability [12-15]. Ir(III) complexes based on PDT agents also exhibit strong anticancer potential by controlling their energy levels to achieve marked ROS generation [16-17]. When this Ir(III) complex exposed to a specific wavelength of light, the excited complex move its energy to the ambient molecular oxygen ($^3O_2$) to generate $^1O_2$ and other toxic reactive oxygen species (ROS), which can lead to the cell death [26](Figure 1.4). In addition, photophysical and biological properties of Ir(III) complexes can be changed due to the easy modification of the ligands.

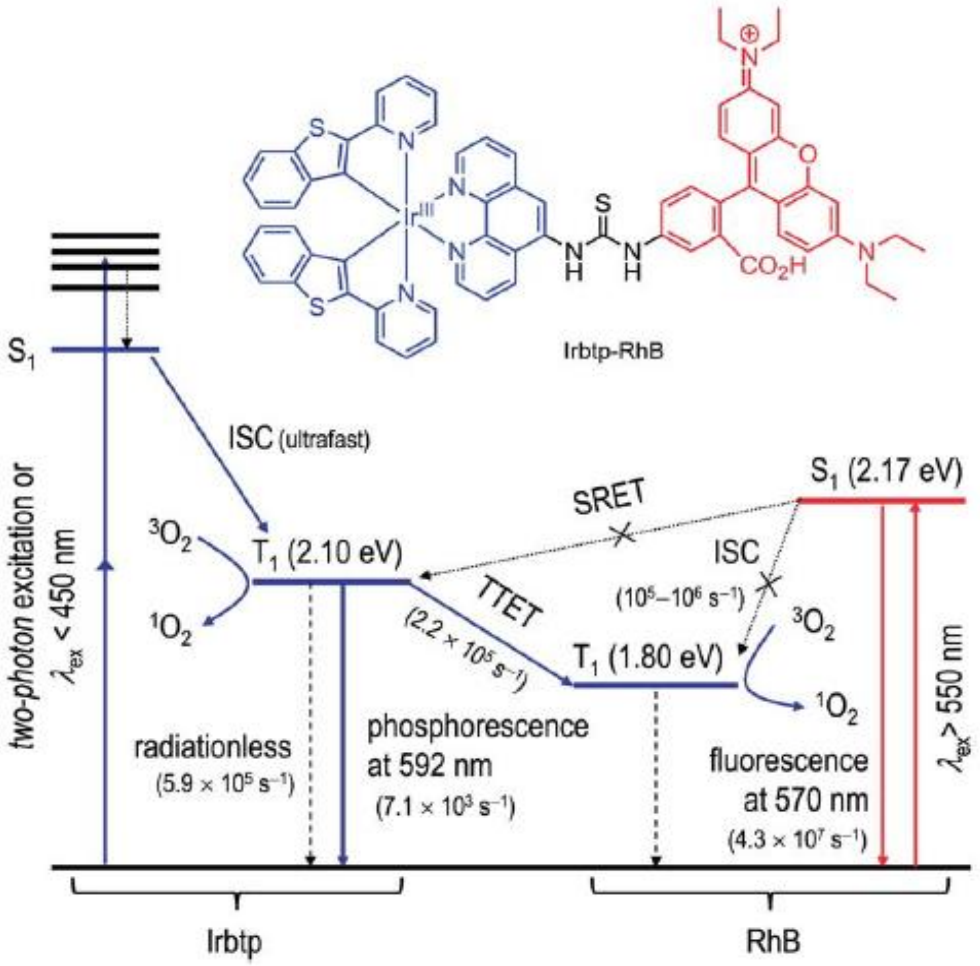

Figure 1. 4 Proposed mechanism for the photophysical processes of Irbtp–RhB [25]. (*Reprinted with permission)

ULSAN NATIONAL INSTITUTE OF SCIENCE AND TECHNOLOGY

1.5 Charge conversion delivery

pH-responsive degradation of chemical bonds is useful tool for stimuli-responsive drug-delivery systems [18]. Various pH-sensitive chemical bonds such as acetal, orthoester, imine, and phosphoramidate moieties have ability to degrade at mild pH changes [19-22]. Recently, Maleic acid amide derivatives are known as candidates of pH-sensitive moiety. Most of them can be able to degrade at mild acidic pH conditions since these moieties can be attributed to the internal reaction of amide carbonyl group by the carboxylate [23-24], inducing change of the chemical structure of maleic acid amide. Also, carboxylate groups within maleic acid amide derivatives exhibit negative charges at basic conditions. But, after degradation at acidic conditions, maleic acid amide bond turn to their original form, maleic acid groups with exposing positively charged amine groups. This negative-to-positive charge conversion in maleic acid amide derivatives have been modified in order to increase the negative charge density of lipids and polymers for the effective pH-triggered drug delivery.

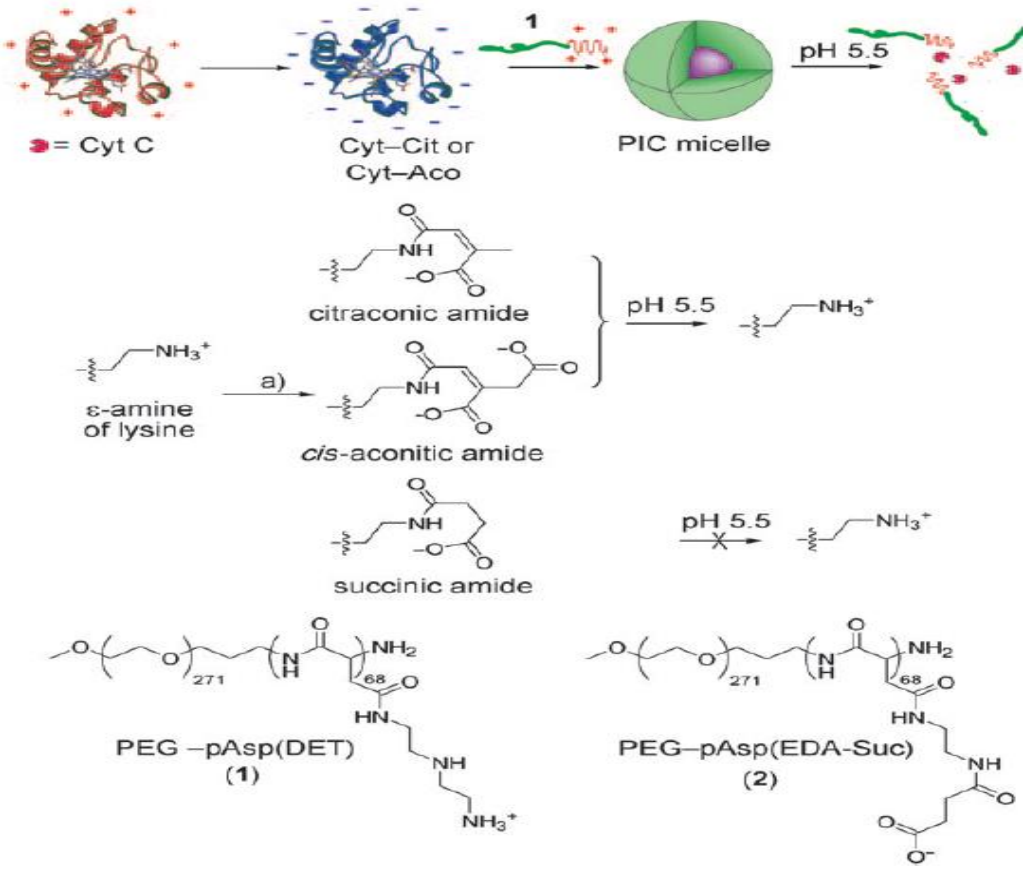

Figure 1. 5 Schematic representation showing the preparation of the charge-conversional PIC micelles [28]. (*Reprinted with permission)

ULSAN NATIONAL INSTITUTE OF
SCIENCE AND TECHNOLOGY

1.6 **Thesis summary**

Mitochondria represents a candidate of interesting targets for organelle-specific cancer chemotherapy, since mitochondria have merits of important role, which possess not only energy production but programmed cell death. However, a significant challenge to access of mitochondrial transporters within this organelle can be difficult, because the inner membrane have the impervious structure of the hydrophobic properties. To solve this issue, mitochondria penetrating peptides (MPPs) have been develop. This MPPs are cell-permeable peptides that are able to enter mitochondria membrane. Moreover, they can accumulate in the mitochondria because of positive charge and liphophlicity within the side chain of peptide. But, these peptide also have some limitations. Since MPPs possess mitochondria targeting ability by charge driven, they can go to mitochondria in normal cell. Although mitochondria in tumor cell is more negative charge than normal cell, charge driven ability of MPPs may affect inhibition of anti-cancer ability. And MPPs can't deliver cargo with high M.W. To overcome this limitation, highly efficient cellular uptake and selectivity ability are the most needed.

In Chapter 2, the synthesis and characterization of newly MPPs coordinated with Ir(III) complex are discussed. Ir(III) coordinated peptides depending on different sequence of mitochondria penetrating peptide and conformation are also described. Designed compound were characterized for PDT. Chapter 3 summarizes the synthesis of charge conversion MPPs and Checks the anti-cancer ability.

ULSAN NATIONAL INSTITUTE OF SCIENCE AND TECHNOLOGY

1.7 References

1. Fantin, V.R.; and Leder, P. *Oncogene*. **2006**, 25, 4787–4797.

2. Galluzzi, L.; Larochette, N.; Zamzami, N.; and Kroemer, G. *Oncogene*. **2006**, 25, 4812–4830.

3. Fernandez-Carneado, J.; Gool, M.V.; Martos, V.; Castel, S.; Prados, P.; deMendoza, J.; and Giralt, E. *J. Am. Chem. Soc*. **2005**, 127, 869–874.

4. Yousif, L.F.; Stewart, K.M.; Horton, K.L.; Kelley, S.O., *ChemBioChem*. **2009**, 10, 2081–2088.

5. Mitchell, D. J.; Kim, D. T.; Steinman, L.; Fathman, C. G.; and Rothbard, J. B.; Pept, J. *Res*, **2000**, 56, 318–325.

6. Wang, X.; Jia, J.; Huang, Z.; Zhou, M.; Fei, H. *Chem.-Eur. J*. **2011**, 17, 8.

7. Ma, D. L.; Wong, W. L.; Chung, W. H.; Chan, F. Y.; So, P. K.; Lai, T. S.; Zhou, Z. Y.; Leung, Y. C.; Wong, K. Y. *Angew. Chem. Int. Ed*. **2008**, 47, 3735.

8. Ma, X.; Jia, J.; Cao, R.; Wang, X.; and Fei, H. *J. Am. Chem. Soc*. **2014**, 136, 17734−17737

9. Lian, W.; Jiang, B.; Qian, Z.; and Pei, Dehua. *J. Am. Chem. Soc*. **2014**, 136 (28), 9830–9833

10. Asrolahi Shirazi, A1.; Tiwari, R.; Chhikara, BS.; Mandal, D.; Parang, K. *Mol Pharm*. **2013**, 10(2), 488-99.

11. Gisela, L. T.; Manuel, P.; Daniel, H.; Joachim, B.; Caroline P. A.; Ingo, M.; Henry, D.; Herce, M.; Cristina, C. *Nature Communications*. **2011**, 10, 1038

12. Lo, K. K. W.; Zhang, K. Y. *RSC Adv*. **2012**, 2, 12069e83.

ULSAN NATIONAL INSTITUTE OF SCIENCE AND TECHNOLOGY

13. You, Y. *Curr Opin Chem Biol*. **2013**,17, 699e707.

14. Zhao, Q.; Huang, C.; Li, F. *Chem Soc Rev*. **2011**, 40, 2508e24.

15. You, Y.; Han, Y.; Lee, Y. M.; Park, S. Y.; Nam, W.; Lippard, S. J. *J Am Chem Soc*. **2011**,133, 11488e91.

16. Hardin, B. E.; Hoke, E. T.; Armstrong, P. B.; Yum, J. H.; Comte, P.; Torres, T.; Frechet, J. M. J.; Nazeeruddin, M. K.; Gratzel, M.; McGehee, *M. D. Nat. Photonics*. **2009**, 3, 406.

17. Yun, M. H.; Lee, E.; Lee, W.; Choi, H.; Lee, B. R.; Song, M. H.; Hong, J. I.; Kwon, T. H.; Kim, J. Y. *J. Mater. Chem*. **2014**, 2, 10195.

18. Fleige, E.; Quadir, M. A.; Haag, R. *Adv. Drug Deliv. Rev*. **2012**, 64, 866.

19. Gillies, E. R.; Goodwin, A. P.; Frechet, J. M. J. *Bioconjugate Chem*. **2004**, 15, 1254.

20. Masson, C.; Garinot, M.; Mignet, N.; Wetzer, B.; Mailhe, P.; Scherman, D.; Bessodes, M. J. Controlled Release 2004, 99, 423.

21. Kramer, M.; Stumbe, J. F.; Turk, H.; Krause, S.; Komp, A.; Delineau, L.; Prokhorova, S.; Kautz, H.; Haag, R. *Angew. Chem. Int. Ed*. **2002**, 41, 4252.

22. Liang, Y.; Narayanasamy, J.; Schinazi, R. F.; Chu, C. K. *Bioorg. Med. Chem*. **2006**, 14, 2178.

23. Kirby, A. J.; Lancaster, P. W. *J. Chem. Soc*. **1972**, 2, 1206.

24. Kirby, A. J.; McDonald, R. S.; Smith, C. R. *J. Chem. Soc*. 1974, 2, 1495.

25. Cho, S.; You, Y.; and Nam, W. W. *RSC Adv*. **2014**, 4, 16913–16916.

26. Shirazi, N.; Tiwari, R.; Bhupender S.; Chhikara, D. M.; and Parang, K. *Mol. Pharmaceutics*. **2013**, 10, 488−499

ULSAN NATIONAL INSTITUTE OF
SCIENCE AND TECHNOLOGY

27. Kristin, L. H.; Kelly, M. S.; Sonali, B. F.; Qian, G.; and Shana, O.K. *Chemistry & Biology*, **2008**, 15, 375–382

28. Lee, Y.; Ishii, T.; Cabral, H.; Kim, H. J.; Seo, J. H.; Nishiyama, N.; Oshima, H.; Osada, K.; and Kataoka, K. *Angew. Chem*, **2009**, 121, 5413 –5416

ULSAN NATIONAL INSTITUTE OF SCIENCE AND TECHNOLOGY

2. Cyclic Mitochondria-penetrating peptides (MPPs) with Ir(III) complex for mitochondria-targeted anticancer theranostics and photodynamic therapy

2.1 Abstract

Selectively targeting and accumulating the PS inside the cancer cells have considerable interest and non-toxic. Herein, we report simple, biocompatible and robust technique for the conjugation of iridium to the MPPs complexes to target the mitochondria of cancer cells. Cyclic [HK(F_xr)$_n$H] and corresponding linear peptide [K(F_xr)$_n$HH] were conjugated with Ir(III) complexes[Red and Green]. Ir(III) complexes and histidine (His) which has positively charged amino acid can easily bind through coordination between imidazole side chain of histidine (His) and metal which is highly efficient and easily synthesized through cyclization procedure. As a result, this effectively develop designed strategy for PDT agent based on Ir(III) complexes, which specifically targeted the mitochondria. Moreover, this cyclic modified complex exhibited an improved PDT effect compared to linear one, meaning of a higher potent mitochondria-targeted PDT agents for cancer therapy.

2.2 Introduction

Increasing modalities by non-invasive techniques are promising strategy for cancer treatment [1]. Recently, these noninvasive treatments have received considerable due to their treatment efficacy and widely used for several therapies including cancer [2]. PDT has been successfully used to treat epidermal cancer by illuminating the photosensitizers (PS) to generate reactive oxygen species (ROS) upon the activation of light [3]. Several photosensitizing agents such as porphyrin, chlorin and zanthenese are conventionally applied and developed for clinics [4]. For instance, photofrins which are porphyrin derivatives clinically generate ROS, to kill the cancer cells [5]. However, the limitations of the photofrins include inefficient light penetration in deep tissues, low molar absorption coefficient (1,170 M^{-1} $Cm^{-1)}$) which needs both high concentrations of sensitizer and long light time, and non-selectivity for tumor [6-8]. Recently, Iridium (III) complexes in PDT have received significant attention due to its stability and efficacy [9-10]. Upon specific wavelength of light, the excited PS relocate its

ULSAN NATIONAL INSTITUTE OF SCIENCE AND TECHNOLOGY

energy to the ambient molecular oxygen ($^3O_2$) to generate $^1O_2$ and other toxic reactive oxygen species (ROS), which can lead to the cell death. Ir(III) complexes have received significantly recognition as bio-imaging agent because of their rich photophysical properties involving large stokes shifts, high quantum yield, long-lived phosphorescence, outstanding color tuning capability and good resistance to photo-bleaching [11-15].Moreover, the photophysical and biological properties of Ir(III) complexes can be readily tuned due to the easy modification of the ligands. Poor solubility and non-selective accumulations in reticuloendothelial systems (RES) may lead to failure of this design and unwanted toxicity. Selectively targeting and accumulating the PS inside the cancer cells have considerable interest and non-toxic.

Peptides received wide interest in targeting the cancer cells. Peptides are known to be biocompatible and highly soluble in several organic solvents and aqueous suspensions. Modifying the amino acid sequence of these peptides, such as cell penetrating peptides can selectively accumulate inside the cancer cells. Cell penetrating peptides (CPPs) such as Tat have the ability to cross the cell membrane [16-17]. Especially, mitochondria penetrating peptides (MPPs) are important CPP, can enter both the plasma and mitochondrial membranes [18]. MPPs are extensively used for targeting cancer cells because they impart positive charge and lipophilic character in the side chains of amino acid, which increase its affinity towards mitochondria [18-19]. Interestingly, cyclic peptides have significant advantages such as enhanced cellular uptake due to cyclic structure with rigidity is ability to result in an ideal interface for interaction with membrane constituent more than flexible structure. Recently, cyclic arginine-rich CPPs showed amplified cellular uptake compared to their linear CPPs with flexibility. Cyclized CPPs are not only able to translocate into living cells with comparable to linear form but exhibit enhanced transduction [20]. Specific organelle targeting in cancer treatment have robust efficacy. Specific organelle localization of the PS improves the treatment efficacy in cancer and investigated in detail [21]. Target specificity of PS can be achieved by controlling the functional groups of the agents and peptides have major role in cancer targeting [22]. PDT agents can be conjugated to peptides under mild reaction condition and can be delivered at the target location. While considering the organelle specific targeting, the mitochondria have received vital merits, upon their ability to induce apoptosis and they become an ideal target for several PDT agents.

Herein, we report simple, biocompatible and robust technique for the conjugation of iridium to the MPPs complexes to target the mitochondria of cancer cells. Cyclic [HK(F_xr)$_n$-H] and corresponding linear peptide [K(F_xr)$_n$-HH] were conjugated with Ir(III) complexes[Red and Green]. Ir(III) complexes and histidine (His) which has positively charged amino acid can easily bind through coordination between imidazole side chain of histidine (His) and metal which is highly efficient and

ULSAN NATIONAL INSTITUTE OF SCIENCE AND TECHNOLOGY

easily synthesized through cyclization procedure [23-24]. As a result, this effectively develop designed strategy for PDT agent based on Ir(III) complexes, which specifically targeted the mitochondria (Scheme 2. 1). Moreover, this cyclic modified complex exhibited an improved PDT effect compared to linear one, meaning of a potent mitochondria-targeted PDT agents for antitumor therapy.

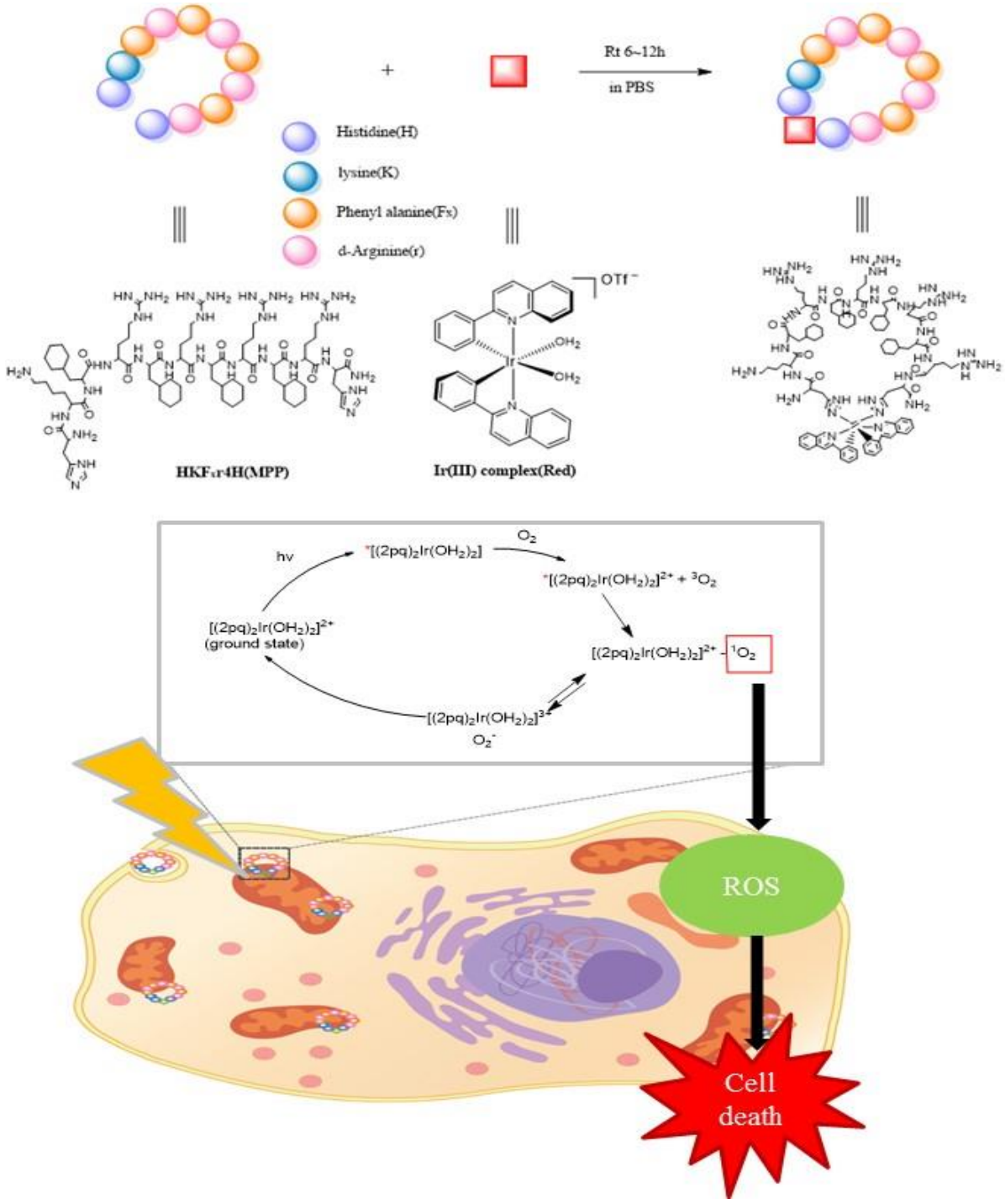

Scheme 2. 1 Schematic representation of overall process for PDT by using Ir(III) complex modifications with MPPs.

ULSAN NATIONAL INSTITUTE OF SCIENCE AND TECHNOLOGY

2.3 Experimental

Materials and Methods

All reagents and chemicals were purchased from commercial sources and used as received. Amino acids (Fmoc-Lys(Boc)-OH, Fmoc-His(Trt)-OH, Fmoc-d-arg(Boc)-OH, Fmoc-Cha-OH) and rink amide MBHA resin were obtained from BeadTech (Korea) and ApexBio (USA), Coupling reagent(*O*-benzotriazole-*N,N,N',N'*-tetramethyluronium hexafluorophosphate, HBTU) was obtained from ApexBio (USA). *N,N*-diisopropylethylamine(DIPEA) and trifluoroacetic acid (TFA) were purchased from TCI (Japan). Triisopropylsilane and piperidine were obtained from Sigma-Aldrich (USA). *N,N*-dimethylformamide(DMF), Methanol and Acetonitrile (ACN) HPLC grade was purchased from DAEJUNG(South Korea) . Iridium(III) chloride hydrate (Strem Chemicals, MA, USA), 2-phenylpyridine (Sigma Aldrich, MO, USA), 2-phenylquinoline (Sigma Aldrich, MO, USA), silver trifluoromethanesulfonate (Alfa Aesar, MA, USA) were used as materials for synthesis and analysis. All of solvents were prepared from SAMCHUN Chemicals, Korea. Analyses for production of reactive oxygen species (e.g., singlet oxygen ($^1O_2$) and superoxide radical ($O_2^{\bullet-}$)) utilized 9,10-anthracenediyl-bis(methylene)dimalonic acid (ABDA) and dihydrorhodamine 123 (DHR123) that were purchased from Sigma Aldrich.

Characterization

$HK(F_xr)_nH$ peptides, $K(F_xr)_nHH$ peptides and Ir(III) complex modified peptides were characterized using MALDI-TOF. Analyses for two synthesized Ir(III) complexes were previously reported [25]. Therefore, utilized two Ir(III) complexes (RED and GREEN) were checked by 1H NMR spectroscopy analysis (UNIST Central Research Facilities, Agilent 400 MR-DD2 NMR spectroscopy, Republic of Korea). Photo-physical studies for each Ir(III) complexes that finish to bind with six peptides (either cyclic or linear) were proceeded by an UV-2600 UV-visible spectrophotometer (Shimadzu, MD, USA), a Varian Cary Eclipse fluorescence spectrophotometer (Agilent, CA, USA), and PicoHarp 300 time-correlated single photon counting (TCSPC) (PicoQuant, Berlin, Germany). The irradiation source for photo-activation of Ir(III) complexes binding with a peptide made use of IQE-200 solar simulator (Newport, CA, USA).

ULSAN NATIONAL INSTITUTE OF SCIENCE AND TECHNOLOGY

Synthesis of peptide ($HK(F_xr)_nH$, $K(F_xr)_nHH$)

Solid phase peptide synthesis (SPPS) was performed by an automated peptide synthesizer. 200 mg of resin was swollen in DMF solution. After 30 min, operate machine to synthesize peptide. Peptide scale is 0.1mM. Amino acid solution was prepared by dissolving Fmoc-His(Trt)-OH 0.372 g in 6ml DMF, Fmoc-Lys(Boc)-OH 0.141 g in 3 mL DMF, Fmoc-d-arg(Boc)-OH 0.195 g(0.195*n) in 3 mL(3*n) DMF,. And Fmoc-Cha-OH 0.117 g(0.117*n) in 3 mL (3*n) DMF. Fmoc deprotection of the Fmoc- amino acids was performed by adding 20% piperidine solution in DMF. HBTU and DIPEA act as coupling reagent and base. After finishing final deprotection of Fmoc protecting group, make cleavage cocktail (TFA: triisopropylsilane: Water = 4.75 mL: 0.25 mL: 0.25 mL). Add cleavage cocktail into resin with stirring for 4 hours at room temperature. Then, precipitate with cold diethyl ether. The peptide is purified through High Performance Liquid Chromatography (HPLC) using water/Acetonitrile.

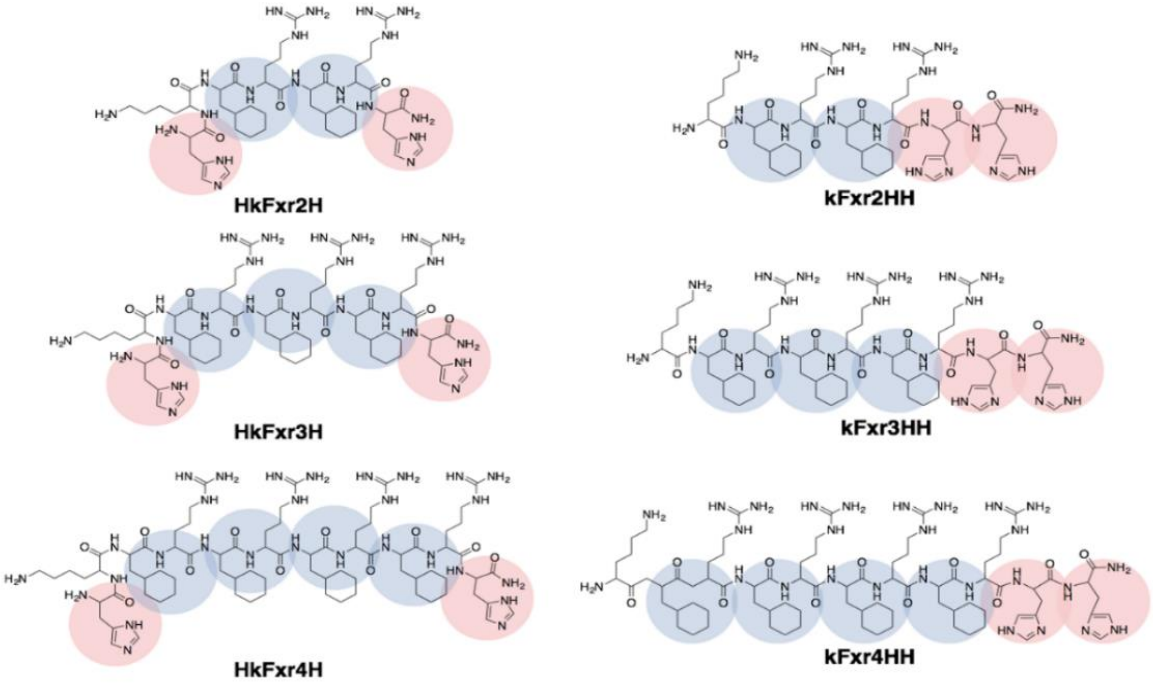

Scheme 2. 2 Molecular structure of newly synthesized mitochondria targeting peptides.

ULSAN NATIONAL INSTITUTE OF SCIENCE AND TECHNOLOGY

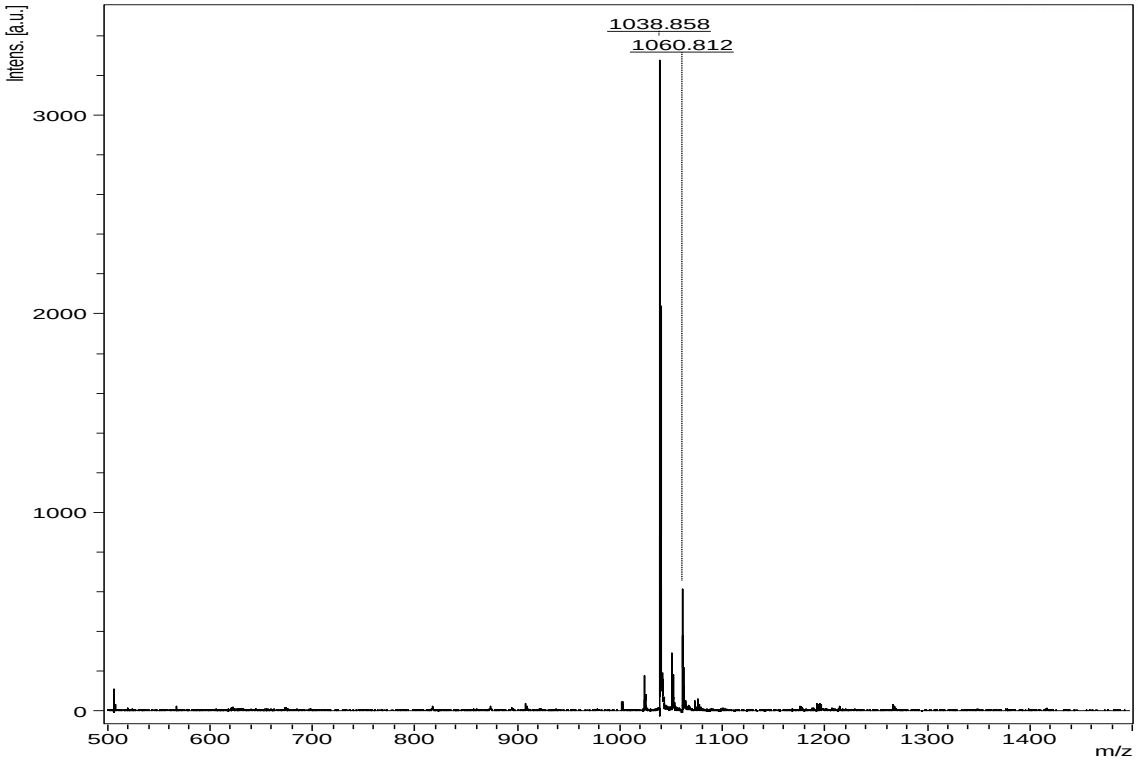

Figure 2. 1 MALDI-MS analysis of HKF_xr2H peptide. (M.W: 1,038 g/mol)

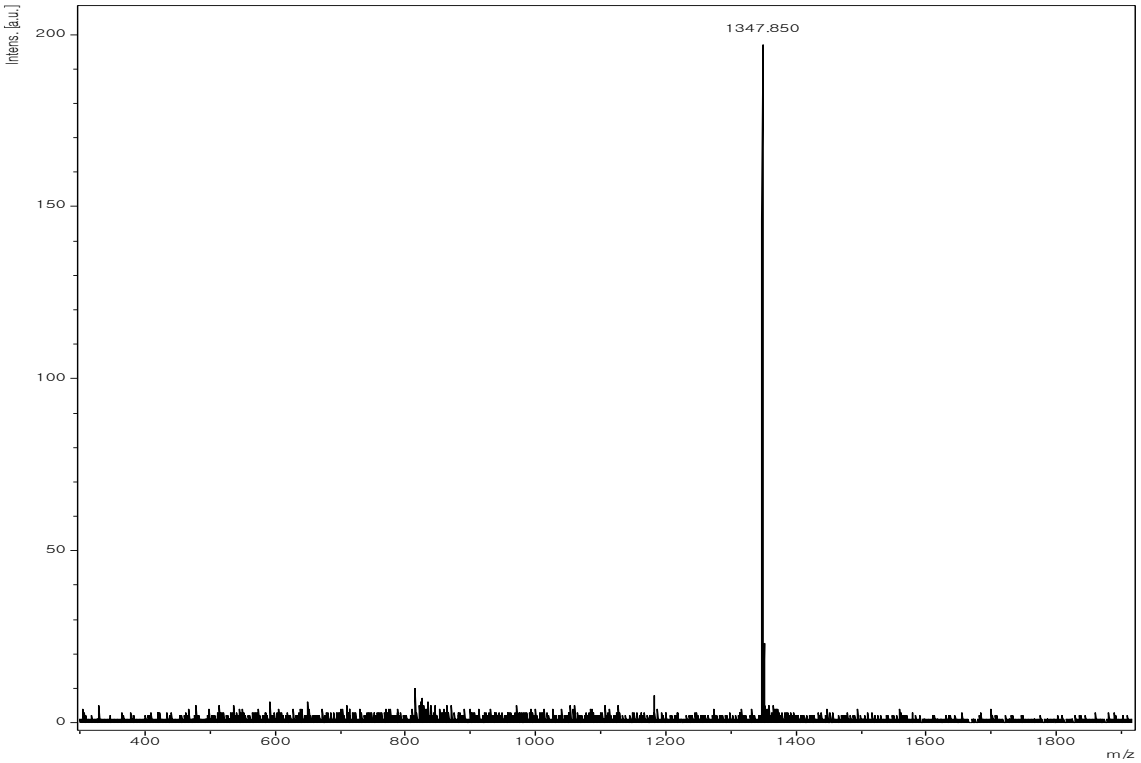

Figure 2. 2 MALDI-MS analysis of HKF_xr3H peptide. (M.W: 1,347 g/mol)

ULSAN NATIONAL INSTITUTE OF SCIENCE AND TECHNOLOGY

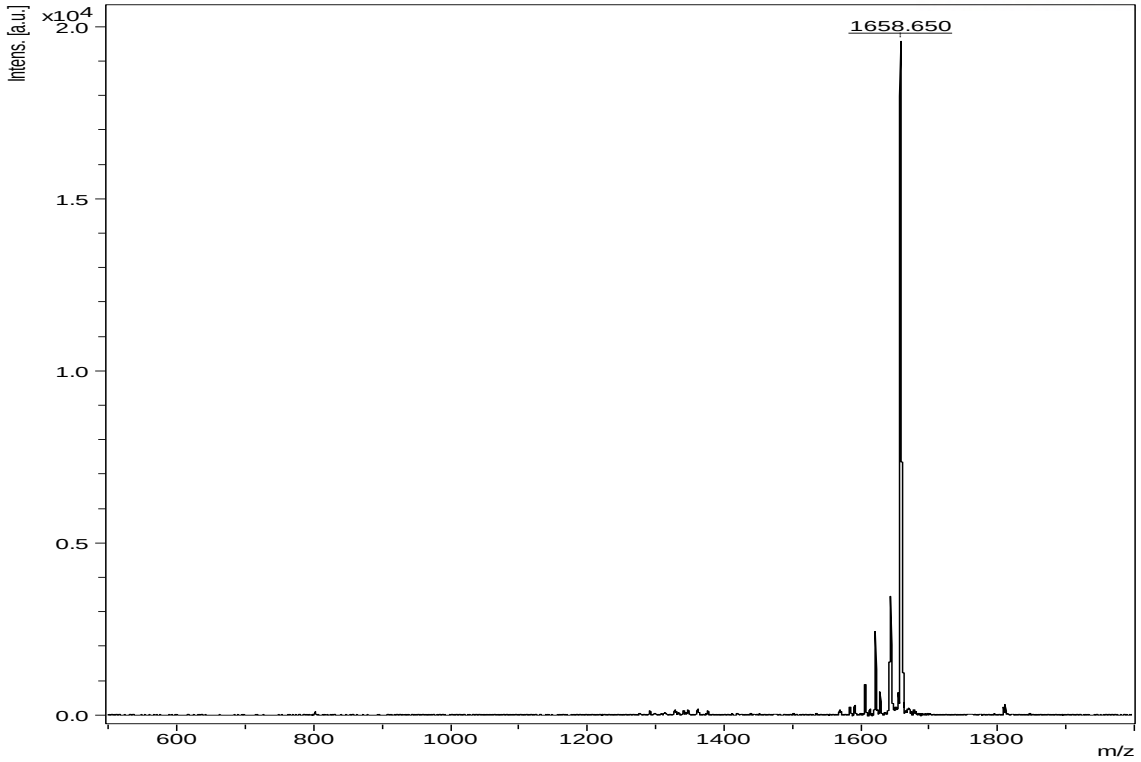

Figure 2. 3 MALDI-MS analysis of HKF$_x$r4H peptide. (M.W: 1,657 g/mol)

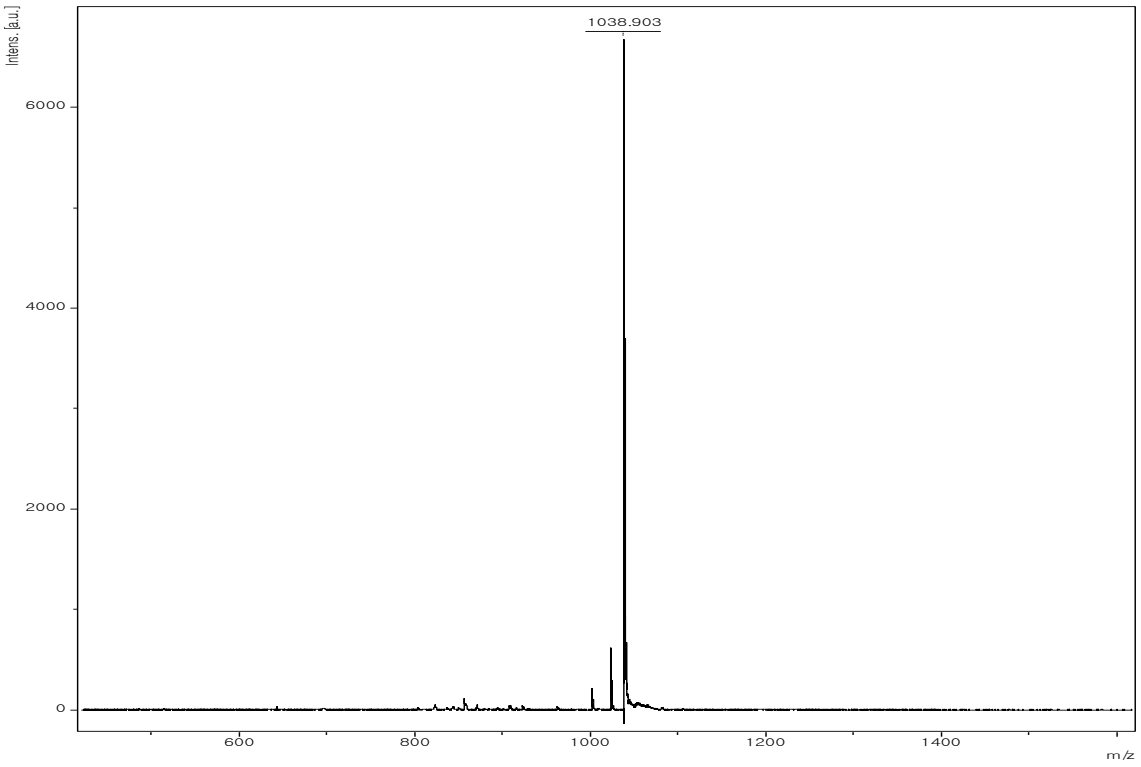

Figure 2. 4 MALDI-MS analysis of KF$_x$r2HH peptide. (M.W: 1,038 g/mol)

ULSAN NATIONAL INSTITUTE OF
SCIENCE AND TECHNOLOGY

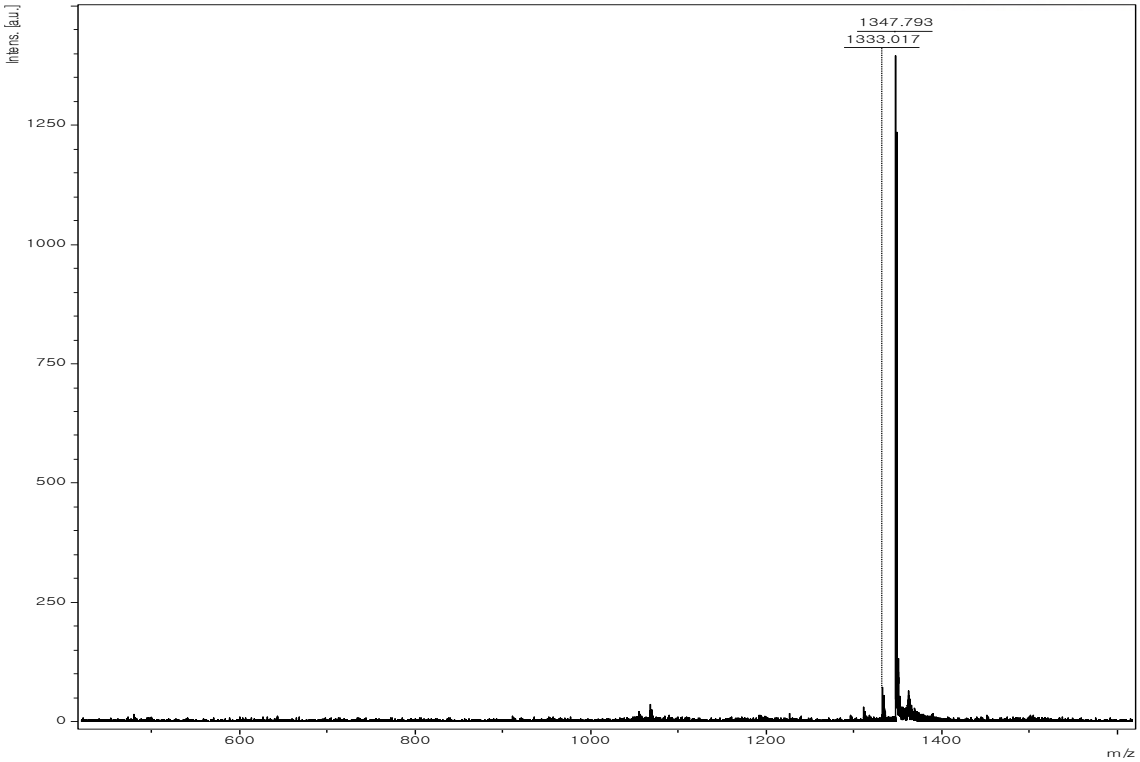

Figure 2. 5 MALDI-MS analysis of KF_xr3HH peptide. (M.W: 1,347 g/mol)

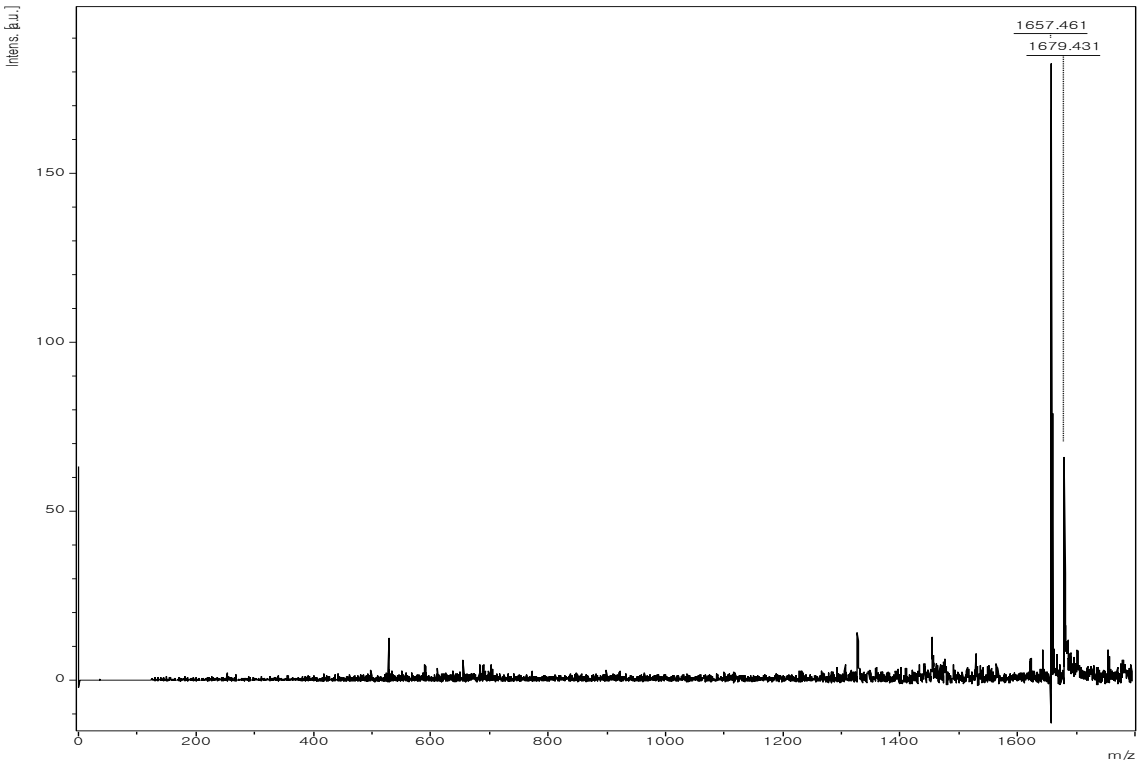

Figure 2. 6 MALDI-MS analysis of KF_xr4HH peptide. (M.W: 1,657 g/mol)

ULSAN NATIONAL INSTITUTE OF SCIENCE AND TECHNOLOGY

Procedure for Ir(III) complexes synthesis (GREEN and RED).

Procedure for synthesizing $[(ppy)_2Ir(OH_2)_2]^+OTf^-$ (GREEN) and $[(2pq)_2Ir(OH_2)_2]^+OTf^-$ (RED) is only two step process. Firstly, Iridium dimers that incorporates each ligand (2-phenylpyridine (ppy) and 2-phenylquinoline (2pq)) were prepared as previously reported method [26].Without further purification for iridium(III) dimers, next step was subsequently proceeded. A solution of dimer (1 equiv.) and silver trifluoromethanesulfonate (AgOTf) (2.2 equiv.) dissolved in EtOH:H_2O = 9:1 (v/v) solvent mixture refluxed for 24 hours. Resident solvent was removed *in vacuo* after cooling down reaction pot. Crude product extracted with CH_2Cl_2. Product was separated from other crude material, utilizing solubility difference. After product separation as much as possible, recrystallization of product with chloroform and pentane. After purification, yellow and orange color powders (GREEN and RED, respectively) were obtained.

$[(ppy)_2Ir(OH_2)_2]^+OTf^-$ (GREEN) ^{1}H NMR (400 MHz, D_2O): δ (ppm) = 8.770 (s, 1H), 7.928 (d, J = 29.9 Hz, 2H), 7.580 (m, 1H), 7.361 (dd, J = 12.0, 6.2 Hz, 1H), 6.788 (dd, J = 11.5, 7.4 Hz, 1H), 6.619 (dd, J = 10.8, 7.0 Hz, 1H), 6.084 (m, 1H).

$[(2pq)_2Ir(OH_2)_2]^+OTf^-$ (RED) ^{1}H NMR (400 MHz, d_6-CD_3CN): δ (ppm) = 8.834 (d, J = 8.9 Hz, 1H), 8.585 (d, J = 8.7 Hz, 1H), 8.273 (d, J = 8.8 Hz, 1H), 8.120 (d, J = 8.1 Hz, 1H), 7.905 (ddd, J = 8.7, 7.0, 1.5 Hz, 1H), 7.864 (d, J = 7.4 Hz, 1H), 7.770 (t, J = 7.5 Hz, 1H), 6.993 (t, J = 7.5 Hz, 1H), 6.704 (dd, J = 11.8, 4.4 Hz, 1H), 6.133 (d, J = 7.4 Hz, 1H).

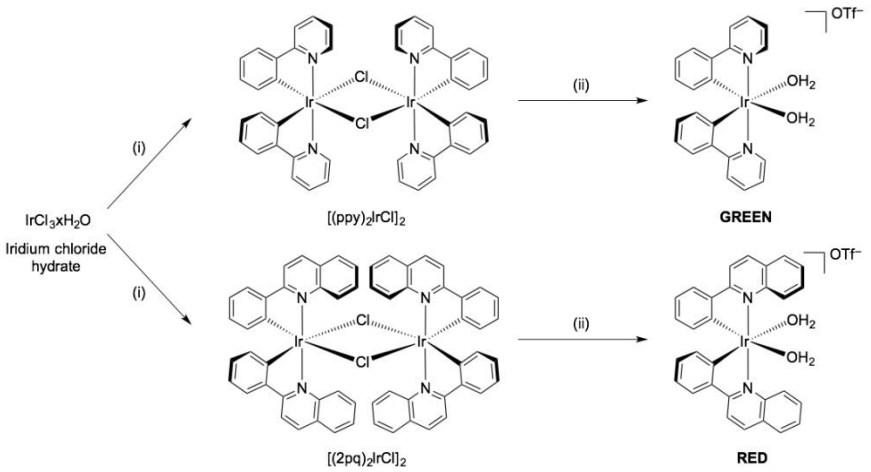

Scheme 2. 3 Synthetic scheme of H2O coordinated Ir(III) complexes (GREEN and RED). (i) ligand (2 equiv.) and 2-methoxyethanol:H2O = 3:1 (v/v). (ii) Silver trifluoromethanesulfonate (AgOTf) (2.2 equiv.) and CH2Cl2:MeOH = 1:1 (v/v).

ULSAN NATIONAL INSTITUTE OF SCIENCE AND TECHNOLOGY

Synthesis of Cyclic and linear form peptide with Ir(III) complexes

Equal molar of peptides and Ir(III) complexes were incubated in water(>1% DMSO) for 2 h at room temperature for Ir-HH cyclization. In order to confirm synthesis, MALDI-MS were performed.

[Green]

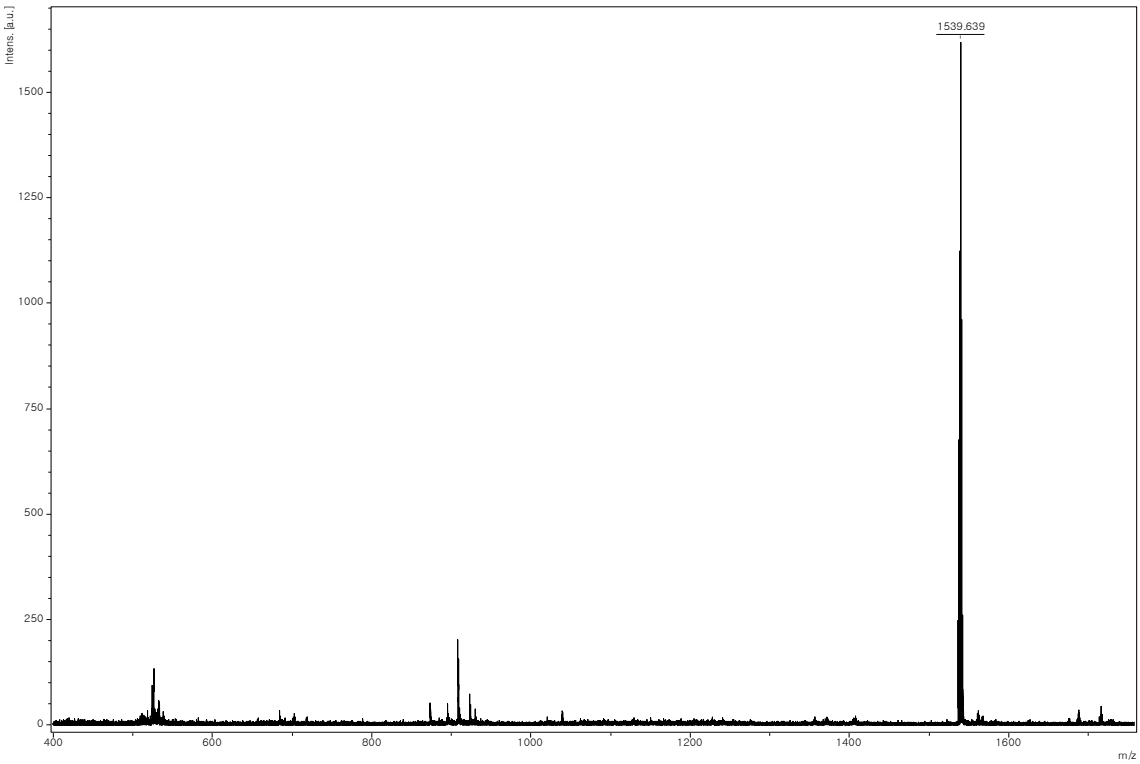

Figure 2. 7 MALDI-MS analysis of HKF_xr2H-Ir(Green). (M.W: 1,538 g/mol)

ULSAN NATIONAL INSTITUTE OF
SCIENCE AND TECHNOLOGY

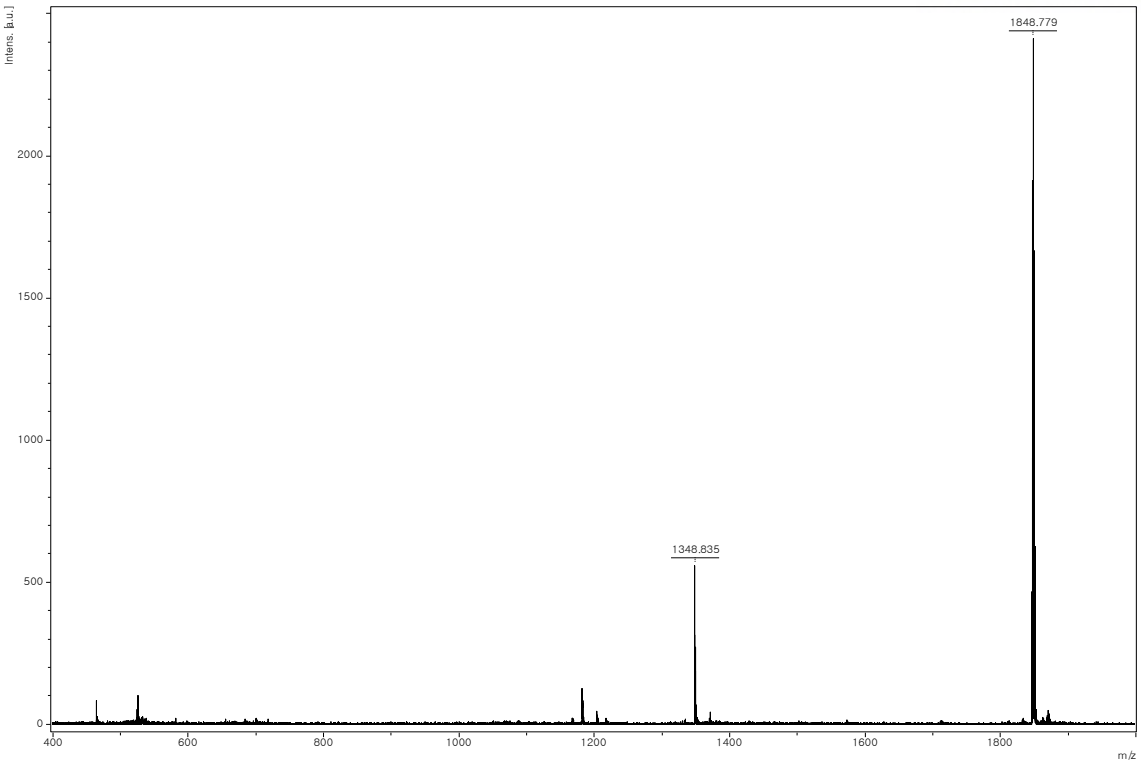

Figure 2. 8 MALDI-MS analysis of HKF_xr3H-Ir(Green). (M.W: 1,848 g/mol)

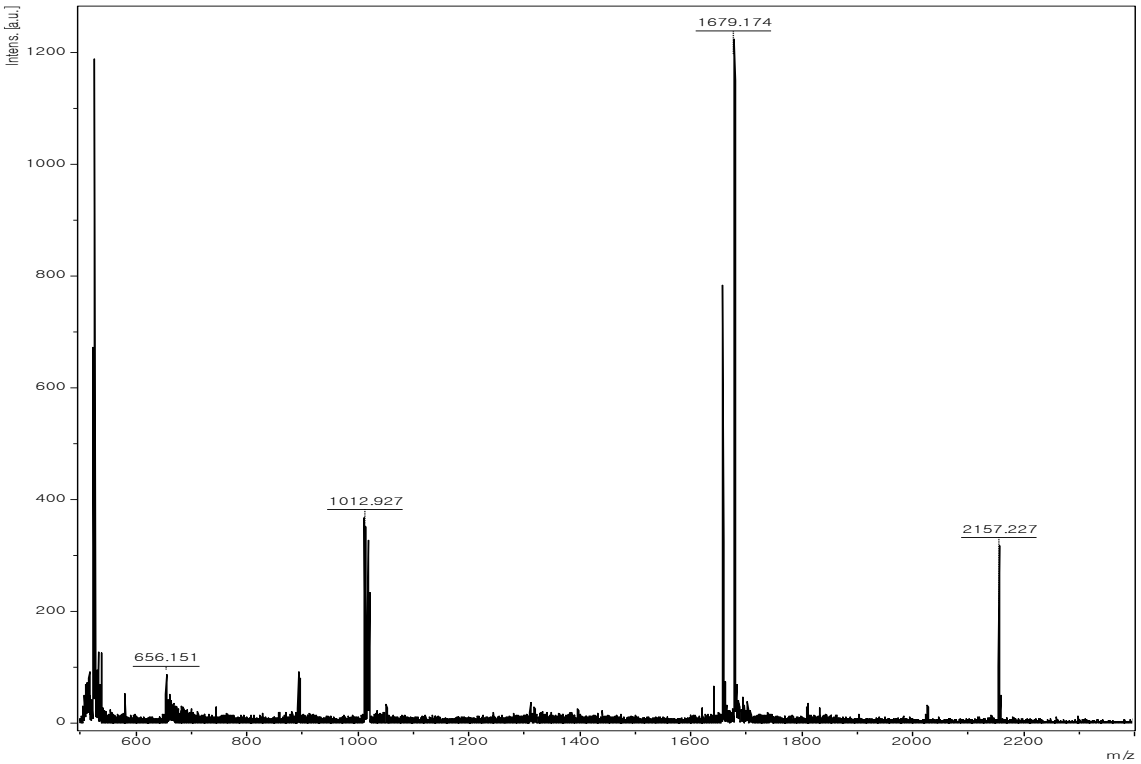

Figure 2. 9 MALDI-MS analysis of HKF_xr4H-Ir(Green). (M.W: 2,157 g/mol)

ULSAN NATIONAL INSTITUTE OF
SCIENCE AND TECHNOLOGY

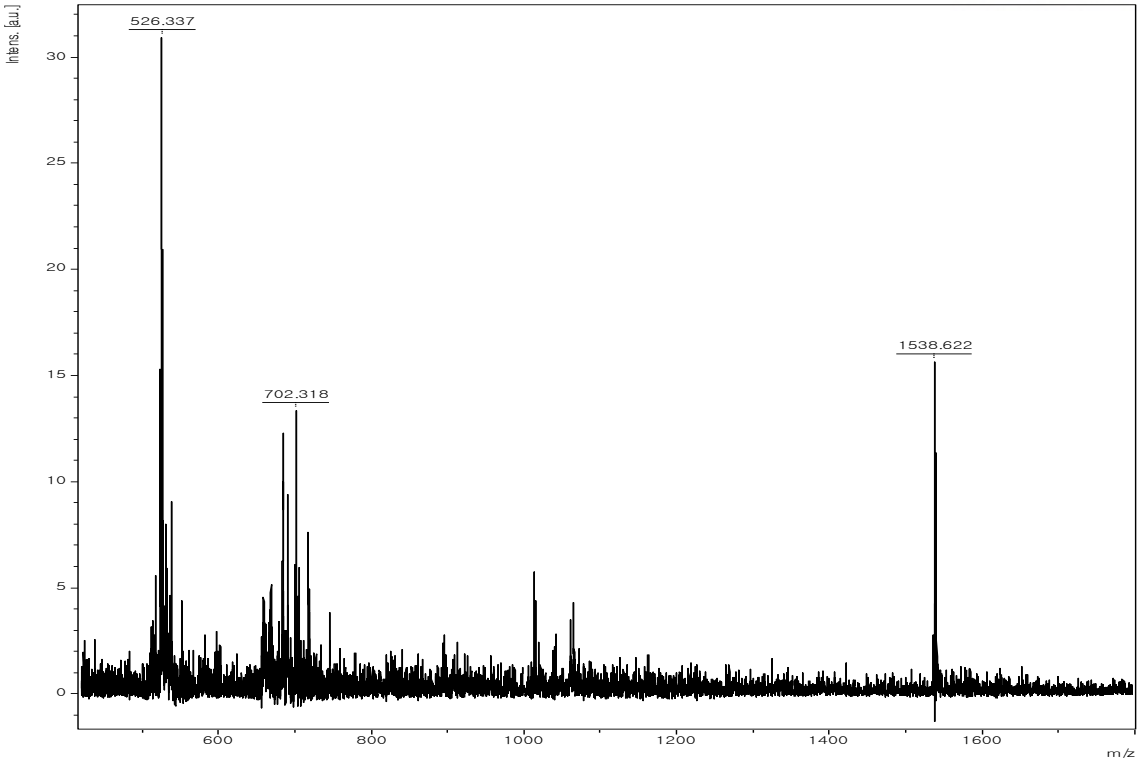

Figure 2. 10 MALDI-MS analysis of KF_xr2HH-Ir(Green). (M.W: 1,538 g/mol)

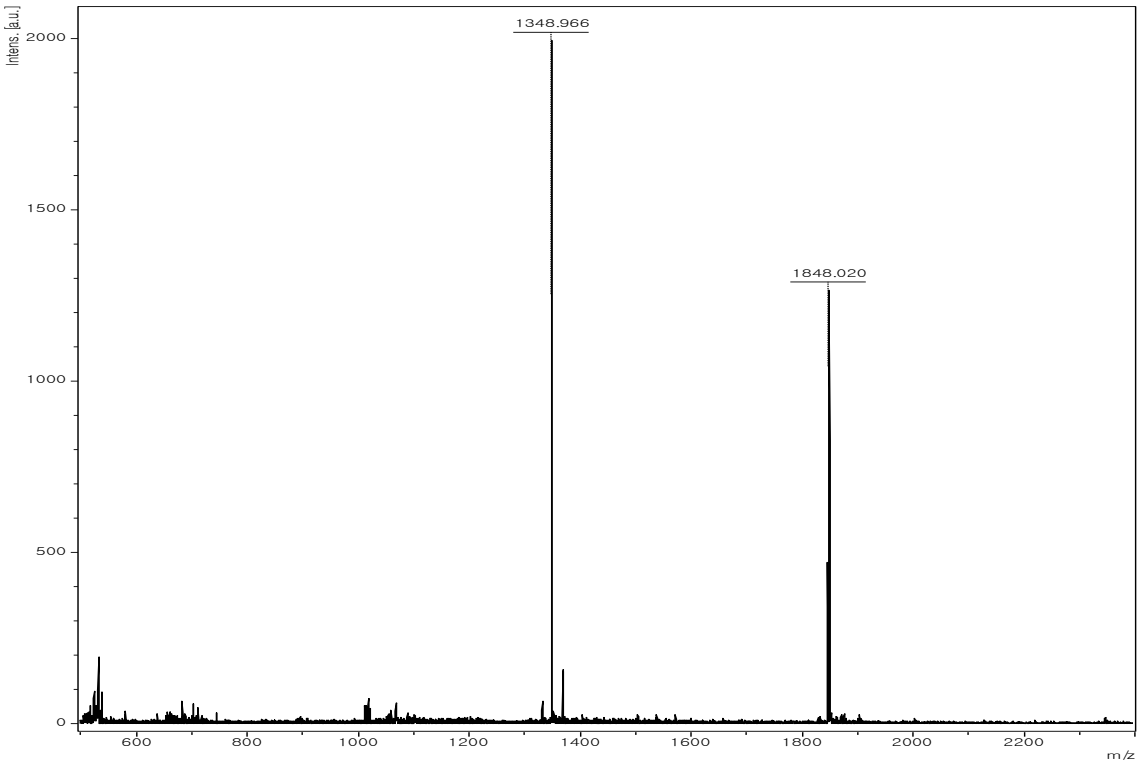

Figure 2. 11 MALDI-MS analysis of KF_xr3HH-Ir(Green). (M.W: 1,848g/mol)

ULSAN NATIONAL INSTITUTE OF
SCIENCE AND TECHNOLOGY

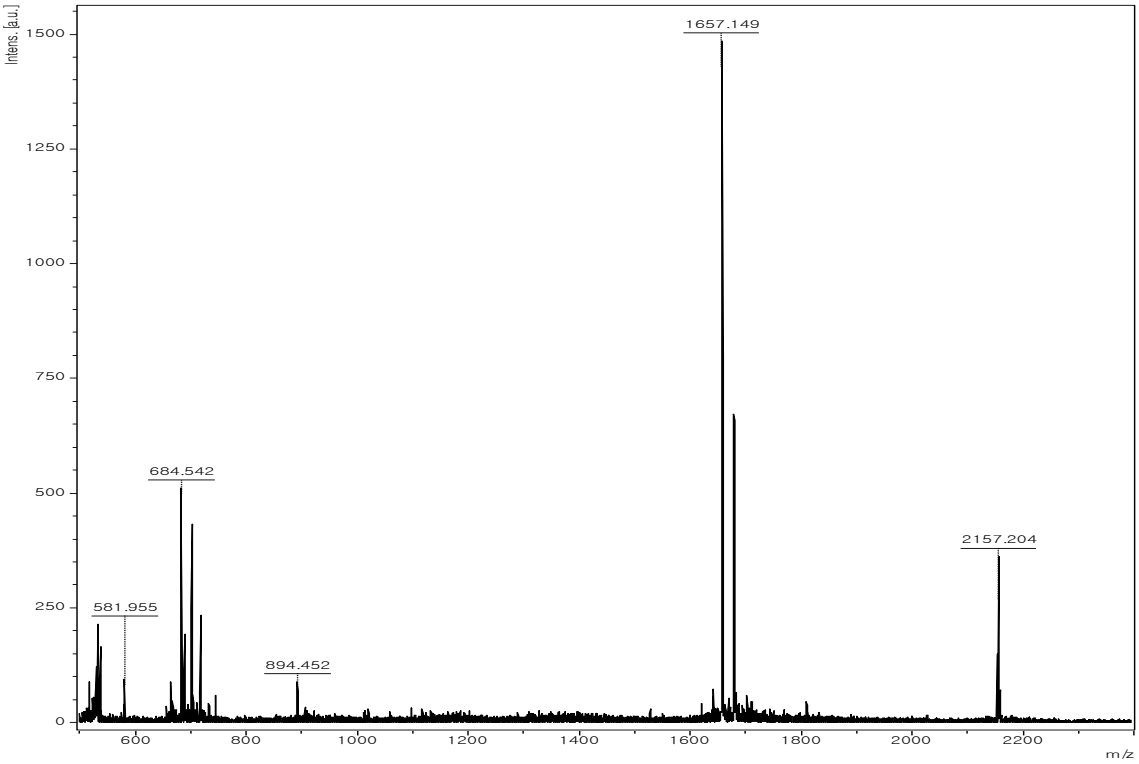

Figure 2. 12 MALDI-MS analysis of KF_xr4HH-Ir(Green). (M.W: 2,157 g/mol)

ULSAN NATIONAL INSTITUTE OF SCIENCE AND TECHNOLOGY

Optical properties of peptide binding Ir(III) complexes.

H_2O:DMSO = 99:1 (v/v%) condition was used to prepare each 20 μM solutions (20 μM Ir(III) complex + 20 μM peptide). Solvent that is used to make solution is degassed with N_2 gas bubbling. A 1 cm × 1 cm cell (Hellma) and 1 cm × 0.2 cm cell (Hellma) for absorbance and emission analysis was used to measure steady-state optical properties, respectively.

Each lifetime for peptide binding Ir(III) complexes was recorded with time-correlated single photon counting (TCSPC). Each sample was prepared as same with UV and PL solution ([Ir(III)] = 20 μM and [Peptide] = 20 μM). TCSPC consists of Ti:sapphire laser, Mira900 (Coherent Inc., CA, USA), monochromator, Acton series SP-2150i (Princeton Instruments, MA, USA), and TCSPC module, PicoHarp 300 (PicoQuant, Berlin, Germany) with a MCP-PMT, R3809U-59 (Hamamatsu Photonics, Japan). Excitation carried out with second harmonic generation (SHG = 420nm) with ~150 fs pulse width and 76 MHz repetition rate. The total instrument response function (IRF) for photon decay was less than 150 ps. The recorded results of phosphorescence lifetime decay for peptide binding Ir(III) complexes were fitted by FluoFit software.

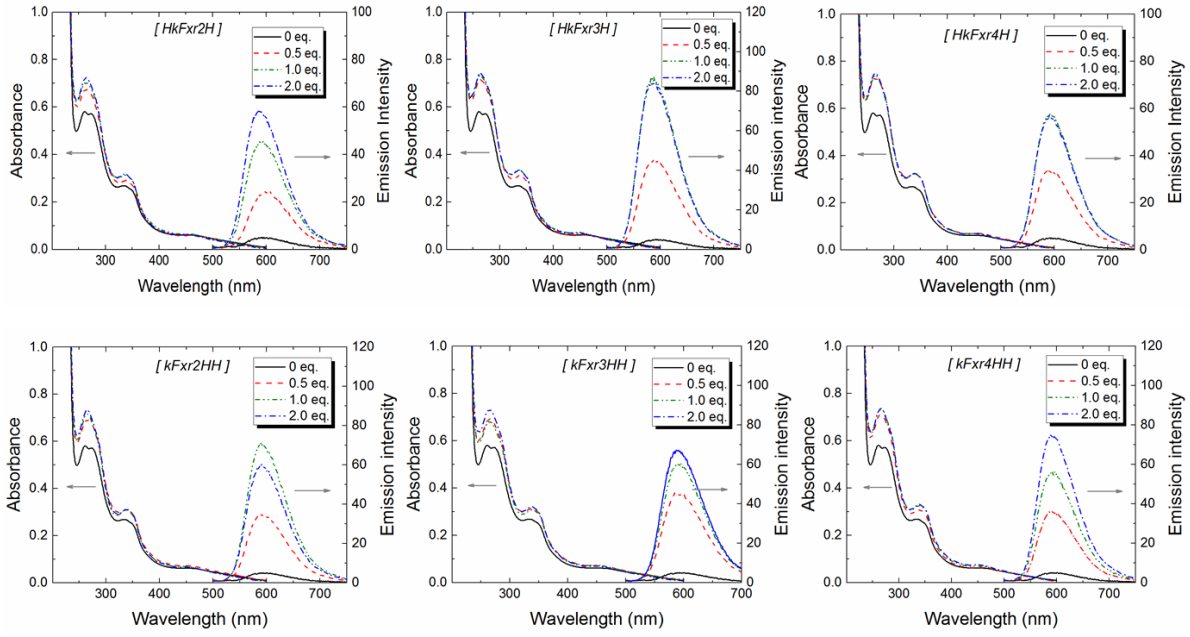

Figure 2. 13 Optical properties of peptide binding Ir(III) complex(Red). Upper images for cyclic peptide and bottom images for linear peptide. Absorbance: 451 nm, emission: 587 nm (DIW: DMSO= 99:1) (This data taken by co-worker, Jung Seung Nam)

ULSAN NATIONAL INSTITUTE OF
SCIENCE AND TECHNOLOGY

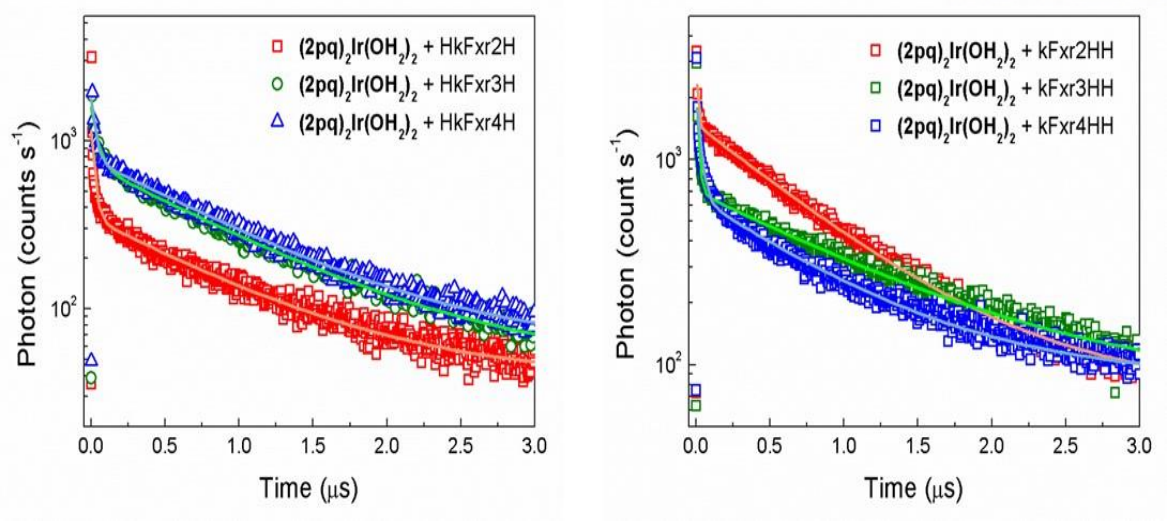

Figure 2. 14 Each lifetime for peptide binding Ir(III) complexes by recording with time-correlated single photon counting (TCSPC).

Table 2. 1 Quantification data of Each lifetime for peptide binding Ir(III) complexes by recording with time-correlated single photon counting (TCSPC). (This data taken by co-worker, Jung Seung Nam)

	HkFxr2H	HkFxr3H	HkFxr4H	kFxr2HH	kFxr3HH	kFxr4HH
t_1 (Peptide)	0.873 ms	0.918 ms	0.912 ms	0.741 ms	1.104 ms	0.829 ms
t_2 (Iridium)	22.1 ns	42.7 ns	27.0 ns	9.42 ns	15.9 ns	30.9 ns

ULSAN NATIONAL INSTITUTE OF SCIENCE AND TECHNOLOGY

Assays for singlet oxygen ($^1O_2$) and superoxide radical generation ($O_2^{\bullet-}$).

Singlet oxygen ($^1O_2$) generation was detected by chemical reaction between $^1O_2$ and 9,10-anthracenediyl-bis(methylene)dimalonic acid (ABDA). Standard ABDA absorbance was gradually declined, disconnecting conjugation of anthracene backbone of ABDA by $^1O_2$ (Scheme 1). Ir(III) complexes and peptide solution were prepared as 10 μM using their stock solution of 1 mM in DMSO and 10 mM in distilled water. ABDA stock solution was prepared as 100mM in DMSO and it was added in Ir(III) complexes solution as 1000:1 volume ratio. These solutions for each peptide-binded Ir(III) complexes were irradiated with solar simulator for which light intensity was about 40% of 100 mW cm^{-2} because ABDA could be decomposed by strong light source. The absorbance change of ABDA according to reaction with photo-activation induced $^1O_2$ was recorded at every 1 minute. Analysis time for absorbance change was up to 5 minutes.

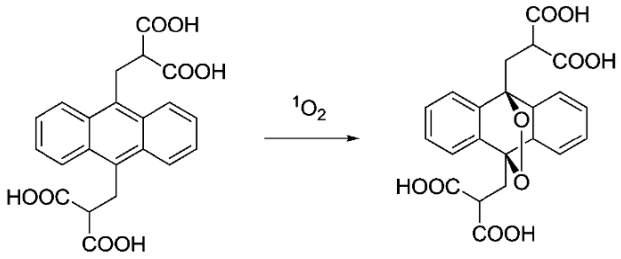

Scheme 2. 4 Breakage of conjugation backbone of ABDA through $^1O_2$ oxidation**.**

To figure out relative amount of superoxide radical ($O_2^{\bullet-}$) generation, furthermore, dihydrorhodamine 123 (DHR 123) was utilized (Scheme 2). Ir(III) complexes (**GREEN** and **RED**) and peptides were prepared as 10 μM:10 μM with same process in ABDA assay (vide supra) and DHR 123 dissolved in DMSO to become 10 mM stock solution. DHR 123 stock was diluted in prepared Ir(III) complex + peptide solution as 1000:1 (v/v). Each sample was loaded in 48-well plate with 1 mL. Light source from solar simulator irradiated the plate that contains each solution with 100 mW cm^{-1} intensity during 5 minutes. Emission intensity change was recorded with fluorometer (λ_{exc} = 505 nm, λ_{emis} = 529 nm).

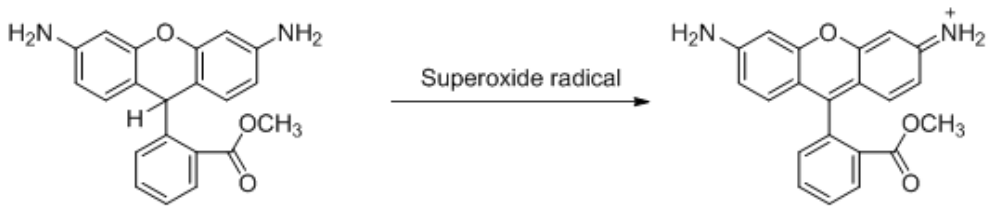

Scheme 2. 5 Formation of new conjugation of DHR 123 through oxidation by $O_2^{\bullet-}$

ULSAN NATIONAL INSTITUTE OF SCIENCE AND TECHNOLOGY

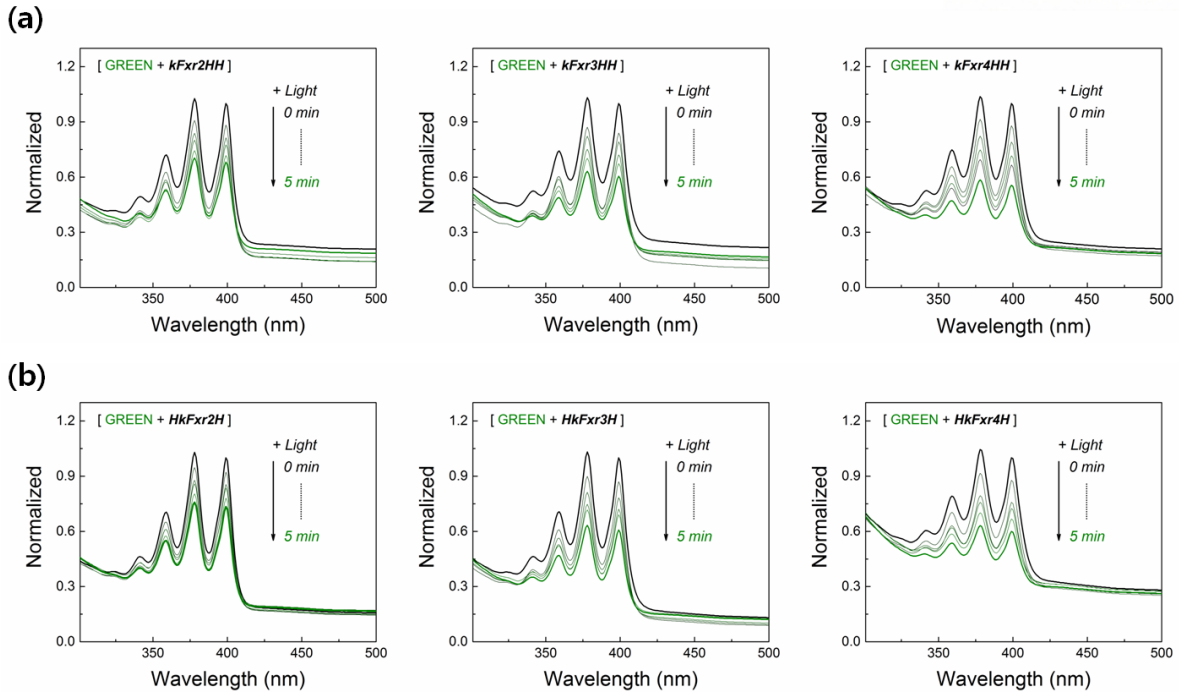

Figure 2. 15 Absorbance change of ABDA for GREEN + peptide complexes. It is correlated with the amount of $^1O_2$ generation by GREEN Ir(III) complex that incorporates either (a) cyclic or (b) linear peptide. (This data taken by co-worker, Jung Seung Nam)

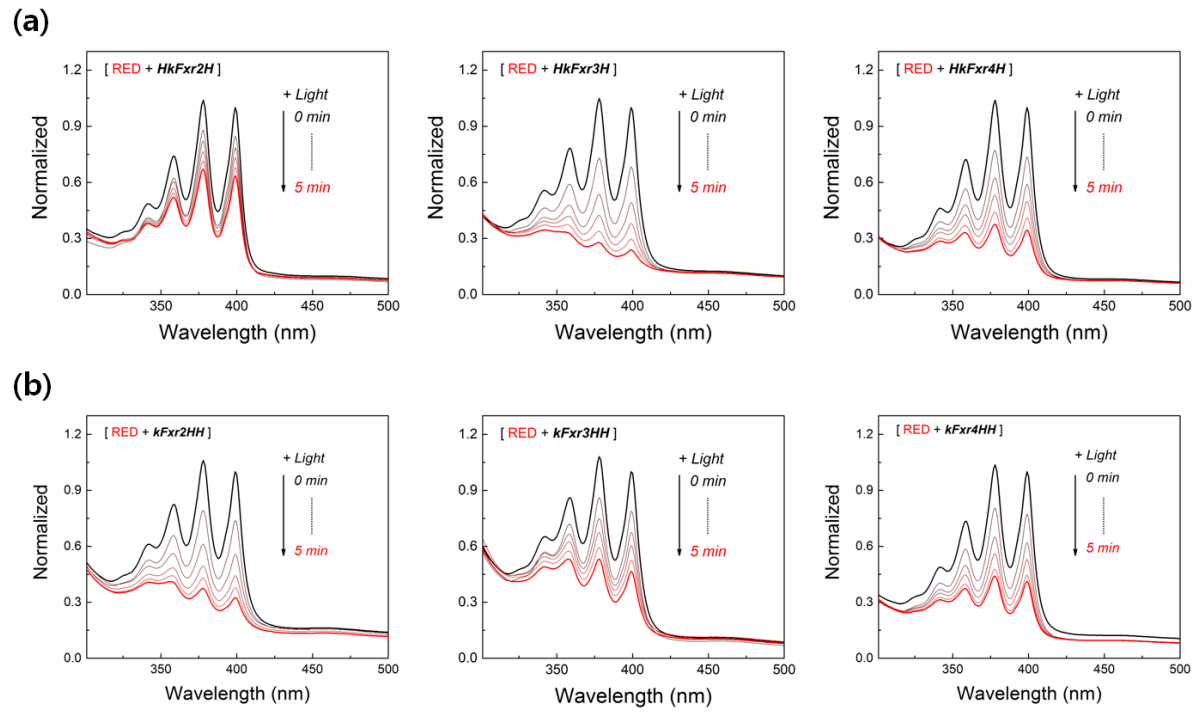

Figure 2. 16 Absorbance change of ABDA for RED + peptide complexes. It is correlated with the amount of $^1O_2$ generation by RED Ir(III) complex that incorporates either (a) cyclic or (b) linear peptides. (This data taken by co-worker, Jung Seung Nam)

ULSAN NATIONAL INSTITUTE OF SCIENCE AND TECHNOLOGY

Cell culture and cell viability analysis.

Human cancer cells originating from cervix (HeLa) and noncancerous fibroblast (HeK293T) cells were obtained and cultured in DMEM, L-15 or RPMI (Life Technologies) containing 10% fetal bovine serum (FBS; Life Technologies) and 1% penicillin/streptomycin (Life Technologies) at 37 ℃ in a humidified atmosphere of 10% CO2. For cytotoxicity analysis, cells were cultured in sterile 96-well Nunc (Thermo Fisher Scientific Inc.) microtiter plate at a seeding density of 5 x 103 cells/well and allowed to settle for 24 h under incubation at 37 ℃ and 5% CO_2 in their respective growth medium (RPMI 1640 and DMEM etc.). In order to check cell viability, the cells were then treated with different concentrations of peptides (0.01, 0.1, 0.5, 1, 2, 3, 5, 10, 15 and 20 μM). After 8h of incubation, stipulated time of light irradiation (3 min, 5 min and 10 min) was performed, Cell viability was measured at 24 h using the alamar blue assay, with each data point measured in triplicate. Fluorescence measurements were made using the plate reader (Tecan Infinite Series, Germany) by setting the excitation wavelength at 565 nm and monitoring emission at 590 nm on the 96 well plates.

Confocal microscope imaging

HELA cells were seeded in one well glass cover glass (Lab Tek II, Thermo Scientific) at a seeding density of 2 x 105 cells/well. In order to check cellular uptake of peptides, the cells were then treated with different concentrations of peptides at 5 μM for 1h. The cellular uptake was monitored periodically using Olympus FV1000 microscope connected to CO_2 incubator.

Flow-cytometry analysis.

HeLa cells were seeded on a 25 mL T-flask (Thermo Scientific) in DMEM (Life Technologies) supplemented with 10% FBS and 1% penicillin/streptomycin at 37 ℃ and 5% CO2. Then the cells were incubated with 10 μM of peptides for a period of 8h and irradiated in light for 5 min. Then the cells were harvested and washed in cold phosphate-buffered saline (PBS). By following the manufacturer's protocol (Life Technologies, V13241), were were incubated with 5 μL Alexa Fluor® 488 annexin V and 1 μL 100 μg/mL PI working solution in 100 μL of annexin-binding buffer solution for 15 min at room temperature. After the incubation period, 400 μL 1X annexin-binding buffer were added, mixed gently and keep the samples on ice. Immediately, analyze the stained cells by flow cytometry (FACS caliber, BD Bioscience), measuring the fluorescence emission at 530 nm (e.g., FL1) and >575 nm (e.g., FL3).

ULSAN NATIONAL INSTITUTE OF SCIENCE AND TECHNOLOGY

2.4 Results and Discussion

1) Characterization of Ir-HH cyclization of peptides of different conformation.

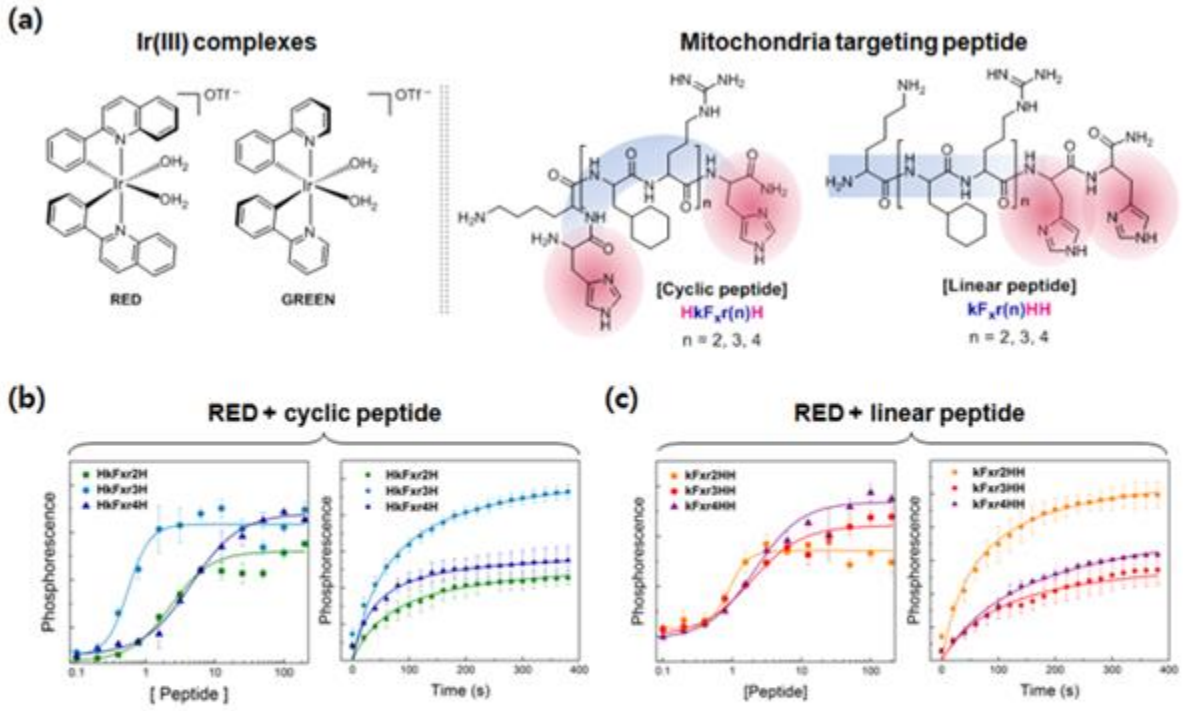

(d)

		HkFxr2H	HkFxr3H	HkFxr4H	kFxr2HH	kFxr3HH	kFxr4HH
RED	EC_{50}(μM)	2.278 ± 0.285	0.556 ± 0.079	4.541 ± 0.464	0.895 ± 0.075	1.875 ± 0.319	2.108 ± 0.154
	K_d(μM)	3.414 ±	0.197 ±	6.581 ±	0.705 ±	2.109 ±	2.599 ±

Figure 2. 17 Analyses for peptide binding with Ir(III) aquo complexes. (a) Molecular structure of Ir(III) aquo complexes and newly synthesized mitochondria targeting peptides. Hill's binding assay and kinetic observation of phosphorescence for RED complex with (b) cyclic or (c) linear peptides. (d) Specific values of EC_{50} and K_d. (This data taken by co-worker, Jung Seung Nam)

We first synthesized a series of model cyclic and linear peptides with increasing number of d-arginine (r) and cyclohexyl alanine (F_x) placed between lysine (K) and histidine (H)(cyclic: $HK(F_xr)_nH$, linear: $HK(F_xr)_nH$, n = 1,2,3)(Figure 2. 23a). These peptides all produced red phosphorescence after 2h of incubation with Ir(III) complex.

The binding affinity between Ir(III) complex and model peptides was determined by Hill's binding

ULSAN NATIONAL INSTITUTE OF SCIENCE AND TECHNOLOGY

assay. In the assay, reaction mixture were prepared with different peptide ratios when concentrations of Ir were fixed at 100 μM. As shown Figure 2. 17b-c, while cyclic peptides have a binding affinity enhancement depending on length of pendant group, linear peptides show no change of binding affinity because of fixed binding motion.

Moreover, we checked the kinetic observation of phosphorescence for red with time dependent (Figure 2. 17b-c). According to time duration, phosphorescence from peptide binding Ir(III) complexes was saturated. From this kinetic analysis, we can calculate k_{off} and k_{on} value from Michaelis-Menten equation based fitting process. This phosphorescence reaction allows a simple estimation of Ir(III)-peptide binding equilibriums (EC_{50}). In the series, cyclic HKF_xr3H exhibited strong binding to Ir(III) than all other peptides(Figure 2. 17d).

ULSAN NATIONAL INSTITUTE OF SCIENCE AND TECHNOLOGY

2) Primary subcellular localization of cyclic MPPs conjugates in living cells.

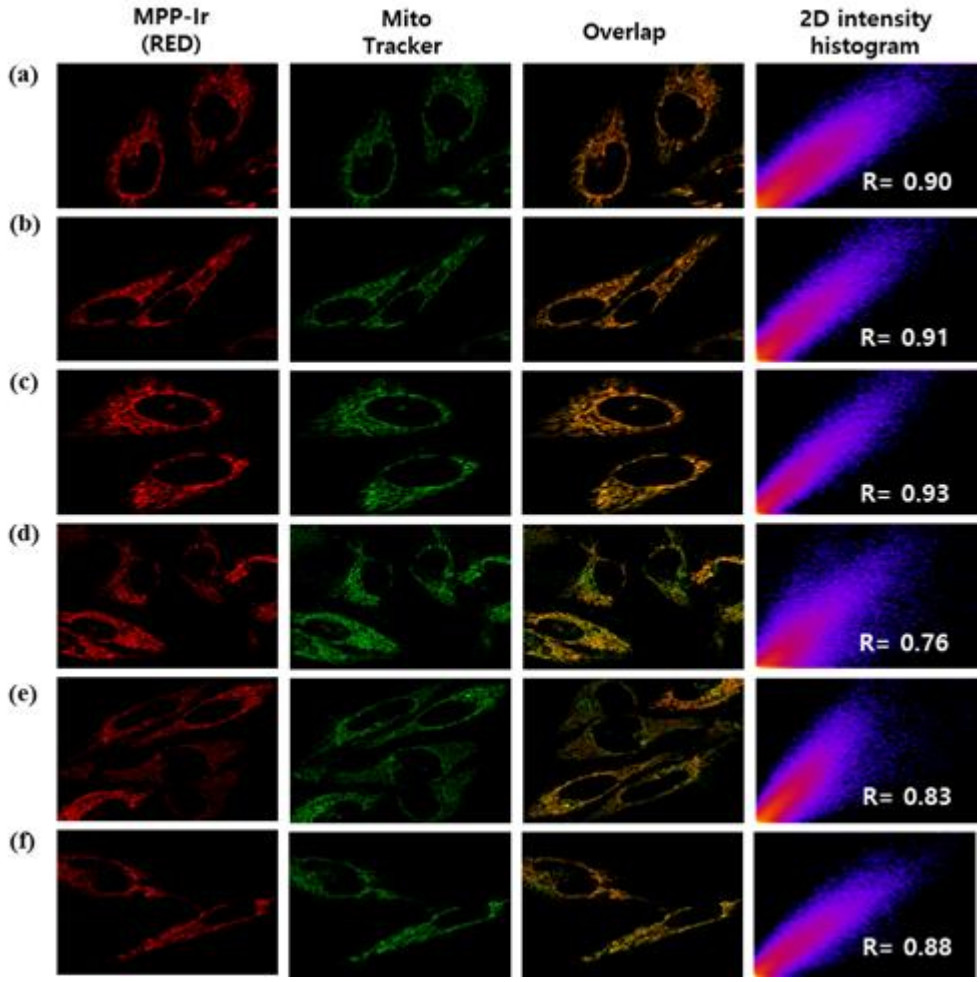

Figure 2. 18 Live-cell confocal microscope images of HeLA cells after incubation with Red-Ir complex (Em: 583 nm) conjugated peptides (linear & cyclic) for 1h. Co-localization analysis with mitotracker green FM (green pallet; Em: 454 nm). 2D histogram images to analyze the extent/significance of location between green pallet and red pallet. R – Pearson correlation value. Cyclic peptide-Ir(red) (upper) and linear peptide-Ir(red) (bottom). Concentration: 10 μM.

To determine the subcellular localization of Ir-peptides, we imaged Ir-peptides localized region in HeLa cell line. with two iridium (III) complexes, respectively. Totally 12 samples are prepared with different conformation (green emitted six samples, red emitted six samples). Cyclic peptides have been already study compare with linear peptides and cyclic peptide with CPPs have high level of cellular uptake more than linear one. Based on this knowledge, we hypothesized that our cyclic form compound also possess more efficient in cellular uptake than linear form one. We check the localization in mitochondria compared with cyclic and linear form model compounds through the

ULSAN NATIONAL INSTITUTE OF SCIENCE AND TECHNOLOGY

confocal microscopy. We treated all samples (10 μM) in the Live HeLA cells with incubation 1h. As shown in Figure 2. 18, we can observe that cyclic MPPs conjugates show higher cellular uptake than linear one. Green Ir-peptides also shows similar results (Figure 2. 19). This data suggest that cyclic MPPs-Ir (III) can be used as improving the cellular delivery.

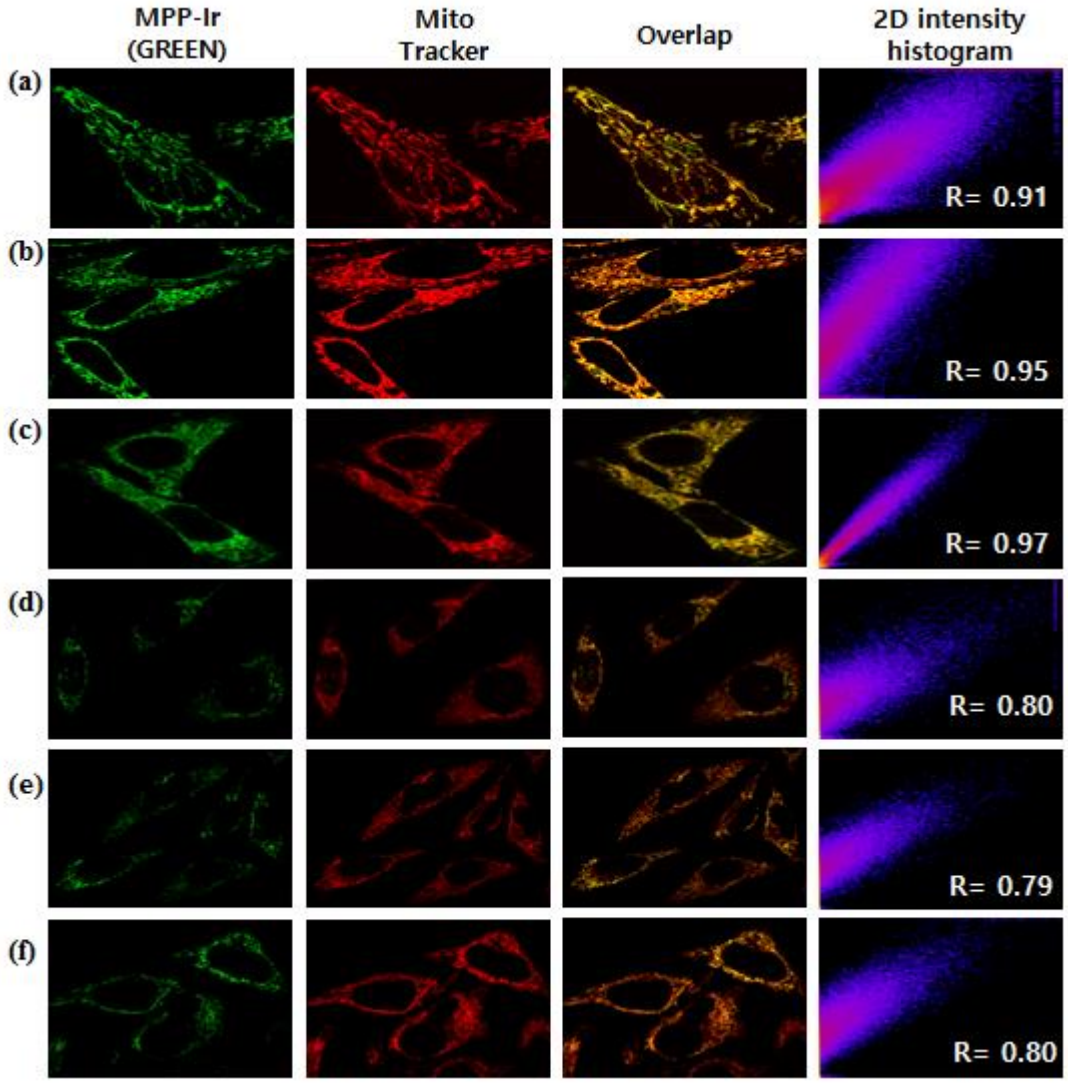

Figure 2. 19 Live-cell confocal microscope images of HeLA cells after incubation with Red-Ir complex (Em: 583 nm) conjugated peptides (linear & cyclic) for 1h. Cyclic peptide-Ir(RED): (a) HKFxr2H-Ir (b) HKFxr3H-Ir (c) HKFxr4H-Ir, Linear peptide-Ir(RED): (d) KFxr2HH-Ir (e) KFxr3HH-Ir (f) KFxr4HH-Ir. Co-localization analysis with mito tracker deep red FM. Green color (Em: 454 nm) and Red –mitotracker (Em: 555 nm). 2D histogram images to analyze the extent/significance of location between green pallet and red pallet. R – Pearson correlation value. Concentration : 10 μM.

ULSAN NATIONAL INSTITUTE OF
SCIENCE AND TECHNOLOGY

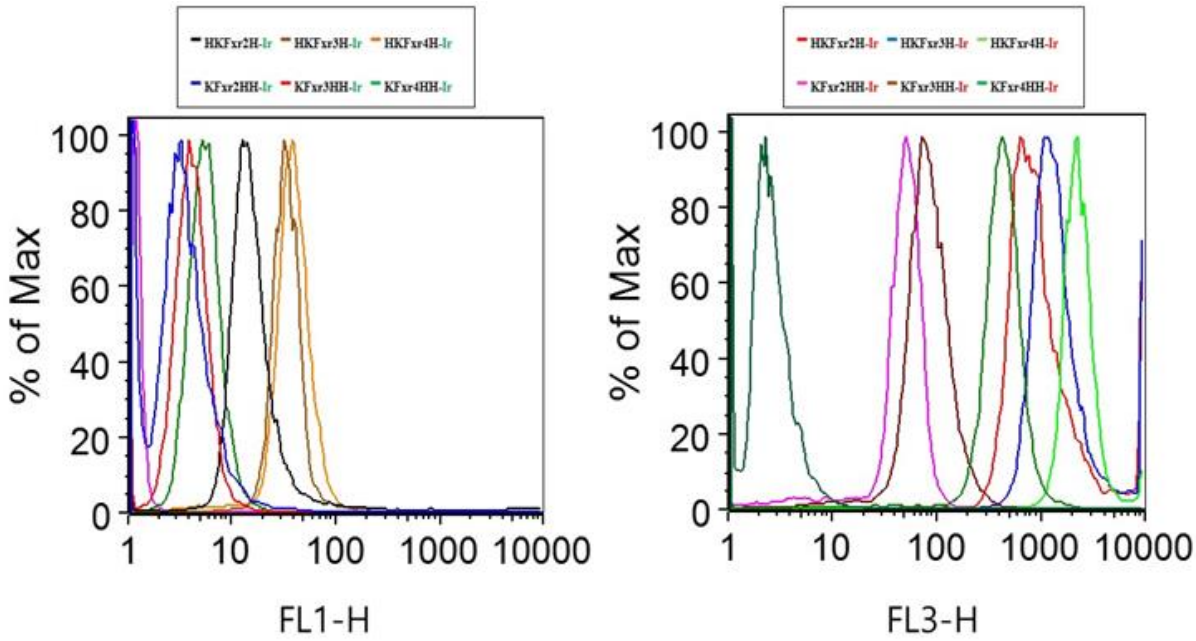

Figure 2. 20 FACS analysis to check the cellular uptake of a) Green Ir and b) Red Ir complex conjugated peptides in HeLA cells after 1h incubation. Concentration: 10 μM.

To check the cellular uptake of Green and Red Ir(II)complex conjugated peptide, we analyzed FACS data in HeLA cells after 1h incubation (Figure 2. 20). We can observe the cyclic peptide are more enter the cell than linear one with both iridium complex conjugates.

ULSAN NATIONAL INSTITUTE OF SCIENCE AND TECHNOLOGY

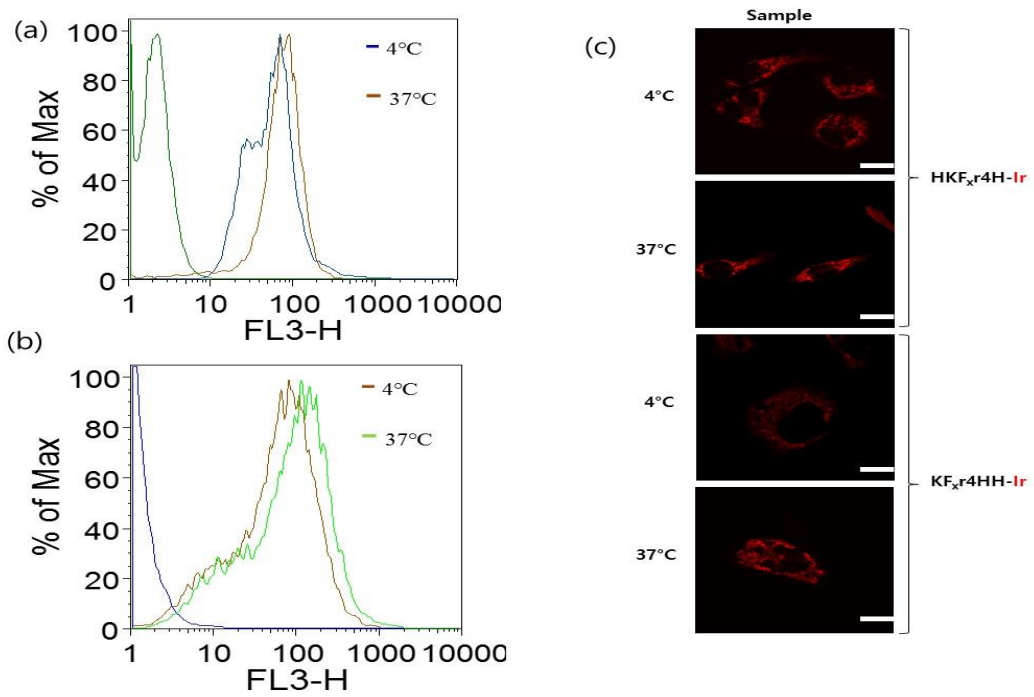

Figure 2. 21 a,b) Flow cytometry analysis to measure the energy independent uptake mechanism in HeLA for cyclic(a) and linear(b) Red Ir peptides after 1h incubation at 37C and 4C. C) Live cell confocal microscope images of HeLA cells after 1h incubation with Red Ir complex conjugated linear(bottom) and cyclic peptides(upper) (Em: 583 nm). Scale bar in 10 μM and 5 μM.

Moreover, we check whether the mechanism of cellular uptake is energy dependent or independent. As a results, these peptides are energy independent process (Figure 2. 21).

ULSAN NATIONAL INSTITUTE OF SCIENCE AND TECHNOLOGY

3) Ir(III)-MPPs as Photodynamic therapy (PDT) Agents.

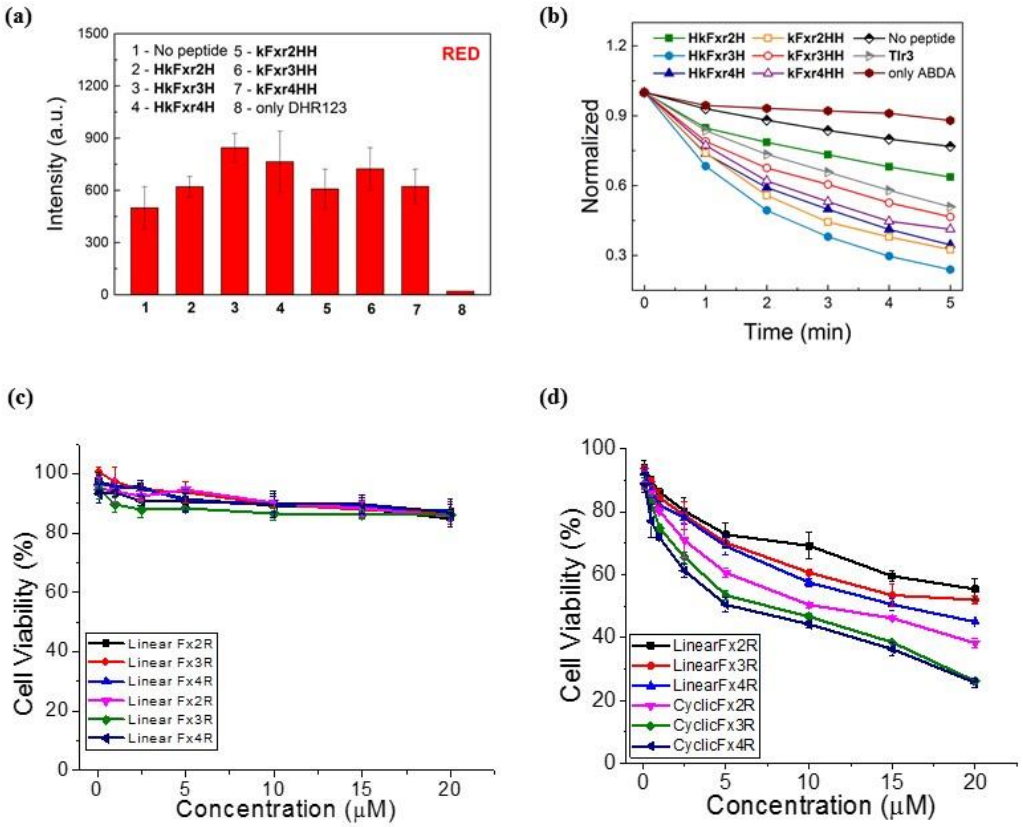

Figure 2. 22 Photodynamic therapy experiment for red iridium complex conjugated peptide. a-b) Estimation of two reactive oxygen species (superoxide radical and $^1O_2$) generation with dihydrorhodamine 123 (DHR 123) or 9, 10-anthracenediyl-bis(methylene)dimalonic acid (ABDA) before/after peptide binding. DHR 123 (left, bar graph) and ABDA assay (right, decay line) with RED. c-d) Cell viability analysis for Ir complex conjugated peptides upon the irradiation (right) and without irradiation(left). Concentration: 10 μM. 100 mW cm^{-2} light; irradiation time = 300 s. (ABDA, DHR data taken by co-worker, Jung Seung Nam)

The ROS generation ability of Ir(III) complexes according to their energy levels was identified by two different analyses: triplet state quenching by O_2, 9,10-anthracenediylbis(methylene) malonic acid (ABDA) assay for $^1O_2$ generation, and dihydrorhodamine (DHR) 123 assay for superoxide radical ($O_2^{\bullet-}$) generation. Triplet state quenching of Ir(III) complexes by O_2 bubbling relates to the amount of formed ROS, because it strongly depends on $^1O_2$ generation and charge transfer interactions from Ir(III) complexes to O_2, resulting in oxygen radical formation. The quenching rate order is HkF_xr3H > HkF_xr4H > HkF_xr2H, suggesting that HkF_xr3H is the best photoactivatable ROS generator for PDT in

ULSAN NATIONAL INSTITUTE OF SCIENCE AND TECHNOLOGY

our system (Figure 2. 22b). In contrast, green iridium complex conjugates produce the little amount of singlet oxygen (Figure 2. 23b). In the DHR 123 assay, the relative rates for $O_2^{\bullet-}$ production are in order of HkF_xr3H > HkF_xr4H > kF_xr3HH > HkF_xr2H = kF_xr2HH= kF_xr4HH> Ir(III) complex(red). Basically, DHR 123 activation ability was shown better in RED complexes than in Green complexes. (Figure 2. 22a, 23a).

Next, we conduct cell-viability with and without irradiation. While we can see the high level of cytotoxicity (20~60%) under irradiation (time: 300s), in the dark site, we don't observe the cytotoxicity (Fig. 2. 22 c-d). This cyclic modified complex exhibited an improved PDT effect compared to linear one. This results suggest that cyclized Ir(III) have a higher potential of mitochondria-targeted PDT agents in cancer therapy. In case of green ir complexes, they don't show photoinduced toxicity effect (Figure 2. 23).

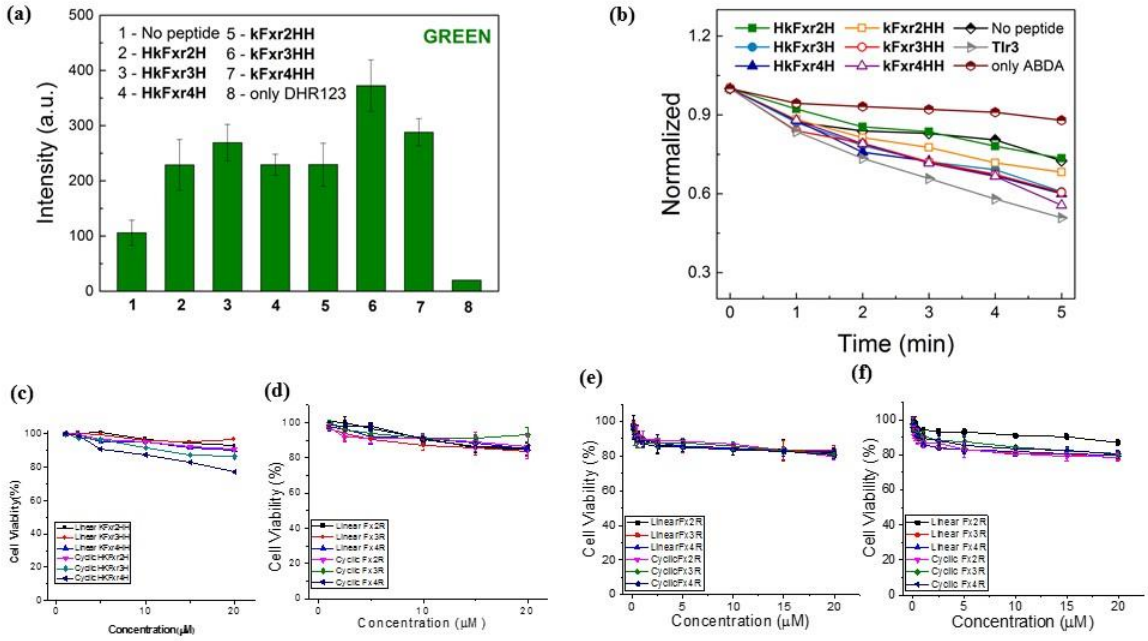

Figure 2. 23 Photodynamic therapy experiment for Green iridium complex . (a-b) Identification of two reactive oxygen species (superoxide radical and $^1O_2$) generation with dihydrorhodamine 123 (DHR 123) or 9, 10-anthracenediyl-bis(methylene)dimalonic acid (ABDA) before/after peptide binding. DHR 123 (left, bar graph) and ABDA assay (right, decay line) with Green. (c-f) Cellviability of Modified peptides with Green emitted iridium complex with(right) and without irradiation(left). Concentration: 10 μM. 100 mW cm^{-2} light; incubation time: 24h , irradiation time = 0(c), 60(d), 300(e), 600s(f). (ABDA, DHR data taken by co-worker, Jung Seung Nam)

ULSAN NATIONAL INSTITUTE OF
SCIENCE AND TECHNOLOGY

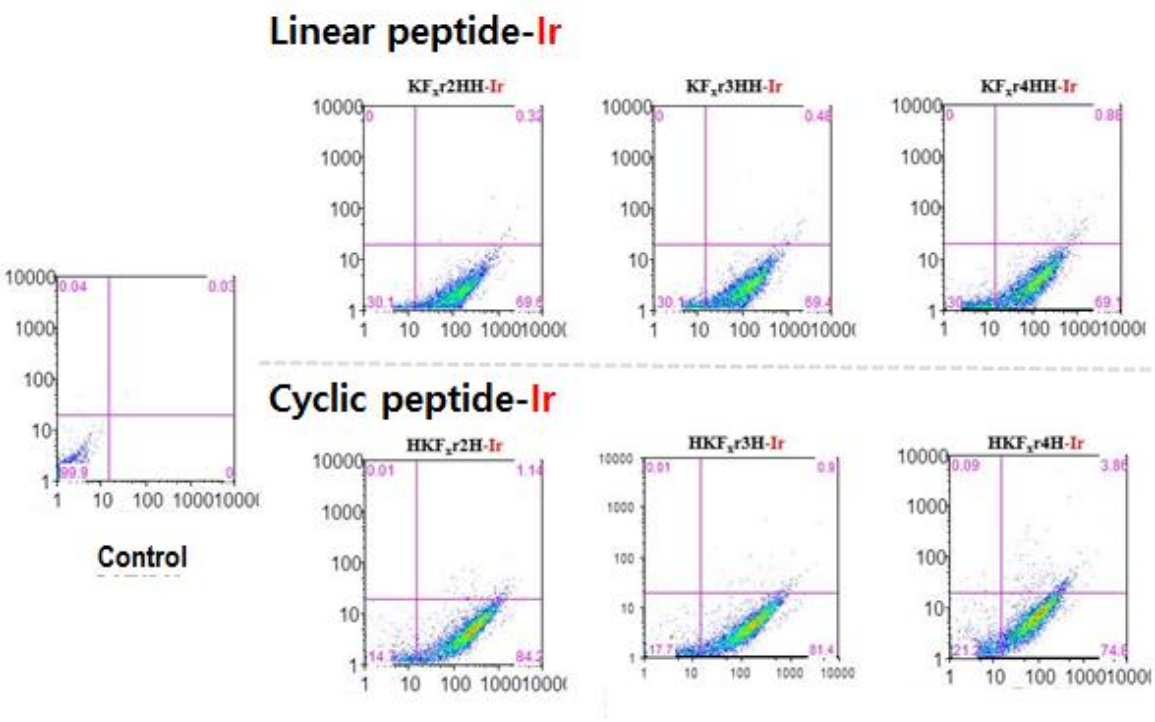

Figure 2. 23 Flow-cytometry analysis to measure the extend of apoptosis mediated cell death in linear & cyclic Red Ir complex conjugated peptides in HeLA cells after 8h incubation and irradiation with light (300s), analyzed by annexin-V-FITC (FL1-H) and propidium iodide (FL3-H) staining assay. 10,000 events were counted to measure extend of apoptosis. Concentration: 20 μM.

The cell death induced by the photo-excited cyclic and linear complexes was further investigated using annexin V/PI apoptosis assays. After treated HeLa cells with modified red one (10 μM) for 1h, sample exposed to irradiation for 5min then incubated for 12 h. As shown in Fig. 2.23, there was an increase in the percentages of cells in early apoptotic phase. While linear modified complexes showed similar percentage (69.1-69.6) of early apoptosis phase, cyclized complexes significantly rose to 84.2% (74.6-84.2) in early apoptosis part. The ability of this model cyclic complexes to induce apoptosis was more efficient their antitumor activity.

ULSAN NATIONAL INSTITUTE OF
SCIENCE AND TECHNOLOGY

2.5 Conclusion

In conclusion, we developed the simple, but, robust and efficient Photodynamic agents for cancer cells using cyclic corporation with selectivity in mitochondria. We design two type of iridium (III) complexes (Green and red emission region). Two complexes exhibited high level of photo physical properties. However, Green emitted iridium (III) complex shows only bioimaging ability. In contract, Red emitted iridium (III) complex shows non-invasive image with NIR region and photo-induced toxicity. By introducing cyclic MPPs to iridium (III) complexes, they enhance the selectivity to mitochondria, cellular uptake, and biocompatibility (soluble in water). Notably, cyclic form iridium (III) complexes were primarily localized in the mitochondria rather than liner form one. Finally, theses coordinated complexes generate ROS under irradiation, indeed, leading to apoptosis. Consequently, we think that this work is meaningful for designing and developing high effective organelle-targeted PDT agents, which has great potential in biomedical fields.

ULSAN NATIONAL INSTITUTE OF SCIENCE AND TECHNOLOGY

2.6 References

1. Mari, C.; Pierroz,V.; Ferrari, S.; Gasser, G. *Chem. Sci*. **2015**, 6, 2660-2686.

2. Yuan, Y.; Kwok, R. T.; Tang , B.Z.; Liu, B. *J Am Chem Soc*. **2014**, 136, 2546e54.

3. Moan, J.; Peng, Q. *Anticancer Res*. **2003**, 23, 3591.

4. Fingar, V. H.; Wieman, T. J.; and Haydon, P. S. *Photochem*. *Photobiol*. **1997**, 66, 513–517.

5. Henderson, B. W.; Fingar, V. H. *Photochem. Photobiol*. 49, 299–304.

6. Gomer, C. J.; Razum, N. J. *Photochem. Photobiol*. **1984**, 40, 435.

7. Triesscheijn, M.; Baas, P.; Schellens, J. H. M.; Stewart, F. A. *Oncologist*. **2006**, 11, 1034.

8. Gollnick, S. O.; Liu, X. N.; Owczarczak, B.; Musser, D. A.; Henderson, B. W. *Cancer Res*. **1997**, 57, 3904.

9. Zhang, S.; Yoshihara, M. T.; Negishi, K.; Iida, Y.; Tobita, S.; Takeuchi, T. *Cancer Res*. **2010**, 70, 4490–4498.

10. Yoshihara, T.; Yamaguchi, Y.; Hosaka, M.; Takeuchi, T.; Tobita, S. *Angew. Chem. Int. Ed*. **2012**, 51, 4148–4151.

11. Lo, K. K. W.; Zhang, K. Y. *RSC Adv*. **2012**, 2, 12069e83.

12. You, Y. *Curr Opin Chem Biol*. **2013**, 17, 699e707.

13. Zhao, Q.; Huang, C.; Li, F. *Chem Soc Rev*. **2011**, 40, 2508e24.

14. You, Y.; Han, Y.; Lee, Y. M.; Park, S. Y.; Nam, W.; Lippard, S. J. *J Am Chem Soc*. **2011**, 133, 11488e91.

15. Frankel, A. D.; Pabo, C. O. *Cell*. **1988**, 55, 1189–1193.

ULSAN NATIONAL INSTITUTE OF SCIENCE AND TECHNOLOGY

16. Green, M.; Loewenstein, P. M. *Cell*. **1988**, 55, 1179–1188.

17. Yousif, L. F.; Stewart, K. M.; Horton, K. L.; Kelley, S. O. *ChemBioChem*. **2009**, 10, 2081–2088.

18. Goun, E. A.; Pillow, T. H.; Jones, L. R.; Rothbard, J. B.; and Wender, P. A. *ChemBioChem*. **2006**, 7, 1497–1515.

19. Gisela, L. T.; Manuel, P.; Daniel, H.; Joachim, B.; Caroline P. A.; Ingo, M.; Henry, D.; Herce, M.; Cristina, C. *Nature Communications*. **2011**, 10, 1038

20. Li, Y.; Tan, C. P.; Zhang, W.; He, L.; Ji, L. N.; Mao, Z. W. *Biomaterials*. **2015**, 39, 95-104.

21. Mandal, S.; Poria, D. K.; Ghosh, R.; Ray, P. S.; and Gupta, P. *Dalton Trans*. **2014**, 43, 17463.

22. Wang, X.; Jia, J.; Huang, Z.; Zhou, M.; Fei, H. *Chem.-Eur. J*. **2011**, 17, 8.

23. Ma, D. L.; Wong, W. L.; Chung, W. H.; Chan, F. Y.; So, P. K.; Lai, T. S.; Zhou, Z. Y.; Leung, Y. C.; Wong, K. Y. *Angew. Chem. Int. Ed*. **2008**, 47, 3735.

24. Ma, X.; Jia, J.; Cao, R.; Wang, X.; and Fei H. *J. Am. Chem. Soc*. **2014**, 136, 17734−17737

25. Bradley Y. W.; M. et al. Group. *Chem. Sci*. **2011**, 2, 917.

26. Nonoyama, M. *Bull. Chem. Soc. Jpn*. **1974**, 47, 767.

ULSAN NATIONAL INSTITUTE OF SCIENCE AND TECHNOLOGY

3. pH-resoponsive Mitochondria Penetrating Peptide with PU-H71 derivatives for efficient anticancer therapy

3.1 Abstract

Stimuli responsive degradation of chemical bonds are useful tools for the development of 'smart materials' which have remarkable applications in stimuli responsive drug delivery system. The pH is commonly applied to the cancer specific drug delivery system, because the pH near the tumor or in the tumor extracellular environment significantly acidic as pH 6-6.5 while the normal physiological pH is around 7.4**.** In this study, we designed and developed mitochondria targeting short peptide with charge conversion depending on pH values. The peptide sequences consists of F_xrF_xKK, possess positive charge and lipophilic character for targeting mitochondria. We conjugated drug (PU-10-ester) as an inhibitor of HSP90 and Maleic derivatives which are play a role of hydrolyzed in MPPs. Once maleic conjugated MPP extravagates into cell membrane through highly permeability, amide bonds within conjugate occur hydrolysis, reproducing intrinsic properties of MPP in the acidic tumor extracellular fluids (pH < 7) for efficient cellular uptake and mitochondria targeting. Moreover, this platforms shows anticancer effect with 40% at 25 μM concentration. Therefore, we hope that this model conjugated peptides have a potent of cancer therapy agent.

3.2 Introduction

Stimuli responsive degradation of chemical bonds are useful tools for the development of 'smart materials' which have remarkable applications in stimuli responsive drug delivery system [1]. Among the various stimuli such as temperature, enzymes, pH etc., the pH is commonly applied to the cancer specific drug delivery system, because the pH near the tumor or in the tumor extracellular environment significantly acidic as pH 6-6.5 while the normal physiological pH is around 7.4 [2]. Moreover the pH of the endosome or lysosomes are even lower (pH 5.0-5.5) [3]. For example, Nano carriers that exhibit charge conversion with the pH-induced cleavage of the amide bond between an amin and 2,3-dimethylmaleic anhydride have been designed [4].

ULSAN NATIONAL INSTITUTE OF SCIENCE AND TECHNOLOGY

Cell-penetrating peptides (CPPs) including mitochondria penetrating peptides (MPPs) are highly cationic peptides usually rich in arginine and lysine amino acids, which have ability to relocate quickly into any live cells. Unfortunately, since they have their inherent non specificity caused by their cationic nature, many in vivo uses are limited. To suppress their nonspecific interaction, the cationic charges of CPPs are masked with poly anions [5]. For example, a CPP was conjugated with an anionic peptide via a cleavable linker in order to shield its nonspecific interactions. Once in the target tissues, hydrolysis of the linker used the disassociation of amide bonds, regenerating the CPP's functions.

The functional groups such as acetal, orthoester, imine, and phosphoramidate etc have ability to degrade under acidic pH (< 6.5) [6-9]. Recently, Maleic acid amide derivatives have been used as candidates of pH-sensitive moiety. They undergo cleavage in the acidic pH, due to the internal reaction of amide carbonyl group by the carboxylate, inducing change of chemical structure of maleic acid amide [10-11]. Upon the pH induced degradation, the negatively charged MA-MPP changes to positively charged MPP and hence facilitate the cellular uptake. This negative-to-positive charge conversion in maleic acid amide derivatives have been modified in order to increase the negative charge density of lipids and polymers for the effective pH-triggered drug delivery. By utilizing pH responsive system, pH-sensitive nanocarriers have been developed for tumor targeted drug delivery. Among them, Mitochondria penetrating peptides (MPPs) provide superior and potent properties; 1) almost MPPs contain lysine residues which can make β-carboxylic amides at neutral pH and quickly hydrolyze at acidic pH to reproduce the corresponding amines. 2) MPPs are CPPs, can enter both the plasma and mitochondrial membranes. So they can be ability to target mitochondria effectively. 3) MPPs can be easily to conjugate organic compound such as anticancer drugs and imaging dye with solubility in water (biocompatible). These strength of MPPs would enhance to selectively pH-triggered drug delivery.

In this study, we designed and developed mitochondria targeting short peptide with charge conversion depending on pH values. The peptide sequences consists of F_xrF_xKK, possess positive charge and lipophilic character for targeting mitochondria. We conjugated drug (PU-10-COOH) as an inhibitor of HSP90 and Maleic derivatives which are play a role of hydrolyzed in MPPs. Once maleic conjugated MPP extravagates into cell membrane through highly permeability, these amides are hydrolyzed, regenerating the pristine functioning MPP in the acidic tumor extracellular fluids (pH < 7) for fast cellular uptake and mitochondria targeting (Scheme 3.1). Moreover, this platforms shows anticancer effect with 40% at 25 μM concentration. Therefore, we hope that this model conjugated peptides have a potent of cancer therapy agent.

ULSAN NATIONAL INSTITUTE OF SCIENCE AND TECHNOLOGY

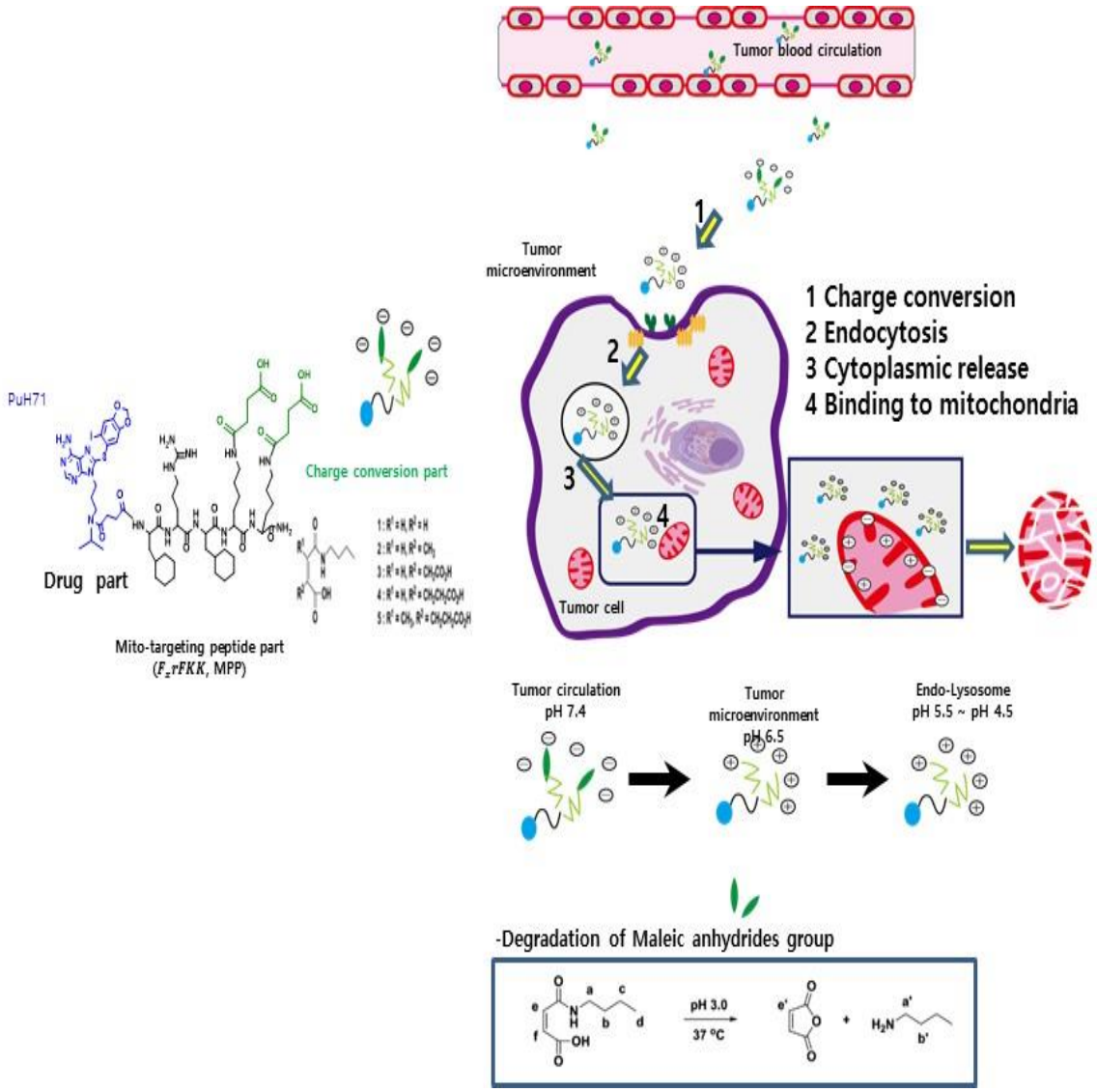

Scheme 3. 1 Schematic representation of charge conversion MPP

ULSAN NATIONAL INSTITUTE OF SCIENCE AND TECHNOLOGY

3 .3 Experimental

3.3.1 Materials and Methods

All reagents and chemicals were purchased from commercial sources and used as received. Amino acids (Fmoc-Lys(Boc)-OH, Fmoc-Phe-OH, Fmoc-d-arg(Boc)-OH, Fmoc-Cha-OH) and rink amide MBHA resin were obtained from BeadTech (Korea) and ApexBio (USA), Coupling reagent(*O*-benzotriazole-*N,N,N',N'*-tetramethyluronium hexafluorophosphate, HBTU) was obtained from ApexBio (USA). *N*,*N*-diisopropylethylamine(DIPEA) and trifluoroacetic acid (TFA) were purchased from TCI (Japan). Triisopropylsilane and piperidine were obtained from Sigma-Aldrich (USA). *N*,*N*-dimethylformamide(DMF), Methanol and Acetonitrile (ACN) HPLC grade was purchased from DAEJUNG(South Korea).Dimethyl sulfoxide (DMSO) HPLC grade was from Fischer chemical (USA). Molecular sieves 4A, 4-8mesh and Magnesium sulfate ($MgSO_4$) obtained from SAMCHUN CHEMICALS (South Korea). 4-Dimethylaminopyridine (DMAP) were purchased from GL Biochem Ltd (Shanghai, China), 12N Hydrochloric acid (HCl) was obtained from OCI Company Ltd (Korea). Methyl 10-hydroxydecanoate and Pyrene-butylic acid were obtained from Sigma-Aldrich (USA). Succinic anhydride, Maleic anhydride, Dimethyl maleic anhydride, Citraconic anhydride and Cis-aconitic anhydride were obtained from Sigma-Aldrich (USA). Ethyl acetate (EtOAc) and DCM were obtained from SK Chemical (Korea). F_xrFKK peptide, Pyrene-F_xrFKK, F_xrFKK-PUH71 and F_xrFKK -10-PU prodrug were characterized using MALDI-TOF. PUH71 and PU-10-ether derivatives were characterized using 400MHz FT-NMR (Agilent Technologies).

3.3.2 Synthesis of peptide (F_xrF_XKK)

Solid phase peptide synthesis (SPPS) was performed by an automated peptide synthesizer. 200 mg of resin was swollen in DMF solution. After 30 min, operate machine to synthesize peptide. Peptide scale is 0.1mM. Amino acid solution was prepared by dissolving Fmoc-Lys(Boc)-OH 0.2821 g in 6 mL DMF, Fmoc-d-arg(Boc)-OH 0.195 g in 3 mL DMF, And Fmoc-Cha-OH 0.117 g in 3 mL DMF. Fmoc deprotection of the Fmoc- amino acids was performed by adding 20% piperidine solution in DMF. HBTU and DIPEA act as coupling reagent and base. After finishing final deprotection of Fmoc protecting group, make cleavage cocktail (TFA: triisopropylsilane: Water = 4.75 mL : 0.25 mL: 0.25 mL). Add cleavage cocktail into resin with stirring for 4 hours at room temperature. Then, precipitate with cold diethyl ether. The peptide is purified through HPLC using water/Acetonitrile.

ULSAN NATIONAL INSTITUTE OF SCIENCE AND TECHNOLOGY

3.3.3 Synthesis of pyrene-F_xrF_xKK

Pyrene- F_xrF_XKK were obtain from manual synthesis. pyrene-butylic acid(200 mg,1eq), F_xrF_xKK peptide(200 mg,1 eq), DIPEA(300 μL,3 eq), and HBTU(298 mg,3 eq) in DMF 1 mL put in the 25 mL RBF and rotate for 24h. After 24h, deprotection of the Fmoc- amino acids was performed by adding 20% piperidine solution in DMF. HBTU and DIEA act as coupling reagent and base. After finishing final deprotection of Fmoc protecting group, make cleavage cocktail (TFA: triisopropylsilane: Water = 4.75 mL: 0.25 mL: 0.25 mL). Add cleavage cocktail into resin with stirring for 4 hours at room temperature. Then, precipitate with cold diethyl ether. The peptide is purified through HPLC using water/Acetonitrile.

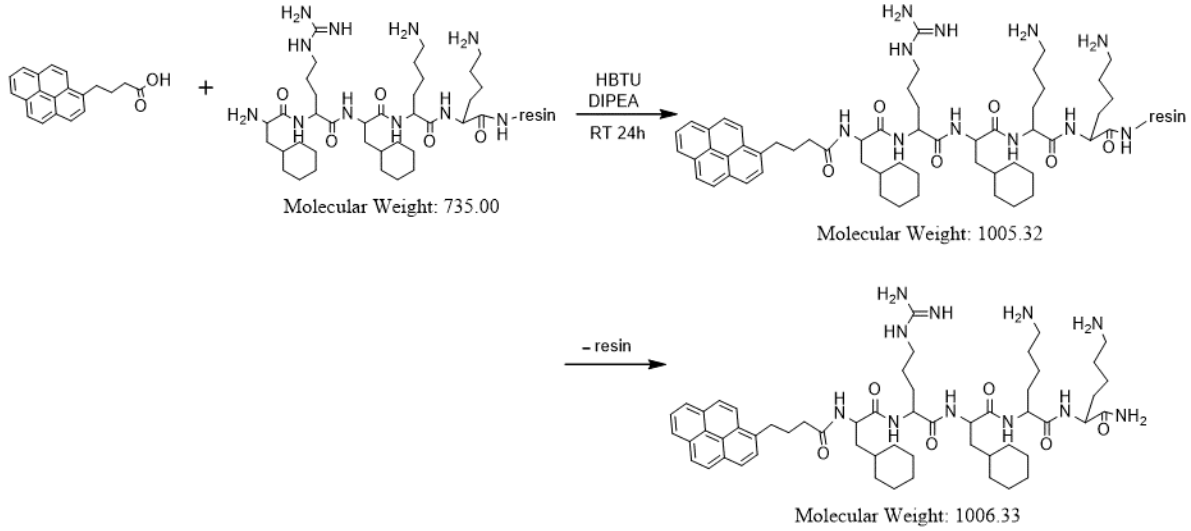

Scheme 3. 2 synthesis of Pyrene- F_xrFKK

ULSAN NATIONAL INSTITUTE OF SCIENCE AND TECHNOLOGY

3.3.4 Synthesis of PUH71- COOH linker

PUH71- COOH was obtain from reaction of between commercial available PHU71and succinic anhydride. PUH71(20 mg,1eq), succinic anhydride(3.9 mg,1eq) and DIPEA(50 mg,1 eq) in DMF 2 mL put in the 25 mL RBF and rotate for 24 h. After 24 h, mixture is purified through HPLC using water/Methanol.

3.3.5 Synthesis of PUH71- F_xrF_xKK

PUH71- F_xrFKK was obtain from reaction of between PHU71-COOH linker and peptide. PUH71(10 mg,1 eq), F_xrFKK peptide(100 mg,10 eq), DIPEA(300 μL,30 eq), and HBTU(298 mg, 30 eq) in DMF 2 mL put in the 25 mL RBF and rotate for 24 h. After 24 h, deprotection of the Fmoc- amino acids was performed by adding 20% piperidine solution in DMF. HBTU and DIEA act as coupling reagent and base. After finishing final deprotection of Fmoc protecting group, make cleavage cocktail (TFA: triisopropylsilane: Water = 4.75 mL: 0.25 mL: 0.25 mL). Add cleavage cocktail into resin with stirring for 4 hours at room temperature. Then, precipitate with cold diethyl ether. The peptide is purified through HPLC using water/Methanol.

3.3.6 Synthesis of PU- 10-COOH linker

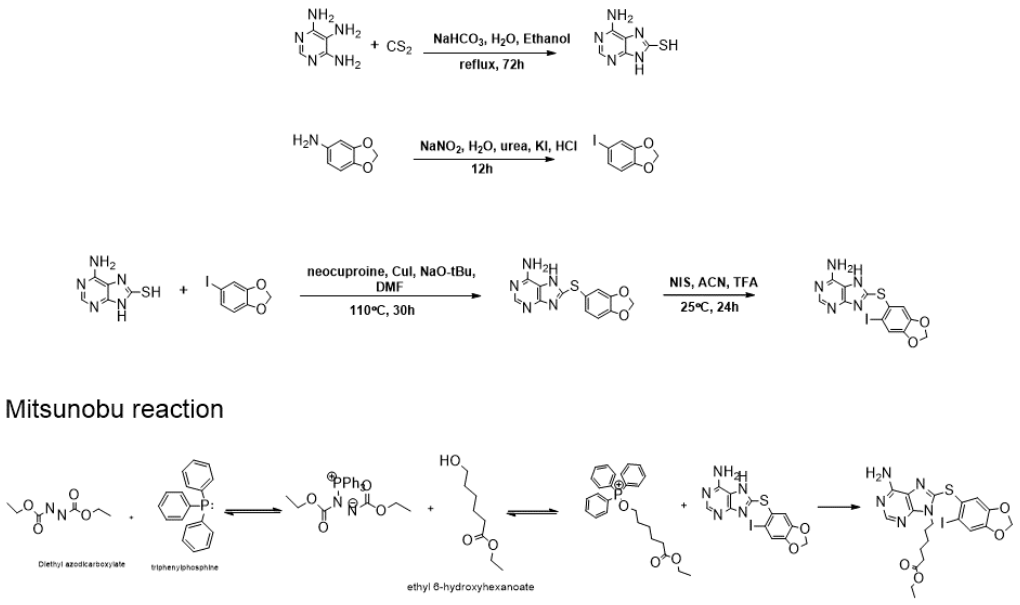

Scheme 3. 3 Overall schematic illustration of PU-10-COOH linker (Mitsunobu reaction[12])

ULSAN NATIONAL INSTITUTE OF SCIENCE AND TECHNOLOGY

3.3.6 a) Synthesis 8-mercaptoadenine

4,5,6-triamino pyrimidine, sodium bicarbonate and carbon disulfide were mixed in H_2O and Ethanol (2:1) solution. And then mixture take a reaction for 72 h by using reflux. After finish the reaction, mixture evaporate to remove carbon disulfide then solid particle were obtain. CH_3COOH 5 mL added this product and then filter some precipitate. δ_H (400 MHz, MeOH) 6.75 (2H, m) , 8.01 (1H, dt), 7.54-7.63 (1H, m), 12.86-13.10 (1H, m).

3.3.6 b) Synthesis 1-iodo-3,4-methylenedioxybenzene

(methylenedioxy)aniline is dissolved in HCl(6.4 mL) and ice. A chilled solution of $NaNO_2$ (6 mL water) was added over a time period of 15 min. then allowed to stir for an additional 10-15min. and sodium nitrile, urea and potassium added to mixture then stirred overnight. After finish the reaction, mixture was purified by extraction and column. Compound come on violet color but after evaporation, compound become dark brown. δ_H (400 MHz, $CDCl_3$) 6.05 (2H, m), 6.54-6.63 (1H, m), 7.16 (2H, m).

3.3.6 c) Synthesis of PU

Mixture contained 8-mercaptoadenine, 1-iodo-3,4-methylenedioxybenzene, Neocuproin, CuI and Nao-tBu was dissolved in dry DMF and boild at 100~120℃ for 24h. δ_H (400 MHz, MeOH) 6.02-6.23 (2H, m). 6.75-7.34 (1H, 1H, 1H, 1H, dt), 8.04-8.13 (1H, m), 12.86-13.10 (1H, m).

3.3.6 d) Synthesis of PU-I

Mixture contained PU, N-iodosuccinimide and TFA was dissolved in ACN and react for 24 h at room temp. After finish the reaction, mixture was purified by extraction and column. δ_H (400 MHz, MeOH) 6.02-6.23 (2H, m). 6.75-7.34 (1H, 1H, 1H, dt), 8.04-8.13 (1H, m), 12.86-13.10 (1H, m).

3.3.6 e) Synthesis of PU-10- $COOCH_3$

Mixture contained PU-I, eyhyl-6-hydroxyhecanoate, tri-phenyl phosphine(PPH_3) and Diethyl azodicarboxylate(DEAD) was dissolved in dry DCM and react for 24 h at room temp. After finish the reaction, mixture was purified by extraction and column. δ_H (400 MHz, MeOH) 1.32 (4H, m). 1.42-1.58(6H, m). 1.64.1.74(3H, m). 1.80-1.95 (3H, m) 2.32 (3H, m). 4.01(3H, m). 4.04(4H, m). 6.02-6.23 (2H, m). 6.75-7.34 (1H, 1H, 1H, dt), 8.04-8.13 (1H, m), 12.86-13.10 (1H, m).

ULSAN NATIONAL INSTITUTE OF SCIENCE AND TECHNOLOGY

3.3.6 f) Synthesis of PU-10- COOH

Mixture contained PU-10-$COOCH_3$ and KOH was dissolved in MeOH to remove methoxy unit and react at room temp for 24 h. After finish the reaction, mixture was purified by extraction and column. δ_H (400 MHz, MeOH) 1.32 (4H, m). 1.42-1.58(6H, m). 1.64.1.74(3H, m). 1.80-1.95 (3H, m) 2.32 (3H, m). 4.04(4H, m). 6.02-6.23 (2H, m). 6.75-7.34 (1H, 1H, 1H, dt), 8.04-8.13 (1H, m), 12.86-13.10 (1H, m).

3.3.7 Synthesis of PU-10- F_xrF_xKK

PU-10-F_xrF_xKK was obtain from reaction of between PH-10-COOH linker and peptide. PU-10-COOH(3 mg,1 eq), F_xrF_xKK peptide(30 mg,10 eq), DIPEA(30 μL,10eq), and HBTU(30 mg,10 eq) in DMF 1ml put in the 10ml RBF and rotate for 24h. After 24h, deprotection of the Fmoc- amino acids was performed by adding 20% piperidine solution in DMF. HBTU and DIEA act as coupling reagent and base. After finishing final deprotection of Fmoc protecting group, make cleavage cocktail (TFA: triisopropylsilane: Water = 4.75 mL: 0.25 mL: 0.25 mL). Add cleavage cocktail into resin with stirring for 4 h at room temperature. Then, precipitate with cold diethyl ether. The peptide is purified through HPLC using water/Methanol.

3.3.8 Synthesis of Pyrene- F_xrFKK –maleic derivatives

Pyrene-F_xrF_xKK-maleic derivatives (Succinic anhydride, Maleic anhydride, Dimethyl maleic anhydride, Citraconic anhydride and Cis-aconitic anhydride) were obtain from manual synthesis. pyrene- F_xrFKK peptide (1mg,1eq), DIPEA(3.5 μL,20 eq), and Maleic derivatives (2, 1.9, 2.5, 2.2, 3.1 mg 20 eq seperatly) in DMF 1ml put in the 10ml RBF and rotate for 24 h. After 24 h, the peptide is through HPLC using water/Methanol.

ULSAN NATIONAL INSTITUTE OF SCIENCE AND TECHNOLOGY

3.3.9 Cell culture and cell viability analysis.

Human cancer cells originating from cervix (HeLa) and noncancerous fibroblast (HeK293T) cells were obtained and cultured in DMEM, L-15 or RPMI (Life Technologies) containing 10% fetal bovine serum (FBS; Life Technologies) and 1% penicillin/streptomycin (Life Technologies) at 37℃ in a humidified atmosphere of 10% CO_2. For cytotoxicity analysis, cells were cultured in sterile 96-well Nunc (Thermo Fisher Scientific Inc.) microtiter plate at a seeding density of 5 x 103 cells/well and allowed to settle for 24 h under incubation at 37 ℃ and 5% CO_2 in their respective growth medium (RPMI 1640 and DMEM etc.). In order to check cell viability, the cells were then treated with different concentrations of peptides (0.01, 0.1, 0.5, 1, 2, 3, 5, 10, 15 and 20 μM). After 8h of incubation, stipulated time of light irradiation (3 min, 5 min and 10 min) was performed, Cell viability was measured at 24 h using the alamar blue assay, with each data point measured in triplicate. Fluorescence measurements were made using the plate reader (Tecan Infinite Series, Germany) by setting the excitation wavelength at 565 nm and monitoring emission at 590 nm on the 96 well plates.

3.3.10 Confocal microscope imaging

HELA cells were seeded in one well glass cover glass (Lab Tek II, Thermo Scientific) at a seeding density of 2 x 105 cells/well. In order to check cellular uptake of peptides, the cells were then treated with different concentrations of peptides at 5 μM for 1h. The cellular uptake was monitored periodically using Olympus FV1000 microscope connected to CO_2 incubator.

ULSAN NATIONAL INSTITUTE OF SCIENCE AND TECHNOLOGY

3.4 Results and Discussion

1) Characteristic of Pyrene-MPP

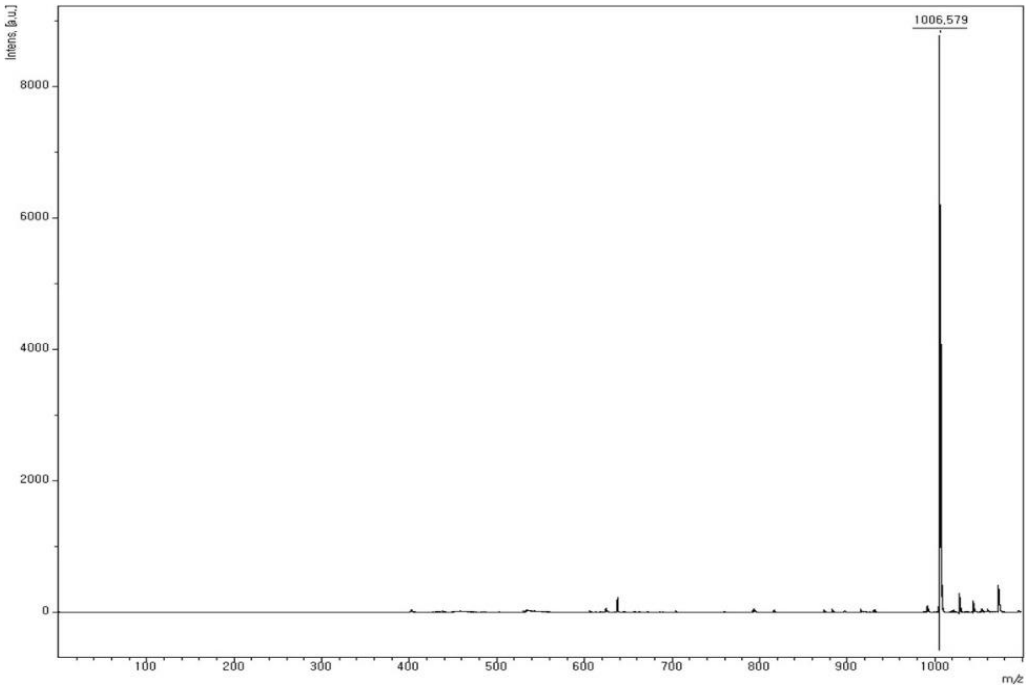

Figure 3. 1 MALDI-MS analysis of Pyrene-F_xrF_xKK. (M.W: 1006g/mol)

We synthesized mitochondria penetrating peptide, which have a sequence of F_xrF_XKK (just call, MPP). To check the predominant mitochondria of peptide, we conjugated Pyene dye to peptide for imaging. As expected, our peptide can be accumulated in the mitochondria (Figure 3. 2)

ULSAN NATIONAL INSTITUTE OF SCIENCE AND TECHNOLOGY

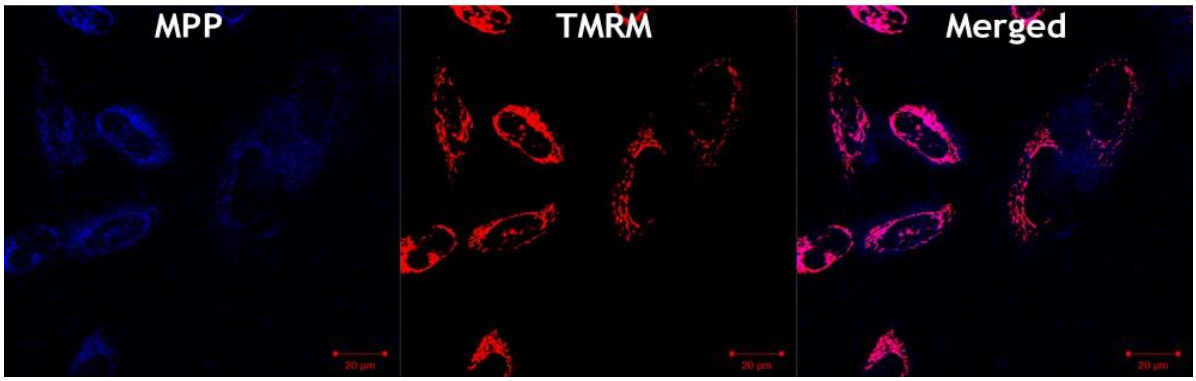

Figure 3. 2 Pyrene with MPP peptide after 1h incubation in HeLA cells

Next, we check the cell viability of conjugated peptide. Modified peptide shows almost non-toxic up to 50 μM with increasing concentration of peptide (Figure 3. 3). So, this peptide can be able to target organelle and possess biocompatibility.

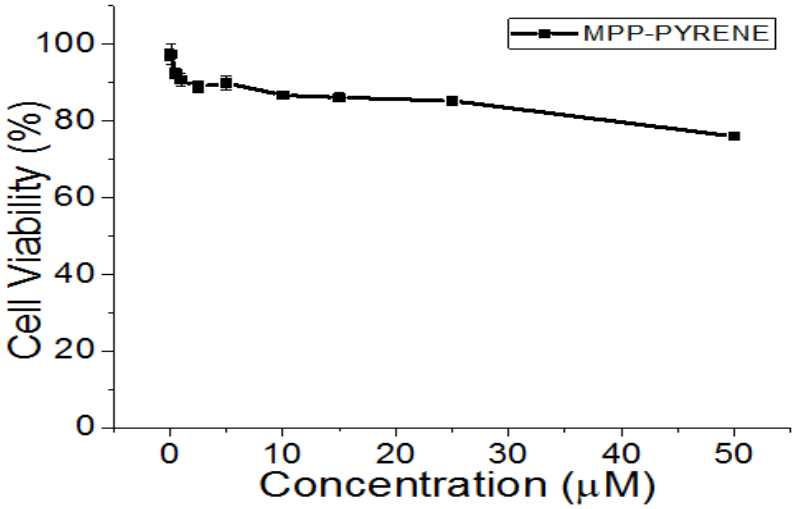

Figure 3. 3 Cell viability analysis for Pyrene-MPP peptides in HeLa cells under 24h incubation

ULSAN NATIONAL INSTITUTE OF SCIENCE AND TECHNOLOGY

2) Cell viability of Drug conjugated MPP (PUH71-MPP)

Before using charge conversion properties, we firstly try to check the cell viability of drug-MPP. We want to know how much affect to anticancer ability without charge conversion units. So, we conjugated drug to peptide. PU-H71 is kind of HSP90 inhibitor and it can be used as an anti-cancer drug. HSP90 can be degraded and suppress the growth of tumor cell. So it is important that block the effect of HSP90 in the cell to treat the cancer. To attach PUH71 into peptide, PUH71was tethered succinic anhydride. Succinic anhydride can be make the carboxylic acid group, which can react with $-NH_2$ in peptide. We make drug-MPP and then confirm cell viability. PUH71-MPP shows toxicity but that much high compared to free drug. We thought about that and we came up with some idea. Since drug is highly closed to peptide residues, drug could be inhibited with turbidity. So, we made new drug with longer linker than previous one in order to reduce turbidity.

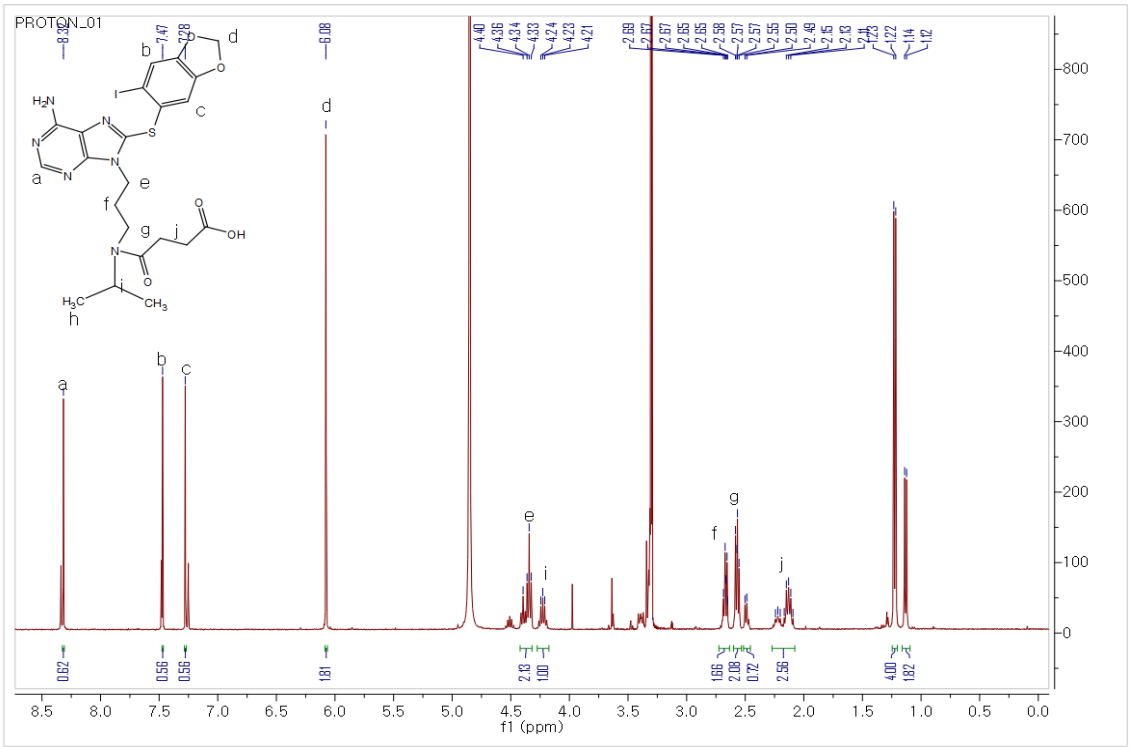

Figure 3. 4 ^{1}H-NMR spectra of PUH71-COOH linker (400MHz, MeOH).

ULSAN NATIONAL INSTITUTE OF SCIENCE AND TECHNOLOGY

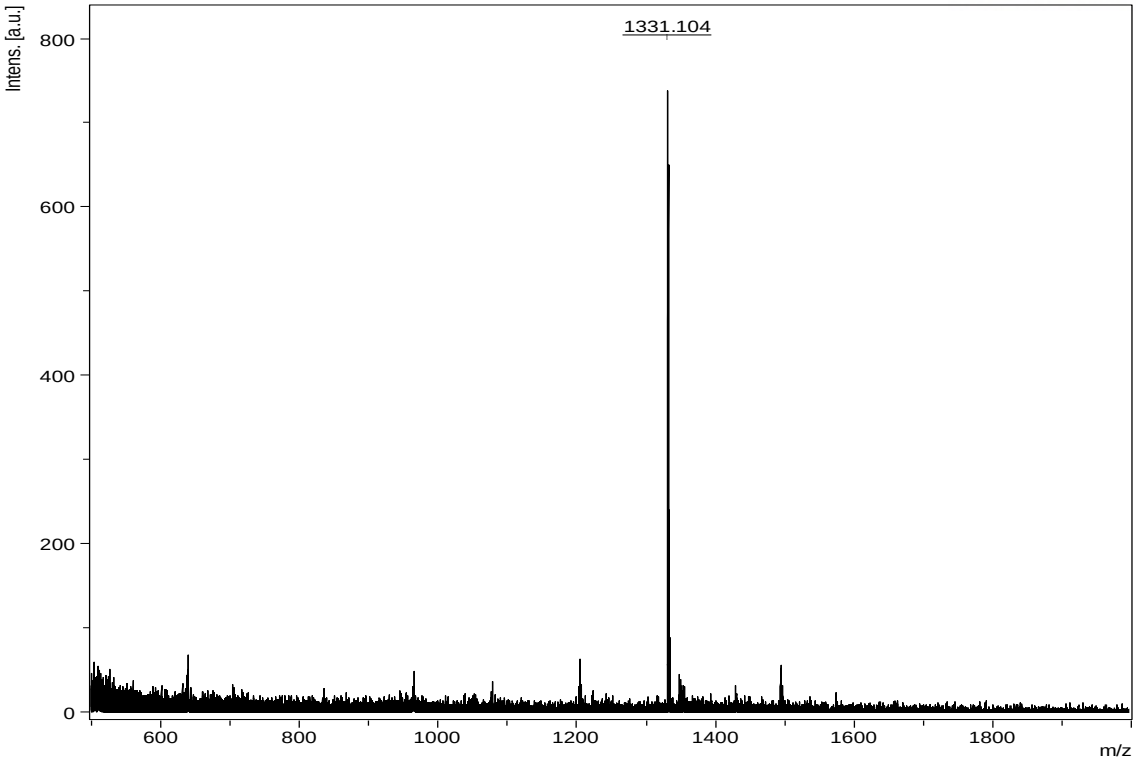

Figure 3. 5 MALDI-MS analysis of PUH71-F_xrF_xKK. (M.W: 1,330 g/mol)

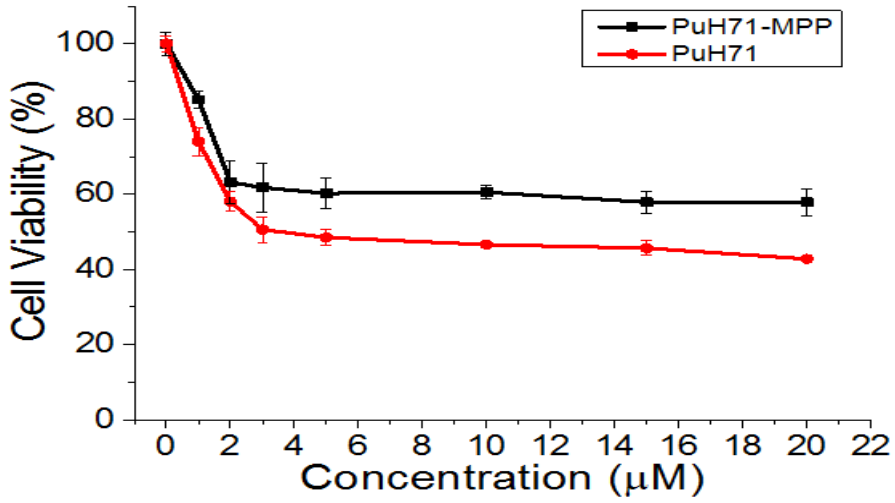

Figure 3. 6 Cell viability analysis for PuH71-MPP peptide and PuH71 drug in HeLa cells after 48h incubation using the Alamar blue dye assay**.**

ULSAN NATIONAL INSTITUTE OF SCIENCE AND TECHNOLOGY

3) Characterization data of PU-10-linker

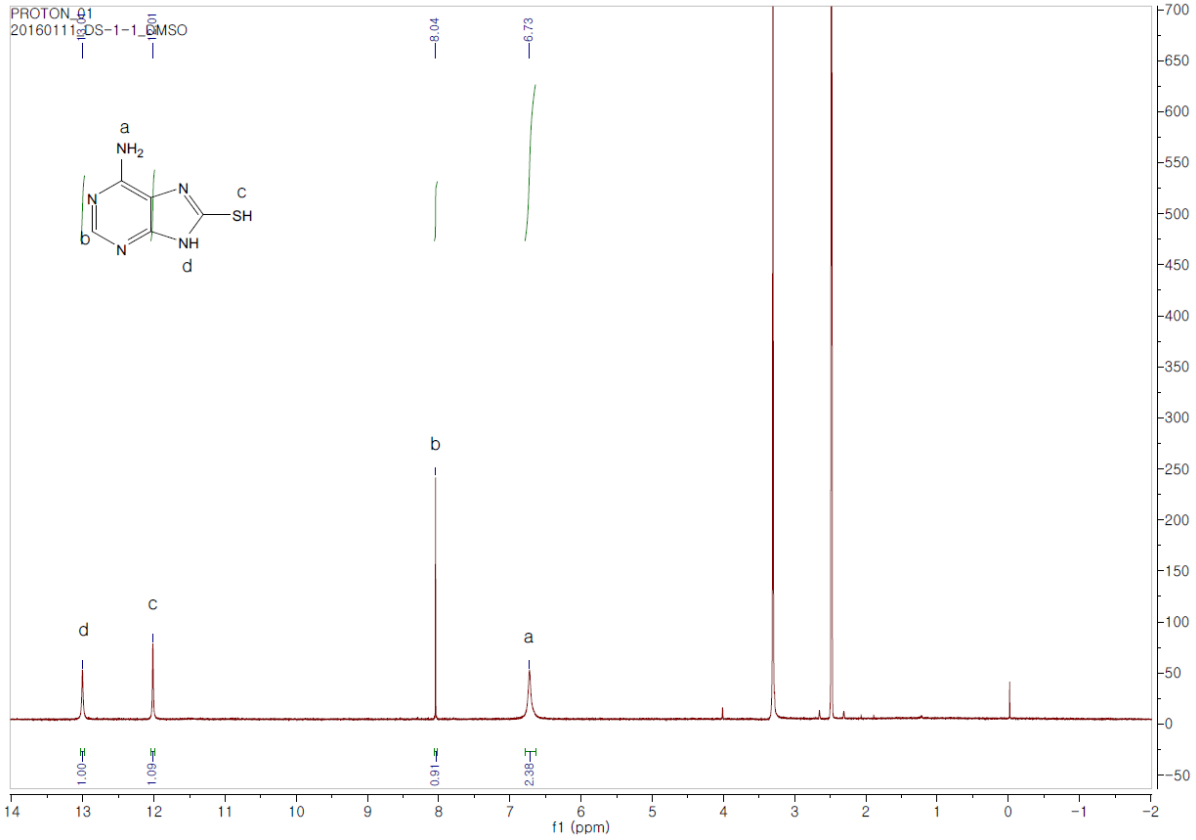

Figure 3. 7 ^{1}H-NMR spectra of 8-mercaptoadenine (400MHz, MeOH).

ULSAN NATIONAL INSTITUTE OF SCIENCE AND TECHNOLOGY

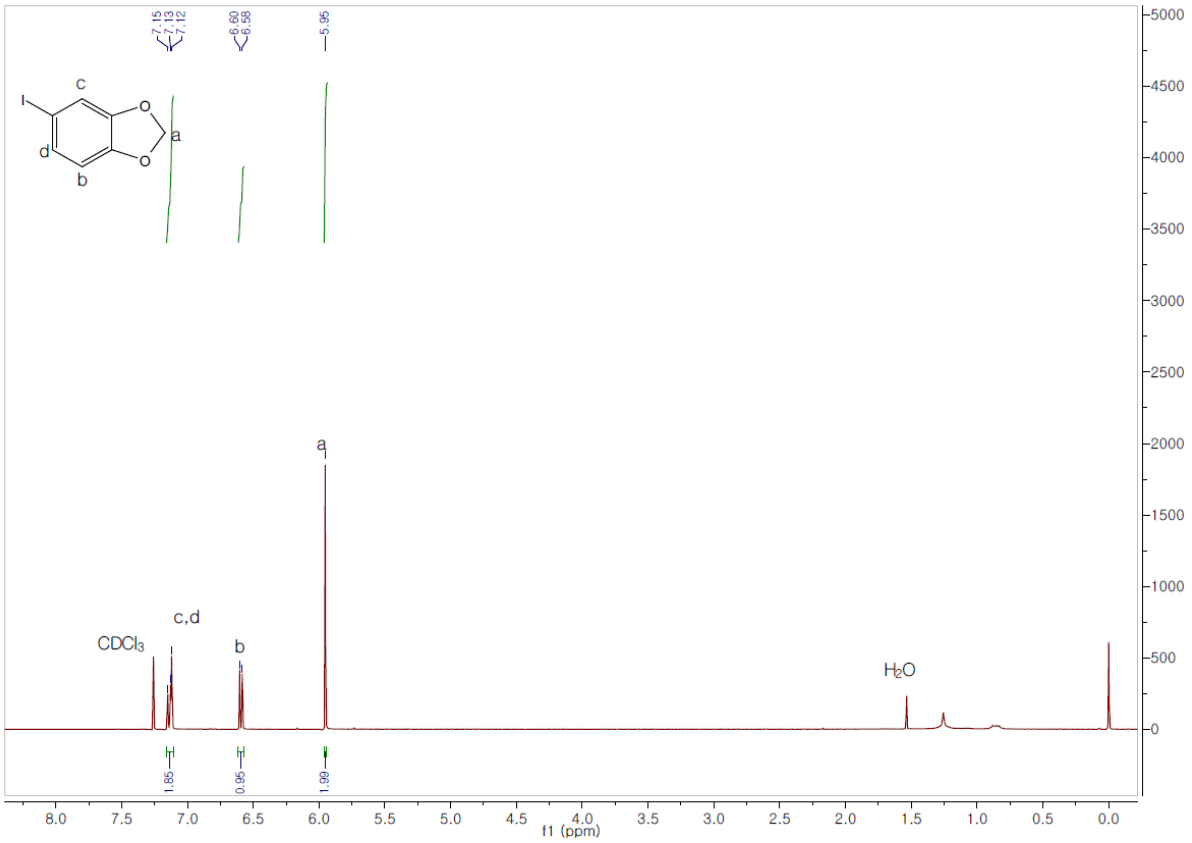

Figure 3. 8 ^{1}H-NMR spectra of 1-iodo-3,4-methylenedioxybenzene (400MHz, $CDCl_3$).

ULSAN NATIONAL INSTITUTE OF SCIENCE AND TECHNOLOGY

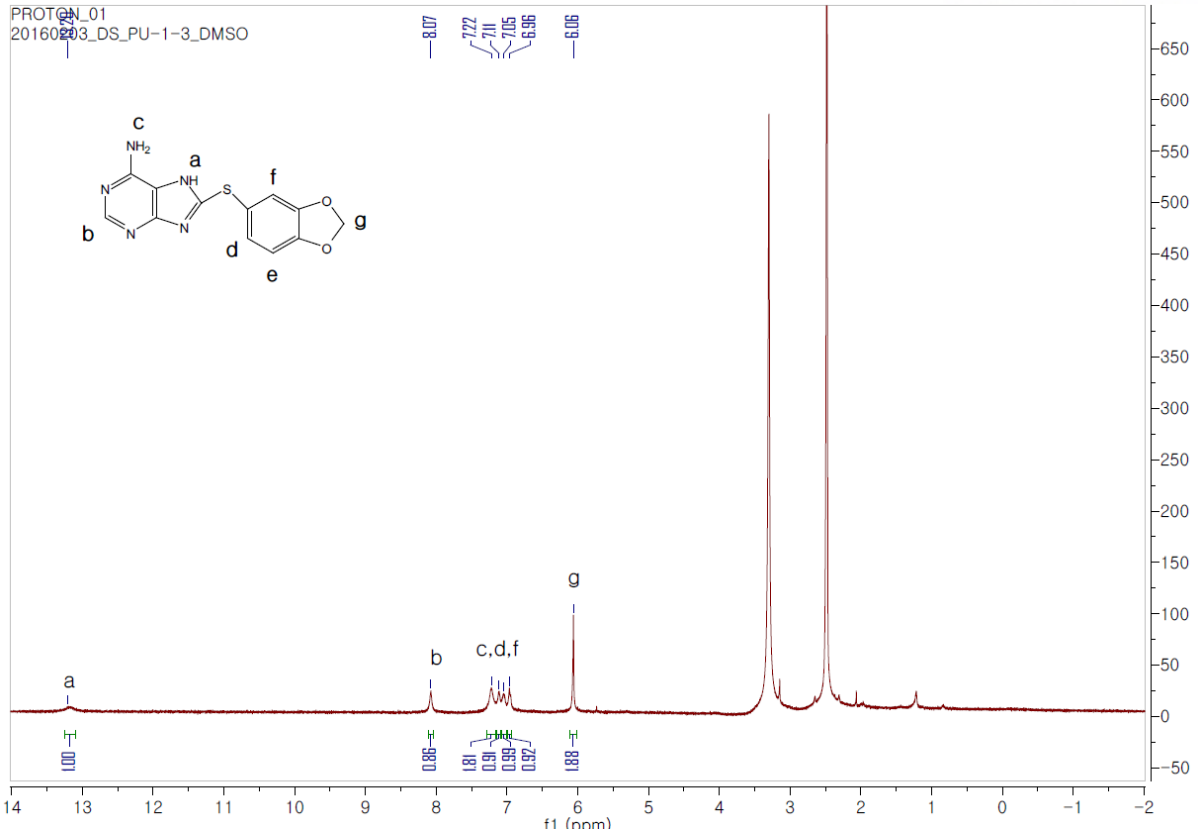

Figure 3. 9 ^{1}H-NMR spectra of PU (400MHz, MeOH).

ULSAN NATIONAL INSTITUTE OF SCIENCE AND TECHNOLOGY

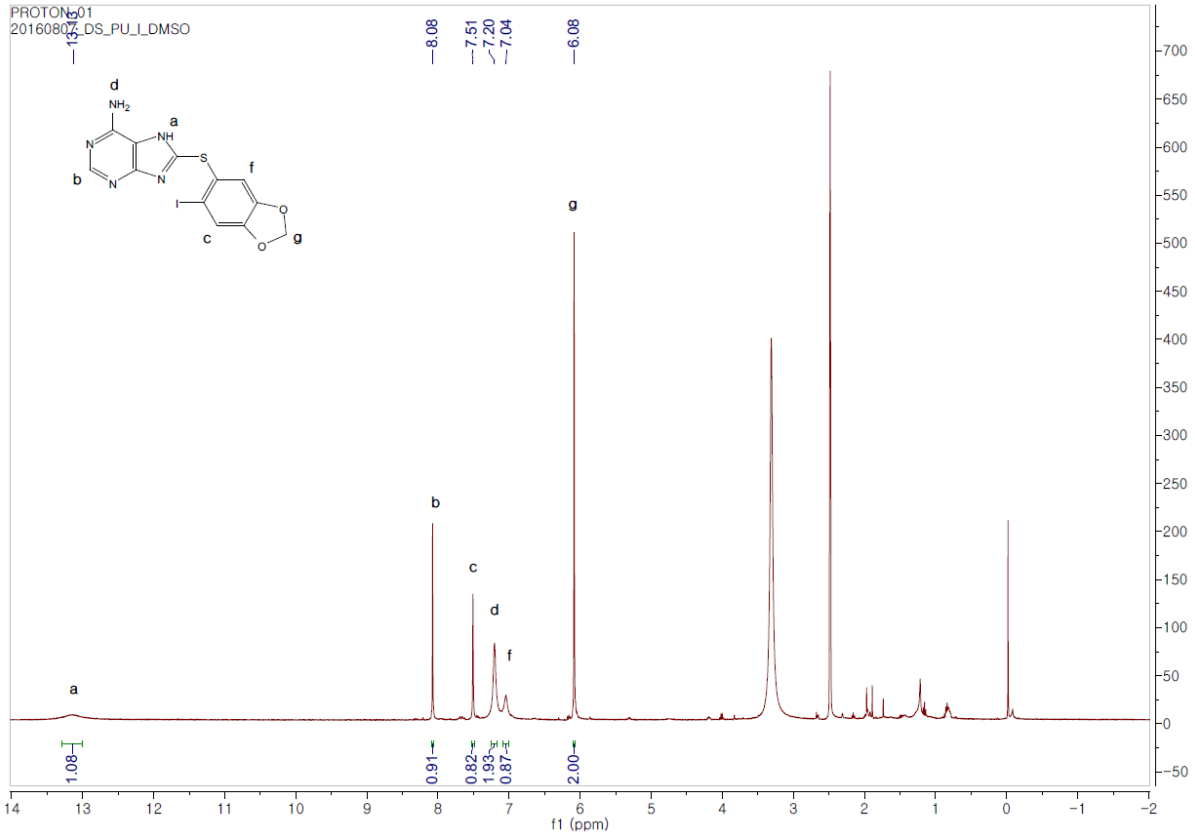

Figure 3. 10 ^{1}H-NMR spectra of PU-I (400MHz, MeOH).

ULSAN NATIONAL INSTITUTE OF
SCIENCE AND TECHNOLOGY

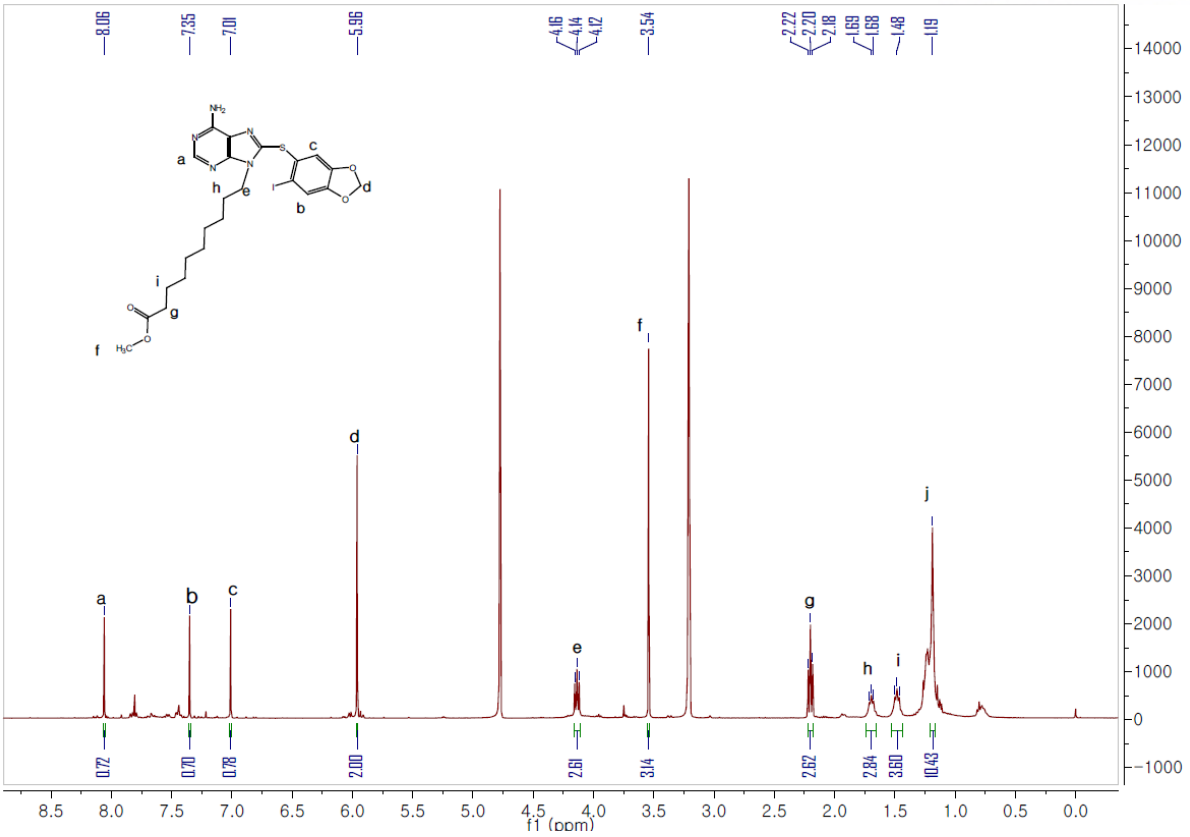

Figure 3. 11 ^{1}H-NMR spectra of PU-10-$COOCH_3$ (400MHz, MeOH).

ULSAN NATIONAL INSTITUTE OF
SCIENCE AND TECHNOLOGY

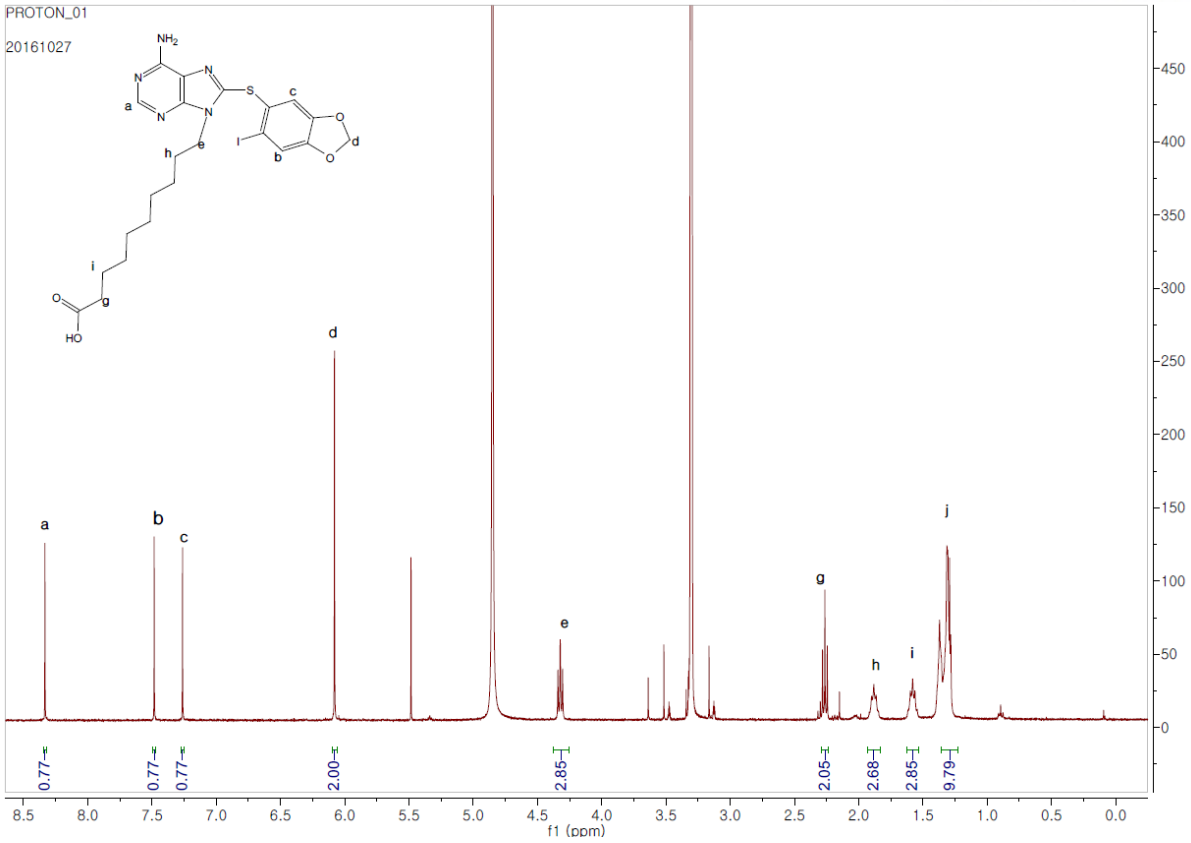

Figure 3. 12 ^{1}H-NMR spectra of PU-10-COOH (400MHz, MeOH).

ULSAN NATIONAL INSTITUTE OF SCIENCE AND TECHNOLOGY

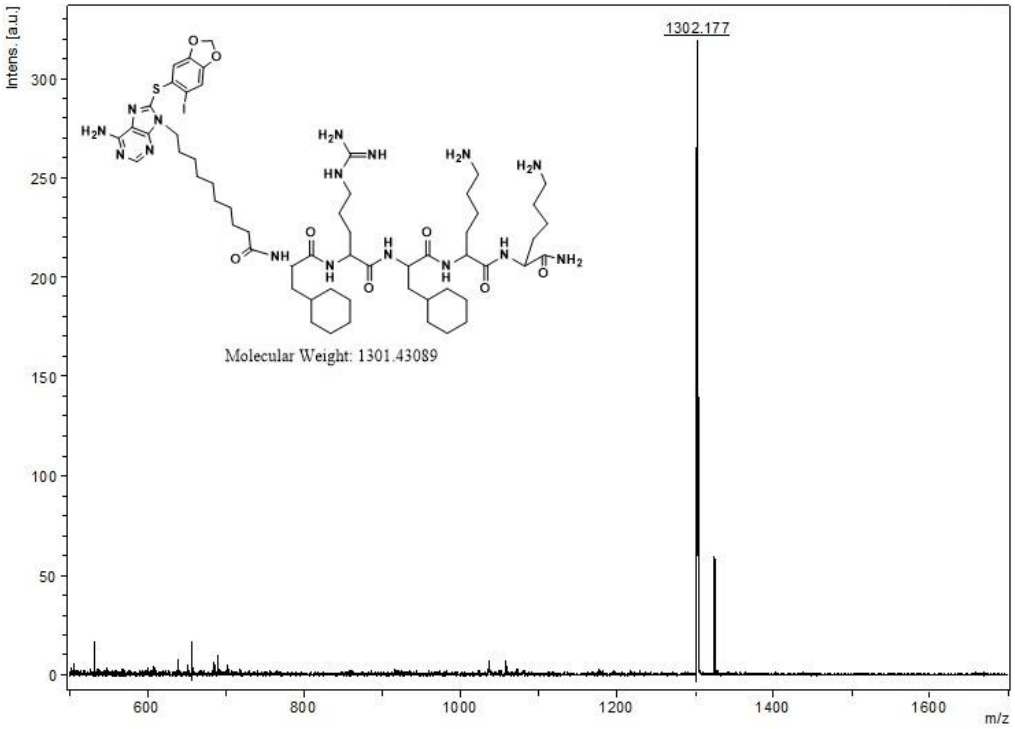

Figure 3. 13 MALDI-MS analysis of PU-10- F_xrF_xKK

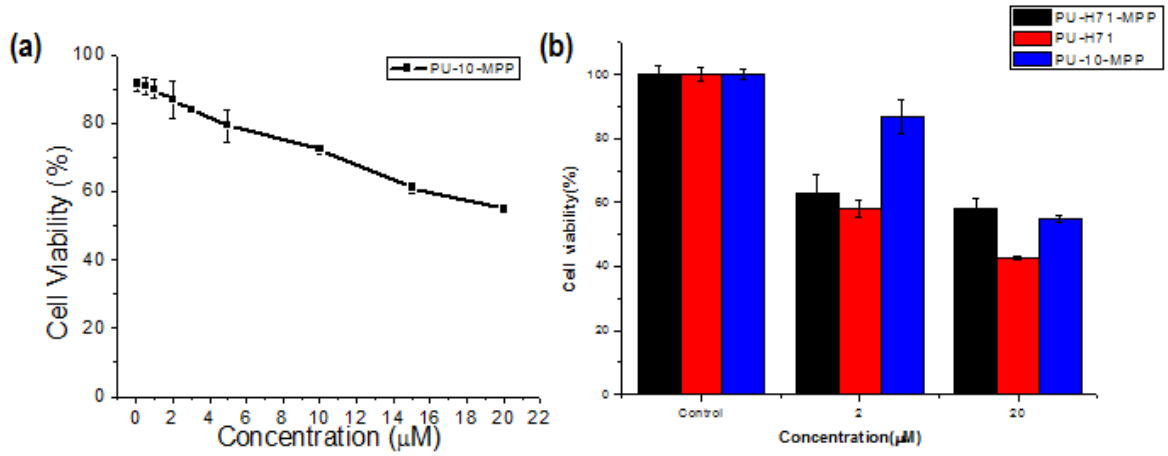

Figure 3. 14 Cell viability analysis for Pu-10-MPP peptide (a) in HeLa cells after 24h incubation. (b) Compared cell viability of PU-H71,PU-H71-MPP and PU-10-MPP at concentration 2, 20 μM.

ULSAN NATIONAL INSTITUTE OF SCIENCE AND TECHNOLOGY

4) Hydrolysis of pyrene-MPP-Maleic derivatives

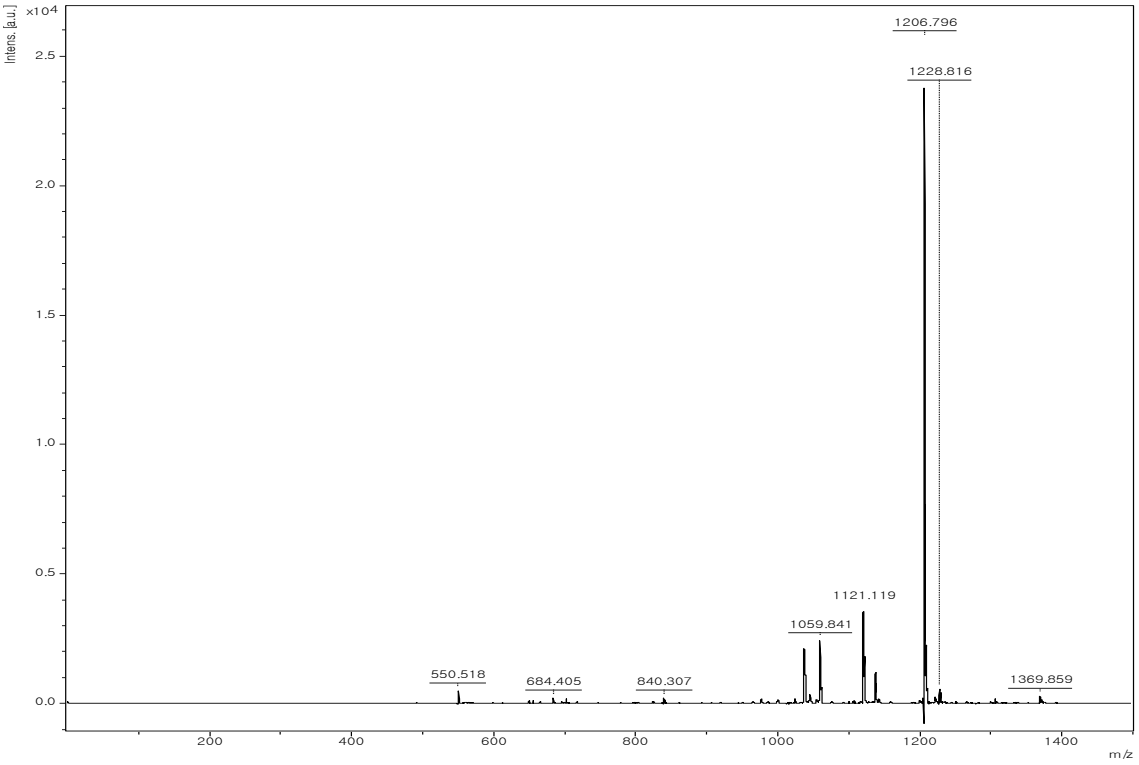

Figure 3. 15 MALDI-MS analysis of Pyene-F_xrF_xKK- succinic anhydride

To utilize charge conversion, we attached maleic derivatives to MPP. Firstly, we try to conjugate succinic anhydride to MPP. We get the succinic-MPP(Figure 3.10). But succinic anhydride group don't show degradation at the mild acidic condition (No data). So, we try to attach maleic derivatives with MPP. Among the maleic group, citraconic anhydride and aconitic anhydride are well kwon as degradation at acidic condition. Based on this knowledge, we synthesize the citraconic-MPP (Figure 3.11). and then we check the degradation of citraconic-MPP. After 1h rotation time at pH 5.5, Citraconic group occur the hydrolysis, which means it also can be used for charge conversion system(Figure 3.15).

ULSAN NATIONAL INSTITUTE OF SCIENCE AND TECHNOLOGY

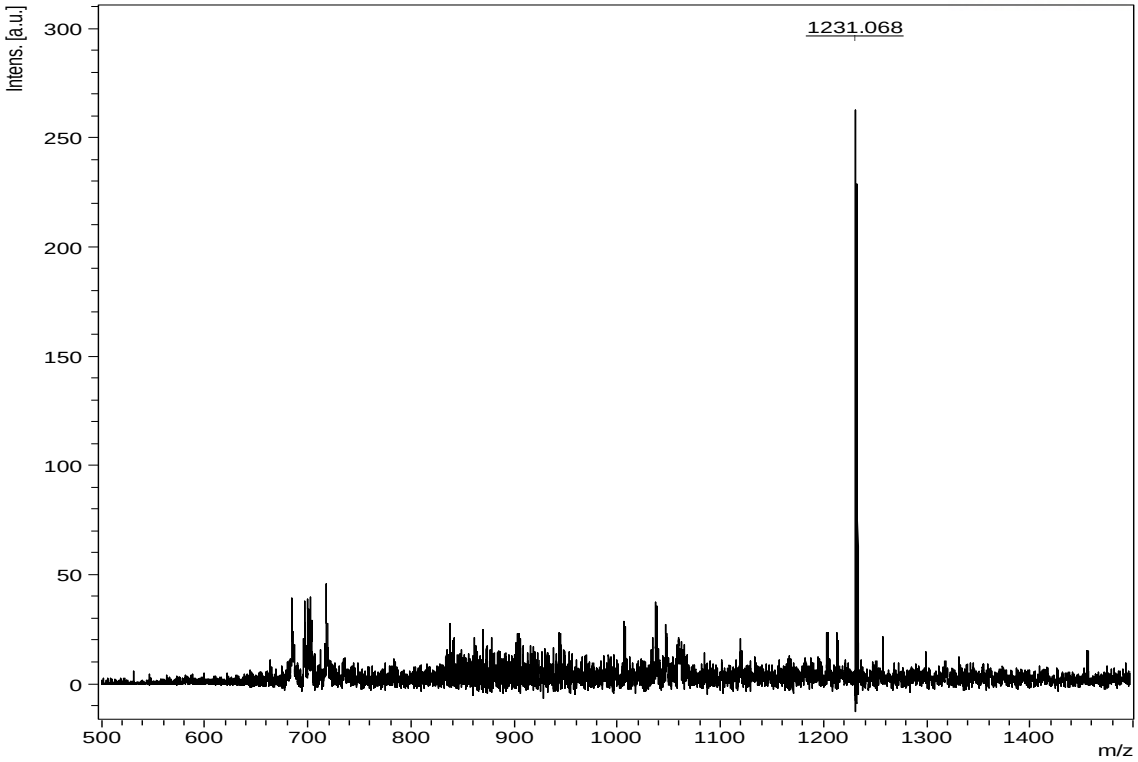

Figure 3. 16 MALDI-MS analysis of Pyene-F_xrF_xKK- citraconic anhydride

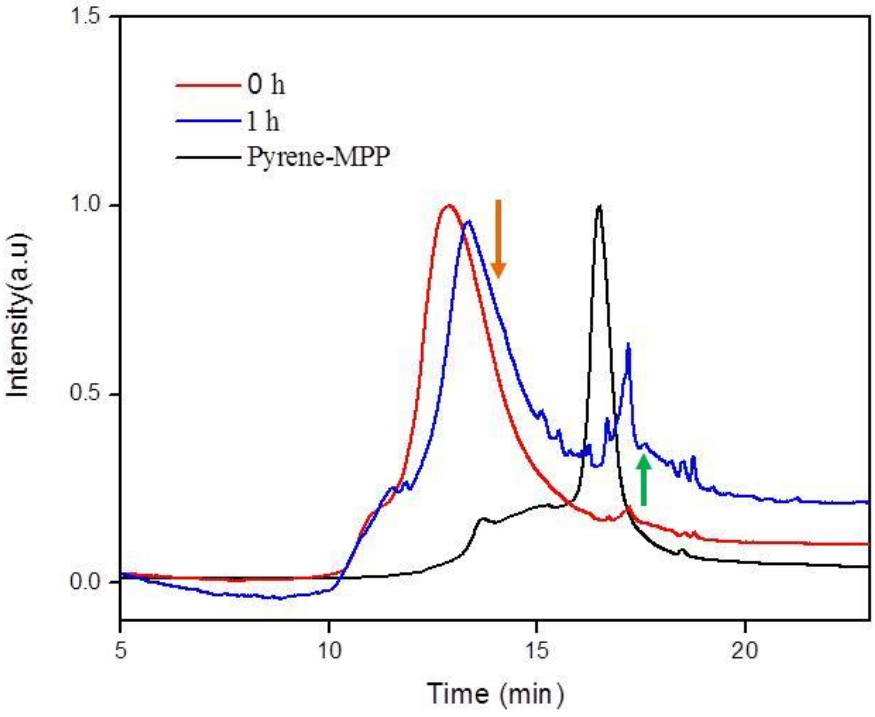

Figure 3. 17 HPLC analysis of MPP-citraconic conjugate depending on reaction time at acidic pH 5.5.

ULSAN NATIONAL INSTITUTE OF SCIENCE AND TECHNOLOGY

3.5 Conclusion and future work

In this research, we synthesize mitochondrial targeting charge conversion of peptide depending on pH**.** The peptide sequences consists of F_xrF_xKK, just called MPP, possess positive charge and lipophilic character for targeting mitochondria. Primary amines of lysine and arginine residues are the main cause of the nonspecific interactions, but they also play a key role in their membrane transduction

PU-H71 is kind of HSP90 inhibitor and it can be used as an anti-cancer drug. HSP90 can be degraded and suppress the growth of tumor cell. So it is important that block the effect of HSP90 in the cell to treat the cancer. To attach PUH71 into peptide, PUH71was tethered succinic anhydride. Succinic anhydride can be make the carboxylic acid group, which can react with $–NH_2$ in peptide. We make drug-MPP and then confirm cell viability. PUH71-MPP shows toxicity but that much high compared to free drug. We thought about that and we came up with some idea. Since drug is highly closed to peptide residues, drug could be inhibited with turbidity. So, we made new drug with longer linker than previous one in order to reduce turbidity. And we conjugated new synthesized drug (PU-10-COOH) as an inhibitor of HSP90. This platforms shows anticancer effect with 55~58% at 20 μM concentration. So, we hope that this model conjugated peptides have a potent of cancer therapy agent.

Finally, some β-carboxylic amides are stable at neutral pH but quickly hydrolyze at acidic pH to regenerate the corresponding amines. Most of maleic derivatives can be able to degrade at mild acidic pH conditions since these moieties can be attributed to the internal attack of amide carbonyl group by the carboxylate, inducing change of the chemical structure of maleic acid amide. Maleic derivatives which are play a role of hydrolyzed in MPPs. Once maleic conjugated MPP extravagates into cell membrane through highly permeability, these amides are hydrolyzed, regenerating the pristine functioning MPP in the acidic tumor extracellular fluids ($pH < 7$) for fast cellular uptake and mitochondria targeting. So our designed peptide also could be more potent to selective ability for targeted organelles. Through this result, we planned detail experiments to get more clear evidence by adjusting maleic derivatives to MPP. Further investigation with drug and targeting efficiency will be examined.

ULSAN NATIONAL INSTITUTE OF SCIENCE AND TECHNOLOGY

REFERENCES

1. Fleige, E.; Quadir, M. A.; Haag, R. *Adv. Drug Deliv. Rev*. **2012**, 64, 866.

2. Cardone , R. A.; Casavola , V.; Reshkin , S. J.; *Nat. Rev. Cancer*. **2005** , 5, 786 .

3. Meyer, M.; Philipp, A.; Oskuee, R.; Schmidt, C.; Wagner, E. *J. Am. Chem. Soc*. **2008**, 130, 3272;

4. Rozema, D. B.; Lewis, D. L. Wakefield, D. H.; Wong, S. C.; Klein, J. J.; Roesch, P. L.; Bertin, S. L.; Reppen, T. W. Chu, Q. A.; Blokhin, V.; Hagstrom, J. E.; and Wolff, J. A. *PNAS*. **2007**, 104(32), 12985.

5. Lee, Yan.; Miyata, K.; Oba, M.; Ishii, T.; Fukushima, S.; Han, M.; Koyama, H.; Nishiyama, N.; and Kataoka, K. Angew. *Chem. Int. Ed*. **2008**, 47, 5163 –5166

6. Gillies, E. R.; Goodwin, A. P.; Frechet, J. M. J. *Bioconjugate Chem*. **2004**, 15, 1254.

7. Masson, C.; Garinot, M.; Mignet, N.; Wetzer, B.; Mailhe, P.; Scherman, D.; Bessodes, M. J. *Controlled Release*. **2004**, 99, 423.

8. Kramer, M.; Stumbe, J. F.; Turk, H.; Krause, S.; Komp, A.; Delineau, L.; Prokhorova, S.; Kautz, H.; Haag, R. *Angew. Chem*. *Int. Ed*. **2002**, 41, 4252.

9. Liang, Y.; Narayanasamy, J.; Schinazi, R. F.; Chu, C. K. *Bioorg. Med. Chem*. **2006**, 14, 2178.

10. Kirby, A. J.; Lancaster, P. W. *J. Chem. Soc. Perkin Trans*. **1972**, 2, 1206.

11. Kirby, A. J.; McDonald, R. S.; Smith, C. R. *J. Chem. Soc. Perkin Trans*. **1974**, 2, 1495.

12. Yuen ,T.; But , S.; Toy, P. H. J. AM. *Chem. Soc*. **2006**, 128, 9636-9637.

ULSAN NATIONAL INSTITUTE OF
SCIENCE AND TECHNOLOGY